Simulation dynamique de perte d'équilibre : Application aux passagers debout de transport en commun

Zohaib Aftab

N° d'ordre 243-2012 Année 2012

Thèse

Simulation dynamique de perte d'équilibre : Application aux passagers debout de transport en commun

Présentée devant
L'UNIVERSITE CLAUDE BERNARD LYON I

Pour l'obtention
du DIPLÔME DE DOCTORAT

Formation doctorale : Biomécanique
École doctorale : École doctorale MEGA

Par

M. Zohaib AFTAB

Soutenue le 21 Novembre 2012 devant la Commission d'examen

Jury

Rapporteur	M. Patrick LACOUTURE	Professeur (Université de Poitiers)
Rapporteur	M. Philippe FRAISSE	Professeur (Université Montpellier 2)
Examinateur	Mme. Laurence CHÈZE	Professeur (Université Lyon 1)
Directeur de thèse	M. Bernard BROGLIATO	Directeur de recherche (INRIA Grenoble)
Co-directeur	M. Thomas ROBERT	Chargé de recherche (IFSTTAR, Bron)
Co-directeur	M. Pierre-Brice WIEBER	Chargé de recherche (INRIA Grenoble)

Laboratoire de Biomécanique et Mécanique des Chocs,
Ifsttar, 25 av. Francois Mitterrand, case 24, 69 675 BRON Cedex

N° d'ordre 243-2012 Année 2012

Thèse

Dynamic Simulation of Balance Recovery: Application to the standing passengers of public transport

Présentée devant
L'UNIVERSITE CLAUDE BERNARD LYON I

Pour l'obtention
du DIPLÔME DE DOCTORAT

Formation doctorale : Biomécanique
École doctorale : École doctorale MEGA

Par

M. Zohaib AFTAB

Soutenue le 21 Novembre 2012 devant la Commission d'examen

Jury

Rapporteur	M. Patrick LACOUTURE	Professeur (Université de Poitiers)
Rapporteur	M. Philippe FRAISSE	Professeur (Université Montpellier 2)
Examinateur	Mme. Laurence CHÈZE	Professeur (Université Lyon 1)
Directeur de thèse	M. Bernard BROGLIATO	Directeur de recherche (INRIA Grenoble)
Co-directeur	M. Thomas ROBERT	Chargé de recherche (IFSTTAR, Bron)
Co-directeur	M. Pierre-Brice WIEBER	Chargé de recherche (INRIA Grenoble)

Laboratoire de Biomécanique et Mécanique des Chocs,
Ifsttar, 25 av. Francois Mitterrand, case 24, 69 675 BRON Cedex

This work was carried out in the Biomechanics and Impact Mechanics Laboratory (LBMC) at IFSTTAR[1] and the Bipop team at INRIA[2]. The project was funded by the Cluster de Recherche, Transport, Territoire et Santé (TTS) put in place by the Région Rhône-Alpes.

[1]French Institute of Science and Technology for Transport, Development and Networks
[2]National Institute for Research in Computer Science and Control

میرے والدین کے نام

"About 5 years ago a young lady gets on the Volvo bus at noon. It's a light load with only 10 or so passengers. She moves to the second ticket machine which is about 2 metres into the bus, so I close the door and release the Park Brake without touching the accelerator. The bus just rolls gently on its own steam at about 5 km/hr (about 3mph) as I check the outside mirror for traffic and gently swing towards the lane. It seems clear and the lady has finished dipping her ticket and I'm about to touch the accelerator when I see this idiot dash between two cars right in front of me. I slammed the brakes and instinctively and instantly stuck my hand out into the aisle area. **Even changing the speed of the bus from 5 km/hr to ZERO was enough to propel the young lady like a rocket towards the front of the bus**. Fortunately with 45 years of karate instincts my arm was out there to stop her from crashing into the front windshield."

(Account of a former bus driver, indicating the level of risk in buses
http://www.empowernetwork.com/ronrichmond/the-bus-and-your-safety/)

Abstract

Loss of balance is a common phenomenon in our society resulting in injuries and even deaths each year. Among other common sources of destabilization such as slips or trips from an obstacle, the public transportation vehicles are a major source of balance-related injuries to its passengers. Accidental data suggest that the passenger casualties in these vehicles are common, especially to the standing and the elderly passengers, mainly due to the sudden acceleration/deceleration changes of the vehicle. These injuries as well as associated discomfort may discourage people from using these means of transport resulting in adverse economic and societal effects. In this context, the security of the standing passengers in these vehicles constitute the main motivation of this work.

Recovering balance from an external disturbance is a complex process which involves a set of phenomenon such as the perception of the disturbance, information processing, decision making and its implementation. Even though experimental research in the fields of biomechanics and neurosciences provide us with a fair understanding of these phenomena separately, we are unaware of a global model which represents the reaction of people in response to the external disturbances to their equilibrium. In this context, the objective of this work is to develop such a numerical tool which can be used for the assessment of risks associated with the loss of balance of the standing passengers. The essential feature of this tool is the prediction of the post-disturbance kinematics of the subjects depending upon the disturbance characteristics (magnitude, duration etc.) as well as the active recovery response. Another key feature is the representation of the reaction of different populations, especially the elderly, by integrating age effects in the model.

For the development of the tool, mathematical modeling (e.g. simplified body representations) and control ideas are borrowed from the field of biped robotics which explicitly deals with the balance issues of bipeds. Further development is done in view of human balance recovery (BR) characteristics. The resulting BR tool shows reasonable predictive capacity of a human balance recovery response confirmed by the comparison of model predictions with experimental balance recovery data.

Acknowledgement

Giving credit where credit is due, I would like to express my deepest gratitude to my supervisors whose support and cooperation were vital to my success. I thank Bernard Brogliato for showing interest in my work and always asking me the good questions (also for signing a bunch of documents every now and then). Especially, I bear a lot of appreciation and respect for Thomas Robert (my everyday mentor) and Pierre-Brice Wieber with whom I worked most of the time. I consider myself lucky to have worked under your supervision. The kind of clarity that you have in your respective domains as well as the your excellent research proposal kept me on track throughout these years. I also appreciate you patience when the things would not progress the way you would have expected (I imagine) but you never made me feel uneasy and kept trusting on me (I know what you are thinking Thomas, "C'est normale").

I would also like to thank all the former and present members of the Ergonomy team whose interest kept me motivated. Your questions and comments certainly improved this work. I would also like to thank Andrei and Mehdi, my former colleagues at INRIA, for the valuable discussions we had during my trips to Grenoble.

And finally, I will take this opportunity to thank the people who were present on the day of my defense, especially the 'seniors': Jean-Pierre Verriest (your remarks were always very encouraging), Philippe Vezin, David Mitton and Xuguang Wang, without forgetting my sister Sidra who came from Denmark for that day.

Zohaib

21.12.2012

Communications

Peer-reviewed

- Zohaib Aftab, Thomas Robert and Pierre-Brice Wieber, Predicting Multiple Step Placements For Human Balance Recovery Tasks *Journal of Biomechanics*, 2012 (in press), doi: http://dx.doi.org/10.1016/j.jbiomech.2012.08.038

- Zohaib Aftab, Thomas Robert and Pierre-Brice Wieber, Ankle, hip and stepping strategies for humanoid balance recovery with a single Model Predictive Control scheme *International Conference on Humanoid Robotics (ICHR)*, 2012

- Zohaib Aftab, Thomas Robert and Pierre-Brice Wieber, Simulating the effect of upper-body inertia on human balance recovery *Computer Methods in Biomechanics and Biomedical Engineering*, 2012, 15(S1), pp.148-150, doi: http://dx.doi.org/10.1080/10255842.2012.713653

Talks

- Zohaib Aftab, Pierre-Brice Wieber and Thomas Robert, Comparison of Capture Point estimation with human foot placement: Applicability and Limitations *5ème Journées Nationales de la Robotique Humanoïde*, June 3-4 2010, Futuroscope Poitiers (France), url: http://hal.archives-ouvertes.fr/hal-00494610

- Thomas Robert, Zohaib Aftab and Pierre-Brice Wieber, Exploring the influence of sensorimotor and cognitive factors on balance recovery using a robotic approach, *2ème Journée du GT8 Robotique et Neurosciences du GDR Robotique*, 26 Janvier 2011, Bron (France)

Table of Contents

Chapter 1

Introduction

The loss of balance in humans, which is the source of a large number of injuries worldwide, is at the heart of this work The issue has attracted some attention in recent times due to its increasing economic burden on public healthcare budgets. Several fall-risk scenarios have been identified such as slips, trips from objects etc. However, a considerable number of balance-related incidents occur to standing passengers in public transportation vehicles due to abrupt acceleration/deceleration changes. These vehicles, which mainly include urban buses and tramways, are an important means of transport for the people of all age-groups, and the safety of their occupants is of primary importance for their accessibility. In this context, the abundance of balance-related incidents in these vehicles, especially to the standing and elderly passengers, constitute the main motivation of this work. The present chapter is aimed at analyzing the risks associated with standing passengers and formulating the objectives of the this thesis accordingly.

Contents

1.1 Background

1.1.1 Falls are a major public health issue

Falls are a common phenomenon in our society. Loss of balance constitutes a major part of injuries worldwide leading to disabilities and even deaths. For instance, in the year 2000, 44% of all types of injuries in the US resulted from the loss of balance which accounted for 30% of injury costs worth $120 billion (Corso et al., 2006). Similar trends are observed elsewhere and an estimated 0.85 to 1.5% of the total healthcare budget is spent on fall-related injuries in the European Union, Australia and in the US (Heinrich et al., 2010). Moreover, the loss of balance is more frequent among the elderly. In France alone, there are 2 million elderly falls each year resulting in 9000 deaths (Sociale, 2001).

1.1.2 Public transportation: a challenging balance scenario

A particular risky balance situation is encountered by the passengers of the Public Transportation Vehicles (PTVs) such as buses and tramways. These vehicles operate in urban and semi-urban environments and involve sudden acceleration and deceleration phases. It is a common observation that their motion present a considerable challenge to the standing human balance and it is generally not possible to stand firmly without an extra support. As a matter of fact, the occurrence of passenger casualties in public transports are quite common and in situations such as emergency braking or sharp turns the passengers have reportedly been swung against the doors (de Graaf and van Weperen, 1997). This situation poses great health risks to standing passengers in public transportation vehicles and may have negative impact on the general behavior of the society towards these means of transport.

The safety of standing passengers in public transport is the focal point of this work. Though the last few decades have seen impressive research on the safety of these vehicles in crash-related incidents, the issue of loss of balance from low intensity disturbances has received much less attention. Yet, as we will explore in the following

paragraphs, the issue is of serious nature in terms of passenger injuries, their associated health costs and general discomfort.

Non-collision incidents constitute a major part of injuries in PTVs

It is an interesting fact that most of the transport-related injuries occur in situations where the vehicle is not involved in a collision. For instance, Bjornstig et al. (2005) reported that 54% of all injured passengers were victims of non-crash incidents in Sweden while 63% of such injuries were reported in Great Britain (Kirk et al., 2003). The major cause of these casualties is the emergency braking or sudden acceleration/deceleration of the vehicle responsible for at least 50% of the injuries (Bjornstig et al., 2005; Halpern et al., 2005). Even though such incidents result in minor injuries in most cases, non-crash victims have a considerable health cost, using upto 57% of all patient-days according to Bjornstig et al. (2005).

Standing and Elderly passengers are the most vulnerable

A majority of the non-crash injuries are endured by standing and elderly passengers. According to Kirk et al. (2003), 49% of serious non-collision injuries occurred to non-seated passengers while Halpern et al. (2005) reported 81% of the injuries occurring to standing or moving passengers in the bus. Moreover, around 56-72% of all injured passengers are older than 55 years of age (Bende, 2000; Halpern et al., 2005).

1.1.3 Degrading factors

These statistics point towards an important public health issue regarding public transports. The prevalence of falls and injuries in the daily-life incidents, as well as the associated discomfort, may actually discourage people from using these means of transport. Moreover, with the increase in population, the proportion of the most exposed groups (standing and elderly passengers) is increasing with time and is expected to do so for many years. For example, it is estimated that about 25% of the French population would be over 60 years of age by the year 2015 while this number may rise to 33% by the year 2050 (Insee, 2006, Figure 1.1). Similar trends are emerging in other Western

countries. Under these circumstances, the problem is expected to become even more acute in the future.

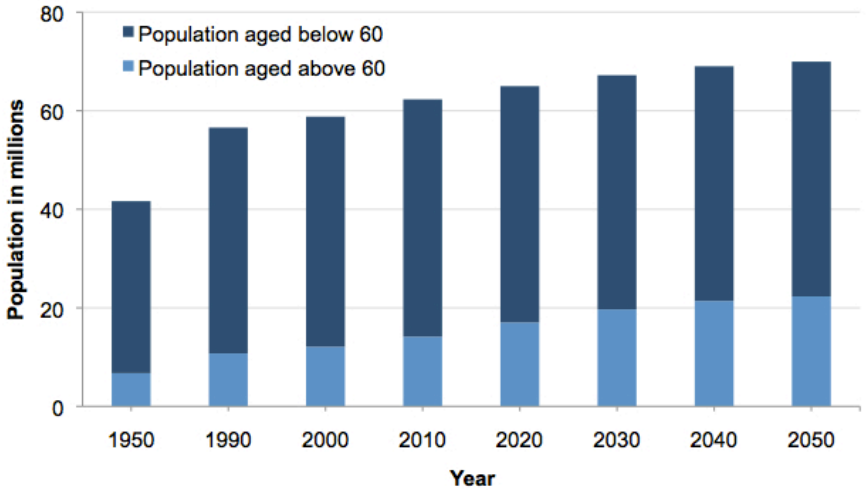

Figure 1.1: Age pattern of the French population from 1950 projected until 2050 by the French National Institute of Statistics and Economic Studies (Insee, 2006). 1 in 3 people will be 60 years of age or more in 2050, compared to 1 in 4 in 2015.

On the other hand, the issue has not been addressed rigorously, both at the level of the conception of vehicles as well as at the operating level. The major reason of balance loss in these vehicles is the sudden acceleration changes. Yet these limits are only vaguely described in the vehicle operating norms. For example, Robert (2006) reported the maximum limits of acceleration and jerk (time derivative of acceleration) defined by RATP (the Parisian transport operator) as 1 $m.s^{-2}$ and 1 $m.s^{-3}$ respectively. For the guided vehicles (tramways, trains etc.), a European norm (Afnor, 2003) specifies performance standards for the vehicle braking system presumably taking into account the effects of acceleration on the passengers' safety and comfort. However, the scientific basis of these norms are not known and these standards are not fully enforced in practice neither (Robert, 2006). Moreover, the interior designs of these vehicles are not fully adapted to ensure maximum occupant safety in case of loss of balance.

1.1.4 Conclusion

To conclude, there is a strong need to address the issue of standing passengers' safety in a systematic way so that these means of transportation remain accessible to all groups of the society. For this purpose, it is important to first understand the process of destabilization caused by the disturbances and the mechanisms of the human balance reaction.

1.2 Existing scientific knowledge

The question of human balance control has mostly been studied in the fields of biomechanics and motor control. The main motivation has been to understand the causes of degeneration of balance due to age and different pathologies. Even though a detailed literature review on this subject is presented in Chapter 2, we briefly summarize the usual approaches alongwith their limitations in the context of the current work.

1.2.1 Classical balance research

Researchers in the fields of biomechanics and neurosciences have concentrated on the human stance control since long time. Several mathematical models have also been proposed for static or quasi-static situations. However, the issue of balance recovery (BR) under strong external disturbances is relatively new and less explored. Most of the research studies are experimental in which real-life scenarios such as slips or trips are reproduced under laboratory conditions. The resulting BR reaction is described in terms of kinematic and dynamic parameters. However, these descriptions are barely applicable to the safety of standing passengers in the PTVs due to contrasting testing procedures and protocols.

On the modeling side, some attempts have been made to model human balance using the simplified representation of human body (usually single or double inverted pendulum supplemented by a foot segment). These models can broadly be divided into two groups. The first category of models predict the possibility of fall or not from a given state using no or single recovery step (e.g. Hof et al., 2005; Mille et al.,

2003; Pai and Patton, 1997). The second category of models try to predict the post-disturbance kinematics (e.g. Barrett and Lichtwark, 2008; Bortolami et al., 2003). However, only small postural disturbances are considered which can be sustained with simple modulation of ankle and/or hip torque and strictly without stepping.

1.2.2 Transport-related experimental research

Most of the vehicle safety research has concentrated on crash-related incidents, where the vehicle is involved in a collision. Crashworthiness is a research field in itself which deals with the ability for the vehicle to withstand an impact and protect its occupants. Laboratory or computer-based simulations of the crash scenarios are often performed. On the other hand, modeling of non-collision incidents has got much less attention so far despite their prevalence in public transportation as it was observed in the previous section. The modeling of these situations fundamentally differs from the crash scenarios since the active recovery reaction of the occupants is not negligible in the later case and needs to be considered to accurately predict the consequences of the disturbance.

Only a few experimental studies specifically address this issue. The scenario is mostly reproduced in a laboratory environment by means of a translating platform on which the human subjects stand (c.f. Figure 1.2). The platform is accelerated unexpectedly and the subjects' reaction is recorded. de Graaf and van Weperen (1997) are among the first to address this issue by exploring the limits of the vehicle acceleration which a standing subject could sustain in longitudinal and sideward directions without holding on or taking a step . It was confirmed that the commonly encountered accelerations in public transport could not be sustained in the standing posture. Moreover, the study highlighted the fact that the jerk of the motion is the decisive factor in such disturbances. However, the study did not report on the recovery reaction of the subjects beyond the acceleration/jerk limits.

The post-disturbance kinematics of the subjects was more thoroughly taken into account in Robert (2006) under the Safetram project[1]. The subjects were put under

[1]SAFETRAM = Passive safety for tramway for Europe, http://www.eurailsafe.net/projects.php

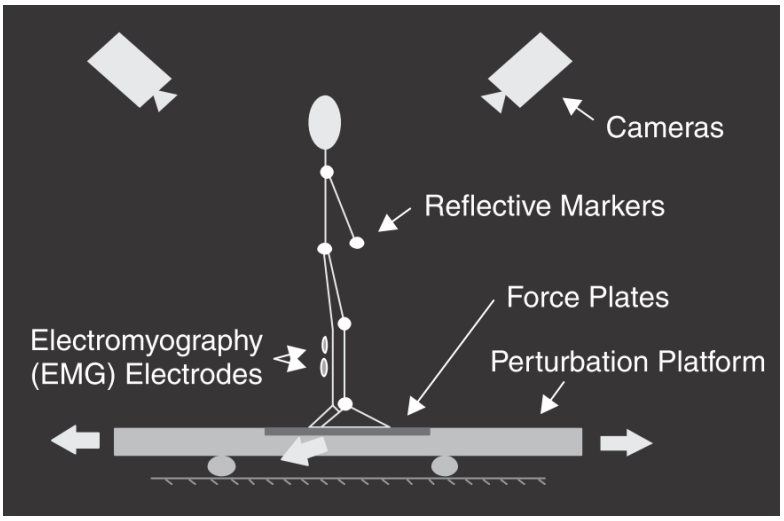

Figure 1.2: A typical disturbance and recording mechanism for simulating transport scenarios (Maki et al., 2003)

the disturbances of various levels and the resulting kinematics was recorded. However, the platform was translated with a non-realistic semi-sinusoidal profile and over a very short duration of time (400 ms). In reality, the disturbances in public transport can persist for several seconds as noted by de Graaf and van Weperen (1997). This discrepancy was addressed in Verriest et al. (2010) where the human subjects were disturbed by an emergency braking profile which lasted for 2s.

The last two studies are interesting in that these specifically consider the effects of disturbance and environmental parameters on the recovery behavior. Apart from these, there are a few other studies which perform similar experiments but the results are difficult to generalize due to non-standard experimental protocols and/or non-realistic acceleration profiles. This aspect will be discussed in more detail in the next chapter.

1.2.3 Remarks

To sum up, the domain of standing balance in humans is a well-researched field and interesting mathematical models have emerged as a result. However, the domain of human balance under strong external disturbances is relatively less known and we are

not aware of a mathematical model which adequately represents the reaction of a human in these circumstances. Given the prevalence of the balance related incidents in the PTVs, a fair degree of understanding about this phenomenon is needed in order to limit its negative effects on the society.

1.3 Objectives of the thesis

The general objective of this work is to develop a numerical tool for the assessment of risks associated with the loss of balance following a strong external disturbance. The primary application of this tool is sought for standing passengers in PTVs which is a high risk and under-researched scenario as we observed in the previous sections. In this regard, the essential part is to predict the post-disturbance kinematics of the subject as a function of the disturbance characteristics (intensity, duration etc.). However, given the reactivity of the human, the post-disturbance kinematics also depends upon the recovery action taken by the subjects. **The modeling of this response is the key feature of this tool and the primary objective of this thesis.**

To this end, the advances in the field of biped robotics could prove beneficial. Owing to the morphological and functional similarities, these machines face similar kind of balance control challenges as humans. Moreover, the field has seen impressive advances in the last few decades resulting in some useful mathematical models and control techniques. Hence, as it will be shown in the next chapters, this knowledge will be helpful in the context of the objectives of this thesis.

A secondary objective of the thesis is to represent the reaction of the elderly people which are the most vulnerable to the balance disturbances. This would require the integration of the effects of ageing on the model parameters.

1.4 Thesis overview

We start by reviewing the relevant literature on the subject of balance in Chapter 2. Both experimental and modeling aspects are discussed along with the fundamental

control concepts in the field of biped robotics. Analysis of the experimental literature affirms that the most prevalent BR strategy in humans is to take a recovery step in the direction of the disturbance. This is thus the subject of Chapter 3 in which various biped stepping control schemes are presented and evaluated. It is shown that in the context of the objectives of this thesis, the Model Predictive Control (MPC) approach is very promising. Our BR controller is thus built on this approach and the complete development of a multiple-strategy MPC scheme is presented in Chapter 4. The model predictions are compared against human BR data showing close resemblance. Finally, in Chapter 5, the BR tool is further developed to include relatively complex situations such as disturbances of longer durations observed in the PTVs. Moreover, a preliminary study on generating an elderly response is carried out in the end by varying selected parameters of the model.

Chapter 2

Literature Review

Human balance is a fairly old subject of research. Although the issue of standing balance has been well studied for a long time, the domain of large disturbances requiring recovery steps is relatively less explored. The problem has mostly been studied with the help of experiments on human subjects and to the author's knowledge, except a few prediction and stance control models, a comprehensive balance control model involving recovery steps is in-existent. The purpose of this chapter is to review existing knowledge about human recovery responses from large disturbances.

The chapter is broadly divided into 2 parts. In the first part (Section 2.1), we review and synthesize experimental findings about the human balance recovery behavior. In the second part (Section 2.2), we focus on the modeling issues. Lastly, we will review the control techniques proposed for the balancing of biped robots which we believe could provide important clues for our balance recovery simulation tool.

Contents

2.1 Experimental Studies of Balance Recovery

A considerable number of experimental studies have focused on the question of disturbed balance. In this section, we review these studies in general and try to synthesize their common findings as well as their limitations. We will particularly be focusing on situations which induce one or several balance recovery steps.

2.1.1 Experimental Mechanisms

The usual procedure of experimental studies consists in disturbing the balance of human subjects by different means in a laboratory created environment. The kinematics and kinetics of the resulting reaction are then recorded using specific instrumentation (reflexive markers, force platforms etc.). One of the most common experimental means of inducing a fall is by a tether-release mechanism. The subjects are inclined in a stationary forward leaning position retained by a tether and a safety harness (c.f. Figure 2.1). The tether is then suddenly released from that unstable posture inducing a loss of balance under the effect of gravity. The method was first introduced by Do et al. (1982) and has been used extensively ever since. Different studies are carried out with different objectives such as recording of stepping properties (Do et al., 1982, 1999; Thelen et al., 1997) and/or age-related differences (Hsiao-Wecksler and Robinovitch, 2007; Madigan and Lloyd, 2005).

The transport-related disturbance scenario, which is the focus of this thesis, is simulated using the translating-platform paradigm. Subjects stand on a support base which can be translated in anterior /posterior direction or sideways. On the basis of the disturbance duration, these studies can be divided into 2 major groups. On one side, there are studies where the platform is translated only for a very brief period and can actually be viewed as a "single destabilizing event" (McIlroy and Maki, 1994). In this case, the associated deceleration phase of the platform can actually facilitate the restabilization of the falling subjects (Bothner and Jensen, 2001). In other studies, the platform motion persists for a longer duration so that its disturbing effect varies during the balance recovery process (McIlroy and Maki, 1996; Robert, 2006; Verriest et al.,

2010). We consider this later scenario closer to the real-time perturbations observed in public transportation vehicles (see e.g. real disturbance profiles in Figure 3 of de Graaf and van Weperen, 1997).

The salient feature of some important moving-platform studies are summarized in Table 2.1.

Table 2.1: A selection of important platform disturbance studies and their characteristics. To be coherent between studies, the disturbance is reported in terms of peak platform acceleration in all cases

Study	Disturbance Direction	Disturbance Profile	Range of peak platform Acceleration	Stepping Allowed ?	Observed Number of Steps	Focus of Study
de Graaf and van Weperen (1997)	Forward, Backward, Sideways	Quasi-Square acceleration profile	0.3-1.6 $m.s^{-2}$ for 2 s	No	0	Limit of balance without stepping
Runge et al. (1999)	Backward	Trapezoidal velocity profile	6.5 - 32 $m.s^{-2}$ for 0.36 - 4 s	No	0	Ankle and Hip strategies
Szturm and Fallang (1998)	Forward, Backward, Sideways	Quasi-semisquare velocity profile	2 - 4 $m.s^{-2}$ for 0.4 - 0.8 s	No	0	Movement Patterns, Motor control
McIlroy and Maki (1996)	Forward, Backward	Square wave acceleration profile	1.5-2 $m.s^{-2}$ for 0.6 s	Yes	> 1	Age-related stepping characteristics
Verriest et al. (2010)	Forward, Backward, Sideways	Quasi-trapezoidal acceleration profile	4 $m.s^{-2}$ for 5 s	Yes	> 2	Kinematics of balance recovery in emergency braking conditions
Robert (2006)	Backward	Semi-sinosoidal acceleration profile	2-10 $m.s^{-2}$ for 0.4 s	Yes	1-4	Kinematics and Kinetics of multiple step balance recovery

Other disturbance scenarios include waist-pull perturbations (Pai et al., 1998; Schulz et al., 2005) and recovery from trips (Pijnappels et al., 2005; Schillings et al., 1996) or slips (Bhatt et al., 2005; Pai et al., 2003). These scenarios are relatively less-common in literature and do not present a particular interest to our research problem.

Throughout the text, we will focus on the two balance recovery scenarios: 1) The tether-release situation due to its simplicity and abundance in the literature, 2) The translating platform paradigm due to its relevance with the transport related disturbances.

2.1.2 Synthesis of Experimental Findings

The experimental studies have given good insight into the basic phenomena associated with the balance recovery. Their main findings can be summarized as follows:

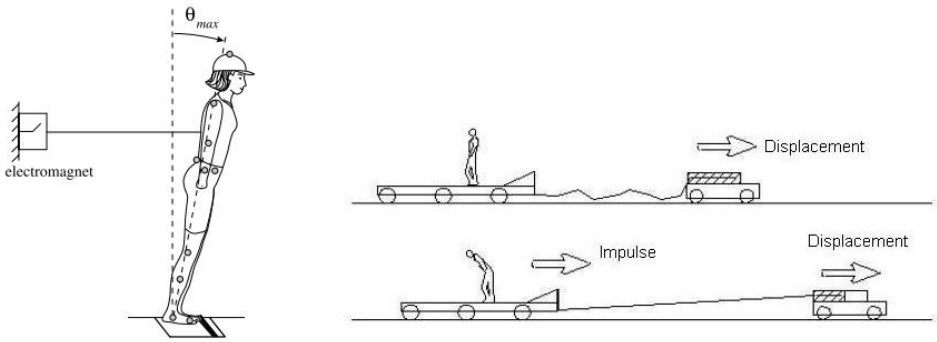

Figure 2.1: Disturbance studies under consideration in this thesis: Tether-release mechanism (Left) and Translating platform paradigm (Right)

Balance Recovery Strategies

Based on numerous experimental observations, the balance strategies can be broadly categorized into 2 classes: 1) Fixed-Support strategies, which include the Ankle and the Hip strategies (Horak and Nashner, 1986; Nashner and McCollum, 1985). The ankle strategy represents the rotation of the whole-body around the ankle joint and is often used to tackle small external disturbances. Hip strategy is characterized by the rotation of the upper-body around the hip joint in the sagittal plane and is usually employed for slightly larger disturbances. 2) Change-of-Support strategies, which involve either the use of compensatory stepping or take an extra support from the environment (Maki and McIlroy, 1997). These strategies are suitable for the large disturbances where the fixed-support strategies are not sufficient to recover balance.

In practice though, the notion of sequential transition from a lower-level strategy to a higher one has been refuted in several studies. Even though the disturbance magnitude remains a relevant parameter for strategy selection, the characteristics of the disturbance (Maki et al., 1994) and the environmental constraints (Horak and Nashner, 1986) also play a role. It has been shown that, when given the choice, the stepping strategy is preferred over the fixed-support hip strategy and is triggered before reaching the theoretical limits of the fixed-support strategies (Maki and McIlroy, 1997; Pai et al., 2000). Similarly, fixed-support strategies often coexist (Maki and McIlroy,

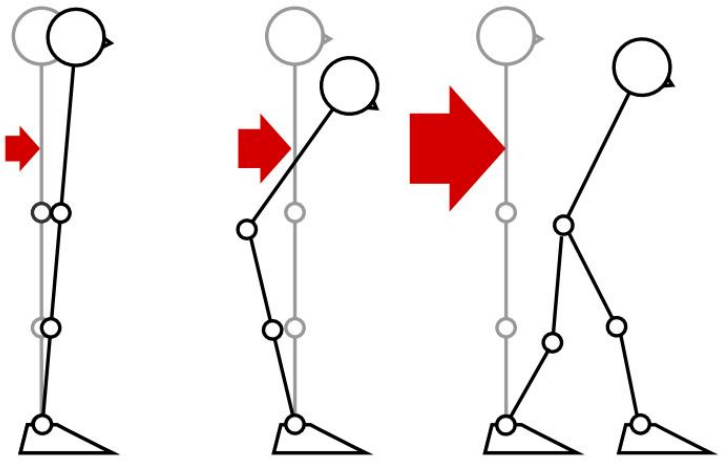

Figure 2.2: Basic movement strategies employed by humans to retain their balance: Ankle (left), Hip (middle) and Stepping (right) (Kanamiya et al., 2010)

1997) in such a way that the relative use of both strategies gradually evolves with the perturbation level (Park et al., 2004).

Temporal phases of Balance Recovery

After the disturbance, a typical reaction can be divided into several temporal phases. To start with, there is an inevitable delay between the application of the disturbance and the outbreak of the first mechanical response. This delay is referred to as Reaction Time or Reaction Delay. Most experimental studies report this delay between 70 - 180 ms (Cyr and Smeesters, 2009b; Do et al., 1982; Karamanidis, 2006; Robert and Verriest, 2007) depending upon the type and sometimes the size of the disturbance.

For the situations involving stepping responses, the step onset is usually defined as the instant where force below the stepping foot is completely zero (with the exception of McIlroy and Maki (1993) who consider the onset of stepping at the point where the vertical force below both feet start to diverge). The delay between the beginning of the mechanical response and the onset of step is referred to as Step Preparation Time or the Weight-Transfer Time. Finally, the Legswing Time is defined as the delay between step onset and step placement on the ground.

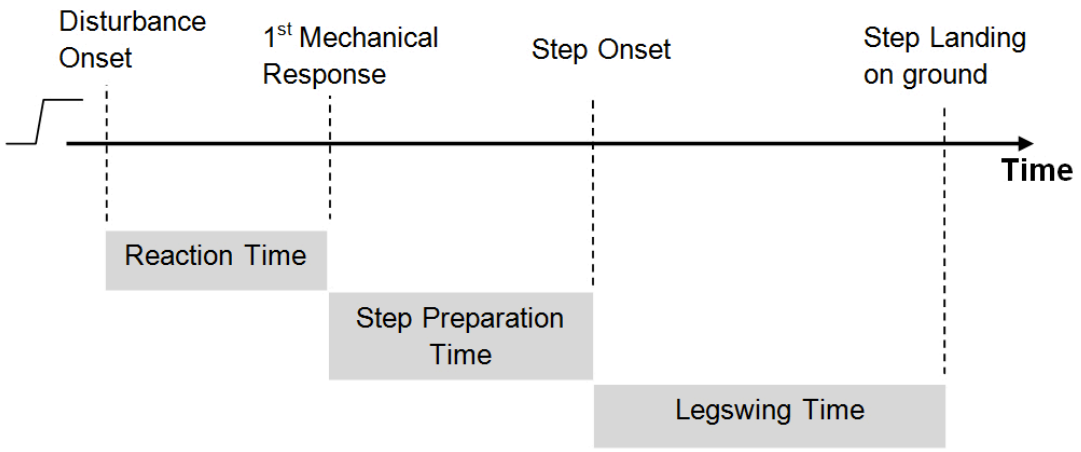

Figure 2.3: The temporal phases of balance recovery involving stepping

The Stepping Variables

Stepping is a common recovery strategy which is characterized by two major variables: Step length and Step time (sum of step preparation and legswing times). Not surprisingly, the recovery ability from a given disturbance is enhanced by taking quicker and larger steps. For example, Owings et al. (2001) found that step onset times and step lengths were decisive factors between failed and successful recoveries in human subjects. Similarly, Hsiao-Wecksler and Robinovitch (2007) showed that the maximum permissible disturbance from which subjects could recover with single step was significantly enhanced by taking larger steps. However, both these variables (step length and step time) are positively correlated. A larger step requires more time to execute during which the system continues to fall. Conversely, a quicker step cannot be placed beyond a certain distance due to actuation constraints. Hence a trade-off is to be found between these two variables for a successful balance recovery.

Effects of Ageing

Several studies have focused on the age-related difference in the balance recovery ability by subjecting young and elderly subjects to various disturbance scenarios and comparing their response. Not surprisingly, recovery ability decreases significantly with age due to musculoskeletal and neurological degradations. It has been shown that the

maximum permissible perturbation level is significantly lesser for the elderly (Hsiao-Wecksler and Robinovitch, 2007; Karamanidis, 2006; Thelen et al., 1997). Moreover, elderly are more likely to employ a stepping strategy (McIlroy and Maki, 1996; Mille et al., 2003) and are further likely to use more number of steps to recover balance than their young counterparts.

The causes of these differences have been associated with different sensory, neural and musculoskeletal degradations with age. Reduced proprioception in the lower limbs, reduced ankle dorsiflexion and quadriceps strength (Lord et al., 1991a,b), increased reaction times (Maki and McIlroy, 1997) and impaired cognitive function have been identified as important discriminators between falling and non-falling elderly.

2.1.3 Inconsistency in Experimental Results

Even though the experimental studies give a good insight into various phenomena of balance recovery, it is still pretty difficult to evaluate and compare results from different studies. This is primarily due to the diversity of the objectives which leads to contrasting experimental configurations. This is particularly the case for the disturbances involving platform translation. We discuss here some of these difficulties briefly:

Disturbance characteristics are not well-defined

For the disturbances involving platform translations, the destabilizing effect on the body is induced mainly by the platform acceleration level (McIlroy and Maki, 1994) and is also affected by initial impetus (jerk) values (de Graaf and van Weperen, 1997). Yet in several studies, the disturbance is characterized in terms of a platform displacement or velocity (e.g. Diener et al., 1988). Though the representative acceleration values are usually reported, acceleration is not used as the driving disturbance variable (see e.g. Runge et al., 1999; Szturm and Fallang, 1998). This leads to strong differences between the findings of two different studies. For example, the maximum level of backward acceleration which a subject could sustain without stepping was reported to be 0.61 $m.s^{-2}$ in de Graaf and van Weperen (1997) while 32 $m.s^{-2}$ in Runge et al. (1999), (Table 2.1). In addition, the transient platform disturbances reported in

many studies do not accurately represent the real-time disturbances observed in the transportation.

Different prior instructions produce different results

In a balance recovery experiment, the reaction can be significantly affected by the instructions given to the subjects prior to the experiment. The most common instruction is about stepping. McIlroy and Maki (1993) reported that subjects tended to step more frequently for the same disturbance when no specific instructions were given about stepping than when they were instructed to keep their feet in place. Yet different studies are carried out under different stepping instructions which sometimes complicates the comparison between otherwise similar parameters.

The reported results may not carry all the information

Given the variety of purposes of different studies, the measured or reported parameters are not the same. For example, among multiple tether-release studies, only Cyr and Smeesters (2009b) have reported the kinematics of successive steps. Similarly, in translating platform studies, only Robert (2006) and Verriest et al. (2010) report the kinematics of multiple steps.

2.1.4 Remarks

To conclude, the experimental studies mainly highlight the biomechanical aspects of balance recovery and enhance our understanding of the basic phenomena involved. However, non-standardization of the testing procedures make it impossible to draw concrete quantitative conclusions about the balance recovery, particularly for the disturbances of moving platform type. For instance, one cannot estimate the effect of individual disturbance parameters (disturbance time, amplitude etc.) separately on the location and number of recovery steps.

2.2 Modeling of human balance

The robust human behavior against external disturbances is by virtue of the highly efficient and accurate balance control system. The exploration of this system and its characteristics is a research field in itself. In this section we will briefly review some of the principal studies which attempt to model human balance.

Human body is a multi-segment, multi-dof system. However, to simplify the task of mathematical modeling and analysis, it is approximated by some simplified representations. The choice of the simplified model is driven by the desired level of complexity of the motion under consideration. Some of the most common representations are discussed below.

2.2.1 Simplified representations of human body

In many balance studies, the human-body is viewed as a sagittal-plane simple inverted pendulum, rotating around the ankle joint (Loram and Lakie, 2002; Morasso and Schieppati, 1999; Winter et al., 1998, 2001). A finite-sized foot is usually supplemented to represent the base of support (Figure 2.4a). All the mass of the system is considered concentrated at the CoM level. The state of the system is characterized by the body sway angle from vertical for quasi-static scenarios or additionally, by the CoM velocity for dynamic conditions (e.g. Pai and Patton, 1997). The model has been largely deemed adequate to represent human standing balance.

However, it has been argued that a single segment approximation of human body is not sufficient to completely explain certain balance properties, even for standing balance (Creath et al., 2005). Moreover, in presence of perturbations (Horak and Nashner, 1986) or secondary tasks (Bardy, 2002), the representation of the anti-phase rotation of the upper and lower body inevitably requires multi-segment representations. In this regard, a common model is the double-inverted pendulum model used in several studies (Bonnet et al., 2007; Martin et al., 2006; Park et al., 2004) (Figure 2.4b). A 3-joint model incorporating a knee has also been employed (Alexandrov et al., 2001;

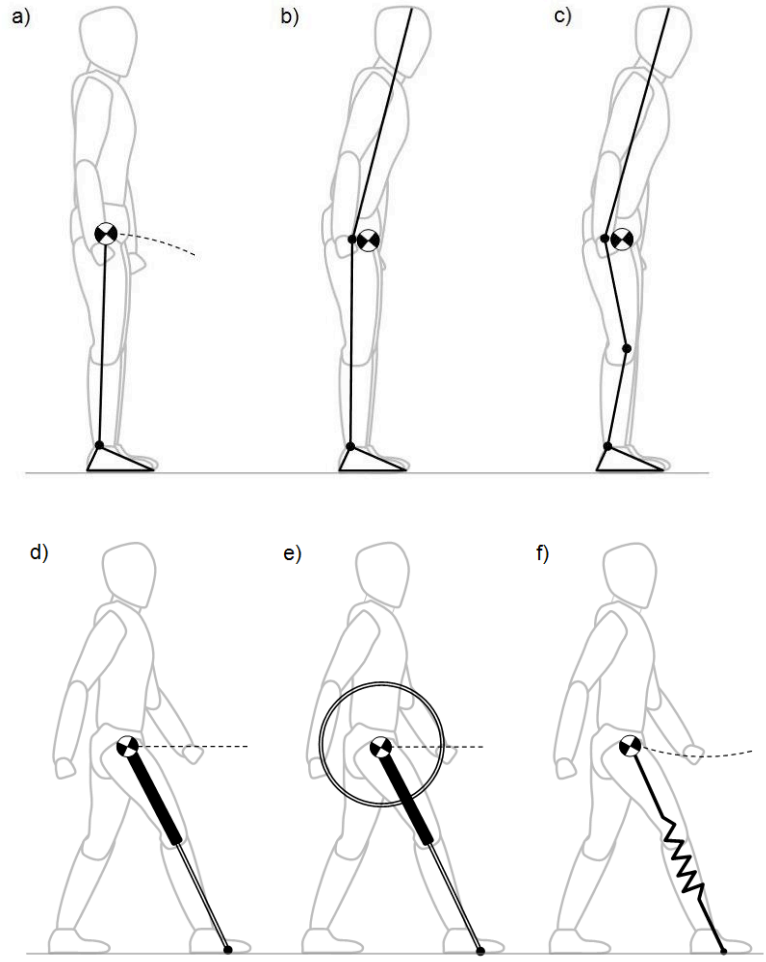

Figure 2.4: Some common simplified models used to approximate multi-articulated human (or robotic) system. The crossed circle represents the Center of Mass position

Alexandrov and AA, 2005; van der Kooij et al., 2001) (Figure 2.4c).

Figure 2.4(d-f) shows a few more simplifications proposed in the domain of biped robotics. The most common model is the the Linear Inverted Pendulum (LIP) model proposed by Kajita and Tani (1991) (Figure 2.4d). This model constrains the CoM to move in a horizontal plane above ground assuming telescopic legs. Though this constraint is less realistic biologically, it linearizes and decouples the CoM dynamics in sagittal and frontal planes which is a valuable property from the control point of view. It additionally neglects the rotational effects of different body parts. A simple way to

include the upper-body inertial effects is by using an inertia wheel centered at the CoM level (Komura et al., 2005; Pratt et al., 2006)(Figure 2.4e). Lastly, to incorporate leg compliance, a spring-mass model was proposed by Geyer et al. (2006)(Figure 2.4f). The model consists of a massless spring attached to a point mass. This model is shown to demonstrate realistic dynamic properties of human walking and running.

2.2.2 Fall predictors

Before moving onto the complete balance control schemes, let us first analyze some prediction models proposed in the biomechanics literature. These models estimate the possibility of falling (or not) from a given system state, using simple representations of human body. The most prominent model in this regard was put forward by Pai and colleagues (Pai et al., 2000; Pai and Patton, 1997; Pai et al., 1998). They used the inverted pendulum model with a foot segment (c.f. Figure 2.4a) to calculate the stability boundary of the ankle strategy in the CoM displacement-velocity zone, using human anatomical and physiological constraints (CoM height, foot size, peak ankle torques etc) (Figure 2.5). The model predictions were also compared against the experimental data. Later a linear version of this concept was proposed by Hof et al. (2005) evolving a reference point called the Extrapolated Center of Mass position (XCoM). These works highlighted the importance of consideration of system velocity, in addition to its position with respect to the foot, for correct predictions in dynamic balance recovery scenarios.

However, this model merely calculates the *theoretical* boundary of the ankle strategy which would imply, in a control scheme, that a step should be initiated when the ankle strategy is not sufficient to restore balance. However, as we have seen in the experimental findings, stepping is a preferred strategy in humans and is usually invoked before reaching the theoretical limits of the fixed-support strategies. In this context, their practical use for the prediction of human responses is quite limited.

A few other studies propose balance threshold lines based on experimental observations. Mille et al. (2003) identified a threshold line beyond which the stepping was triggered when the participants were pulled forward unexpectedly. Moglo and

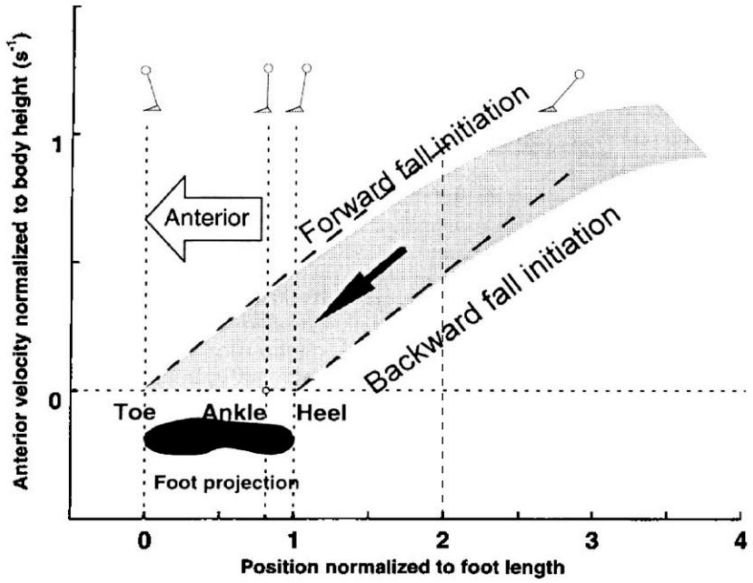

Figure 2.5: The stability of ankle strategy calculated in Pai and Patton (1997) (shaded region) and approximated by Hof et al. (2005) (dotted line) using a simple inverted pendulum model. (Figure taken from Hof et al. (2005))

Smeesters (2005) proposed a similar threshold line between recoveries and falls but included a single-step forward. They also showed that the threshold of balance recovery, in terms of its CoM displacement-velocity state, did not change with the type of perturbation applied.

However, all these predictions only state if a given state will result in a recovery or a fall without giving much idea about the nature of the recovery action necessary to avoid this fall.

2.2.3 Control schemes

There are several studies that model human balance control based upon the basic human balance control principles and the simplified human-body representations described above. Perhaps the most simple stance control model was proposed by Winter et al. (1998). It considers the body sway stabilization being a purely **passive** process. Considering the human body to sway like a simple inverted pendulum, the model limits the role of the Central Nervous System (CNS) to the regulation of muscle tone

such that it keeps the body upright with little swaying. However, contradictory views exist (e.g. Morasso and Schieppati, 1999) which consider the ankle muscle stiffness insufficient to keep the body upright.

Most researchers model the human balance control as an **active** feedback system. The level of complexity varies between studies. Most of the models consider a perfect estimation of the system state variables and employ positional and derivative feedback gains (Maurer et al., 2006; Mergner et al., 2003; Park et al., 2004; Peterka, 2002). For example, Park et al. (2004) proposed a linear feedback model which used a single set of feedback gains (c.f. Figure 2.6) for different perturbations. The model employed the double-inverted pendulum representation to consider upper-body rotation. The model of Peterka (2002) used a similar feedback loop but additionally contained the idea of sensory re-weighting based on environmental conditions and perturbation amplitude. The model considered contributions from both active and passive torques for stance control but showed that the active feedback torques were mainly responsible for postural stability.

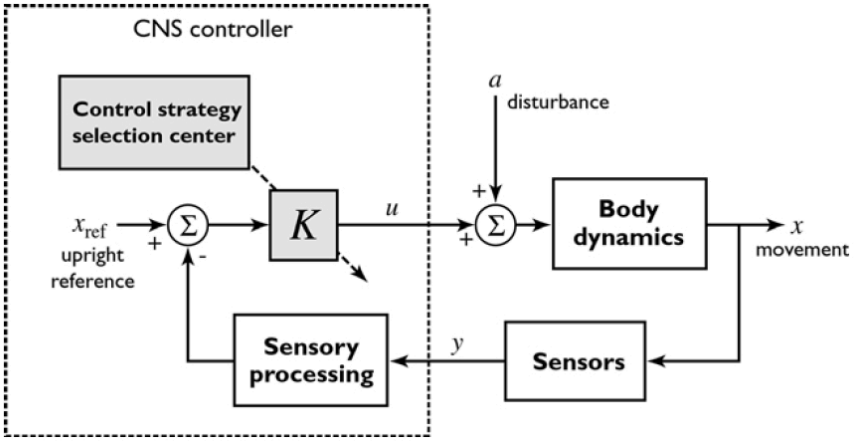

Figure 2.6: A linear feedback control model, where K is a matrix of feedback gains producing joint torque commands u as a function of body movement x (Park et al., 2004).

A more sophisticated stance control system was proposed by van der Kooij et al. (1999) using complex sensor dynamic models (Borah et al., 1988) and intersensory interactions (c.f. Figure 2.7). The modeled sensory systems included the visual, vestibu-

lar and somatosensory components which are considered vital in maintaining balance in humans. The sensor dynamic model comprises of transfer functions representing input-output relations of various sensory systems. The sensory integration was performed using an extended Kalman filter model, while neural delays were compensated by using a predictive element in the controller. In addition, the body dynamics was represented by a three-link segment model of a standing human on a movable support base.

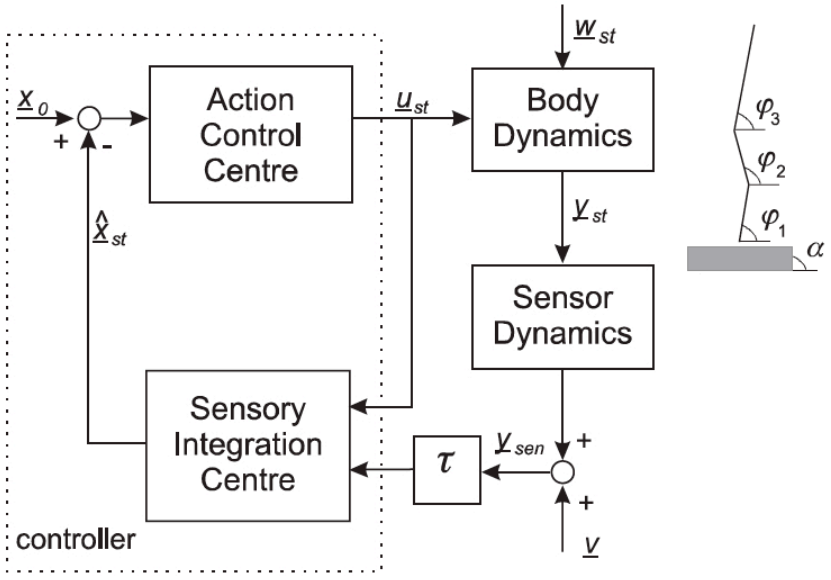

Figure 2.7: Flow diagram of the human stance control model proposed by van der Kooij et al. (1999). The unknown disturbances w_{st} are successfully offset by the muscle actions u_{st}. In addition to sensory input, the sensory control center also inputs muscle actions for best estimate of the body sway

An alternative approach to the continuous feedback control is the **intermittent** or **sliding-mode** control. It consists in generating intermittent control bursts when the system state leaves an area around the reference point (Bottaro et al., 2005, 2008; Loram and Lakie, 2002). The model has been simulated for human postural control.

2.2.4 Remarks

The above-mentioned control schemes demonstrate close resemblance to actual human standing balance and are also useful for understanding the underlying equilibrium

mechanisms. However, all of these control schemes only consider small body sways and/or disturbances that would be compensated by simple modulation of ankle or hip joint and particularly without stepping. This is quite a limitation in the context of the objectives of this thesis, which has a much broader scope than just standing balance. Being interested in modeling responses from larger disturbances, stepping is an important balance strategy to have, as it was noted in the previous section.

2.3 Dynamic equilibrium and stability

The modeling of strongly disturbed balance is a more complex issue. Owing to the fact that the velocity of the motion is not negligible and the system may have intermittent contact phases with the environment (e.g. during stepping), the interpretation of equilibrium and the estimation of instability is not quite straightforward. These issues have been more directly taken up in the field of robotics. Owing to the morphological and functional similarities, the two-legged (biped) robots are subjected to similar kind of balance control challenges as humans. The field has seen impressive advances in the last decades and the continuing efforts have given the roboticists a good understanding of the stability characteristics of motion. Several stable walking controllers have been developed and implemented. We estimate that this knowledge, taking the form of the mathematical formulations and tools, can prove very helpful in context of the objectives of this thesis.

However, the modeling of balance has to be rely on reliable criteria to estimate the system instability, which define equilibrium and stability in a particular way. Before we review the studies related to the control of biped robots, it is important to clarify the meaning of these terms relative to the biped systems. Let us start by simple textbook descriptions of equilibrium for a mechanical system and gradually move to more specific case of bipeds.

Equilibrium and stability are two distinct concepts. A mechanical system is said to be in a state of equilibrium if it has zero acceleration. That is to say, either the

system is at rest (**static equilibrium**) or is moving with a constant velocity (**dynamic equilibrium**). In other words, a system is in equilibrium if all the applied and inertial forces (if any) acting on it are in perfect balance.

On the other hand, the term **stability** describes the state of an equilibrium. An equilibrium can be stable or unstable (Azevedo et al., 2004). An equilibrium is called stable if the system only temporarily leaves its equilibrium position (due to a disturbance for example), but comes back to it when the disturbance is removed. A simple pendulum at rest is an example of stable equilibrium (or more precisely, asymptotically stable in control theory). If the same pendulum is inverted, its equilibrium becomes unstable, that is, only a small disturbance is sufficient to permanently lose its equilibrium upright position.

2.3.1 Equilibrium of Biped Systems

Let's consider again the standard definition of dynamic equilibrium and adapt it for the biped systems. It states that, for a rigid body, the total wrench of the external forces must be strictly equal to the dynamic wrench of the body. In case of a biped locomotion, the external forces include the gravitational and contact forces between feet and the ground. This condition can then be represented as (Barthelemy and Bidaud, 2007):

$$W^i = W^g + W^c \tag{2.1}$$

where W^i, W^g and W^c are respectively the inertial, gravitational and contact wrenches.

Any motion trajectory of a biped must obey this principle. **Given that the gravitational force (W^g) is constant and contact forces (W^c) between feet and ground are limited, the movements that can be achieved are also very limited**. Furthermore, the contact forces being constrained by the friction and the unilaterality conditions, this condition of dynamic equilibrium simply refers to a motion which obeys the laws of mechanics and system constraints.

Note that we have not yet introduced the possibility of unknown external disturbing

forces and the possible control actions such as stepping. Before we do that, let's first introduce the famous Zero Moment Point (ZMP) concept.

Zero Moment Point

Zero Moment Point (ZMP) (or more precisely, zero tipping moment point) was first introduced by Vukobratovic and (1969). It is the point on ground where the tipping moment acting on the biped, due to gravity and inertial forces, is equal to zero. The tipping moment is defined as the component of the moment which is tangential to the supporting surface (Sardain and Bessonnet, 2004). For co-planar contacts, this is the same point where the tangential component of the moment of contact forces is zero, also known as CoP.

Due to the unilaterality condition, the ZMP (or CoP) can only reside inside the support polygon (also called the Base of Support (BoS)) defined by the foot/feet on ground. Moreover, if all the contacts between biped and the environment are in the same plane, the question of verifying dynamic equilibrium condition (2.1) boils down to verifying if ZMP is in the BoS or not. This way the ZMP criterion provides a handy tool to test the motion conformity with respect to the laws of mechanics.

2.3.2 Defining Stability for the biped systems

However, the standard definition (2.1) of dynamic equilibrium ($\simeq$ "ZMP in BoS" condition) is not sufficient to completely address the stability issue of bipeds. While it successfully discriminates between physically realizable and non-realizable motion, this description does not answer one critical question related to biped stability i.e. the possibility of fall or not from a given state. Given a state of the biped, it can be considered in **dynamic equilibrium** if it is possible to generate a motion trajectory which does not result in a fall (Wieber, 2008, 2002). In this context, the condition (2.1) is more a constraint (conformity to the laws of mechanics) than a criterion. In fact, during a real fall, the laws of mechanics are perfectly obeyed (Barthelemy and Bidaud, 2007). Moreover, for equilibrium to be considered **stable**, the biped does not have to come back to its initial equilibrium state but can acquire a different equilibrium state (e.g when a step is placed) (Azevedo et al., 2004).

An attempt was made (Goswami, 1999; Popovic et al., 2005) to define the biped instability in terms of Foot Rotation Indicator (FRI) and the Centroidal Moment Pivot (CMP) reference points. As a whole, these stability criteria require a certain constraint to be obeyed (no foot rotation or zero centroidal moment of the biped) for the system to be considered *stable*. The distance of these reference points with respect to the ZMP and/or support polygon is regarded as an indicator of the level of stability/instability. However, later it was argued that none of these arbitrary conditions are necessary nor sufficient for predicting impending fall or not in humans (Pratt et al., 2006; Wieber, 2005).

What is missing in the usual equilibrium description is the consideration of possible recovery actions. A biped, whether human or a robot, is an active system and the question of fall (or not) from a given state primarily depends upon the type of actions that can be taken to stabilize the system. That is to say, what kind of forces can be generated, which strategies can be used etc. In this context, a more relevant way to look Condition (2.1) is the other way round: **Given that the gravitational force is constant, the only way to achieve a desired motion is to somehow be able to change the contact forces**. The three basic recovery strategies (ankle, hip and stepping) described earlier should actually be considered a way to accomplish this task.

This question of fall has been more directly addressed in the field of biomechanics. Pai and Patton (1997) can be rightly credited for evolving a zone of stability in the system's state space from where fall could be avoided using only the ankle strategy (c.f. section 2.2.2). This concept was later simplified by Hof et al. (2005) by solving the dynamics of the inverted pendulum. Though these formulations consider only the actions pertaining to inverted pendulum model i.e. the ankle strategy, it is a step forward in the right direction.

2.3.3 The XCoM point, a step forward towards fall estimation

The model of Hof et al. (2005) employs the well-regarded inverted pendulum analogy, supplemented by a foot (Figure 2.8). The whole mass m of the system is considered concentrated at the CoM while the forces below the foot are represented by a single force acting at the CoP, which is constrained to remain within the foot. Let

l be the length of pendulum,
j the moment of inertia,
α the angular acceleration of the mass,
$\ddot{c}_x$ the linear acceleration of the mass,
p_x and c_x the horizontal co-ordinates of the CoP and CoM respectively,

then the dynamics in the sagittal plane of this system can be approximated as:

$$mg(p_x - c_x) = j\alpha \approx -ml^2\frac{\ddot{c}_x}{l} \tag{2.2}$$

$$\ddot{c}_x = \omega_0^2(c_x - p_x) \tag{2.3}$$

where $\omega_0 = \sqrt{g/l}$ is equivalent to the natural frequency of a hanging pendulum.

The above differential equation can be solved, under the condition that the CoP is constant, giving:

$$c_x(t) = p_x + (c_x(0) - p_x)cosh(\omega_0 t) + \frac{\dot{c}_x(0)}{\omega_0}sinh(\omega_0 t) \tag{2.4}$$

Solving the above equation for $c_x(t) \leq p_x$ results in a simple condition for dynamic stability:

$$\boxed{c_x + \frac{\dot{c}_x}{\omega_0} \leq p_x} \tag{2.5}$$

Since the CoP cannot leave the support polygon (or BoS), Hof's dynamic stability condition for standing balance simply requires the quantity $c_x + \frac{\dot{c}_x}{\omega_0}$ to be within the BoS. This point is called the Extrapolated Center of Mass (XCoM). Hence, a biped is

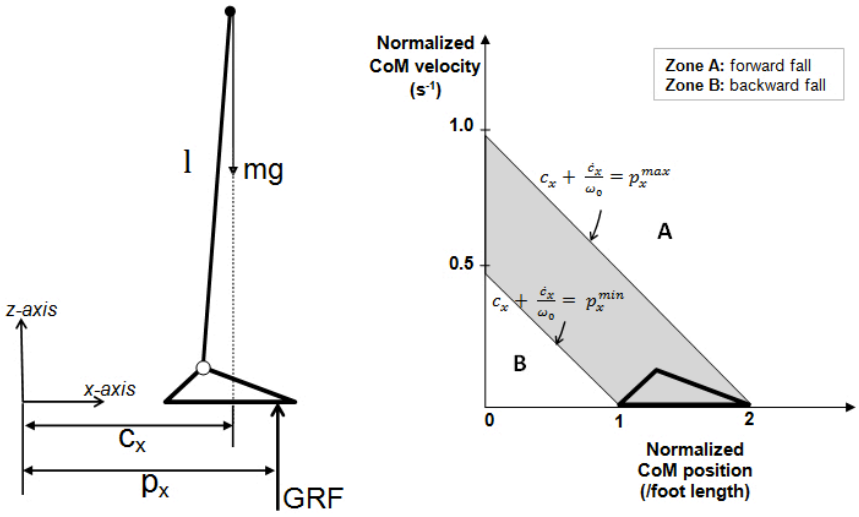

Figure 2.8: Left: The simple Inverted Pendulum (IP) + Foot model assumes point mass concentrated at CoM. The ground reaction force (GRF) acts at the CoP which is constrained to remain within the foot. Right: The limits of the dynamic stability region (grey area) for standing balance. Any state that lies within this region would successfully terminate its motion over the BoS (foot).

in dynamic equilibrium (i.e. will not fall over) if XCoM is within the support polygon ($\simeq$ the state of the system lies in the grey zone in Figure 2.8).

XCoM point is a step forward in the right direction i.e. estimating the possibility of recovery or fall from a given state, using a certain recovery action (ankle strategy). However, one can imagine that if more recovery actions were available (e.g. steps), the stability area in Figure 2.8 would be much larger. This leads us to the more general framework of Viability.

2.3.4 Viability Kernel

The recovery ability or fall estimation is comprehensively described in terms of Viability (Aubin, 1991; Wieber, 2008, 2002). In simple terms, it defines a set of states F where the biped has fallen and a set of states V from where the system is going to fall not matter what action is taken. Hence these two sets of states should be absolutely avoided. The complement of these two sets is then called the Viabil-

ity Kernel assembling a set of states from where a movement will never result in F or V.

The Viability concept is comprehensive enough to define fall or recovery from a given state, but at the same time is too computationally intensive to be implemented numerically as note by Wieber (2002). Given the complex dynamics of a biped system, it is difficult to establish if there exists a way to avoid the undesirable set of states F or V.

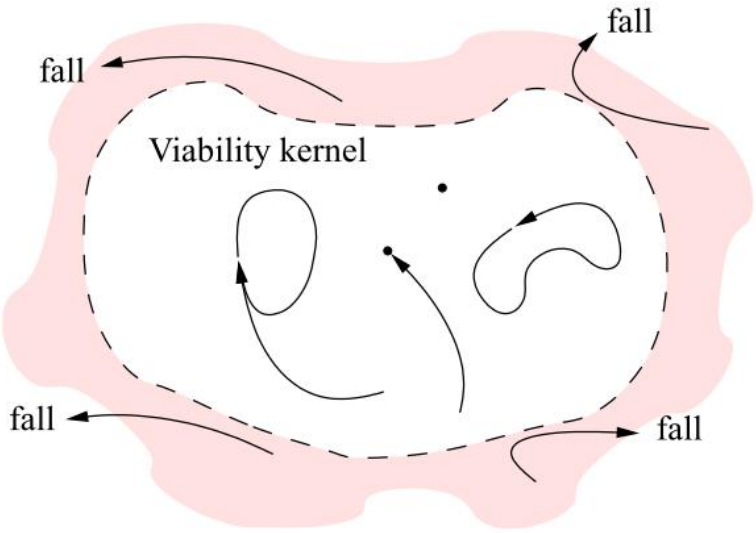

Figure 2.9: The viability kernel gathers all the states from which it is possible to avoid to fall. Leaving it immediately implies an unavoidable fall (Wieber, 2002)

A practical solution

While the calculation of complete viability kernel might be practically infeasible, an intelligent way to generate a stable biped motion is to minimize a derivative of its motion. In fact, it is argued in Wieber (2008) that, while considering a biped equivalent to the well-known cart-table analogy, the objective of avoiding to fall boils down to avoiding cart-table model to diverge to infinity. More specifically, for diverging ($\simeq$ falling) motions, the integrals of the norms of CoM derivatives $\int_{t_k}^{t_k+T} \|c_x^{(n)}\|^2 dt$ will have infinite values and minimizing any of these derivatives would generate stable

motion trajectories, if possible. A practical demonstration of this has been shown where the minimization of CoM jerk (Kajita et al., 2003) or velocity (Herdt et al., 2010a) resulted in stable waking motions.

2.3.5 Concluding remarks

However, above discussion is not intended to deprive ZMP of its importance. In fact, its usefulness lies in the way we exploit it. Though the "ZMP in BoS" criterion cannot ensure the stability (in terms of falling) of a biped, it can discriminate realizable and non-realizable motions and should therefore be considered as a necessary condition in control algorithms.

2.4 Biped control schemes

In view of the above discussion, let us review some common control approaches used for the biped robots' control. Almost all biped walking controllers exploit the ZMP criterion in one way or another. Most controllers based on the ZMP control paradigm rely on the offline trajectory calculations. It amounts to fixing the future feet positions and generating the CoM trajectories such that the ZMP remains within the support polygon throughout the motion. The biped system is then made to follow these predefined trajectories using a control law. Such a setting results in stable walking motions as shown in several works (Hirai et al., 1998; Kagami et al., 2002; Kajita et al., 2003; Lim and Takanishi, 2000; Nishtwaki et al., 1999). Few schemes propose to modify the ongoing motion in case of an external disturbances (Park and Cho, 2000; Wieber and Chevallereau, 2006).

However, the main drawback of the ZMP tracking controllers is that they lead to poor robustness to external disturbances where CoM deviates significantly from the predefined path. In fact, owing to little or no adaptation of the pre-generated ZMP trajectory, the contact forces below the feet cannot be adequately adjusted according to the changing conditions. This parallels our description of the condition (2.1): for a biped to achieve a desired motion (or to change an ongoing motion), the only way is to be able to change the contact forces below feet. Larger the external disturbance,

more substantial the required change in the contact forces.

2.4.1 ZMP as a motion driver and adaptive stepping

Hence the biped motion control is the inverse problem of the usual trajectory tracking algorithms: the ZMP position (which is directly related to the contact forces) should be actively adjusted to drive the CoM dynamics. It is the merit of Pratt et al. (2006) who first used this principle to address the balance recovery issue. They proposed a general velocity-based formulation to calculate a reference point on ground where a biped must step in order to recover balance. The point is called the Capture Point and is the function of the instantaneous state (CoM position and velocity) of the system. The Capture Point is actually the *effective* ZMP position which if maintained would result in static biped posture. Similar points were derived for non-linear pendular dynamics (Wight et al., 2008) while an extension for non-flat ground was proposed by Yun and Goswami (2011).

In another interesting development, Hofmann (2006) analyzed the effect of a forward step on the system's kinetic energy and consequently the on CoM velocity. This idea was later extended by Stephens (2007) to explicitly calculate the recovery step location and timing.

Lastly, one option to deal explicitly with the complex dynamics of the walking systems is with Model Predictive Control (MPC), such as introduced in Wieber (2008). It globally amounts to repeatedly solving online a series of optimal control problems, always taking into account the latest observation of the real state of the system. However, only the formulation from (Herdt et al., 2010a) propose a completely variable stepping positions. The stability of the system is ensured by regulating the CoM velocity (c.f. discussion in Section 2.3.4) whereas the ZMP in BoS constraint is exploited to generate the adaptive stepping positions. We estimate that these schemes can be a good starting point for prediction of human balance recovery responses involving steps.

2.5 Conclusion

The purpose of this chapter was to review the existing knowledge about the issue of disturbed balance and its modeling. An important feature of this kind of balance is the frequent use of stepping responses observed in numerous experimental studies. However, the experimental results are generally limited to a specific study due to contrasting experimental conditions and cannot be used to predict a general recovery response. On the other hand, the existing control models (c.f. Section 2.2) are limited to the standing balance control and do not predict the stepping responses either. In the end, we identified at least a few formulations in the area of biped robots' control which have the capacity to involve an adaptive stepping response based on the perturbed system state. We present these formulations in detail in the next chapter and evaluate their performance with respect to the actual human balance recovery data.

Chapter 3

Balance Recovery by Stepping

Stepping is one of the most efficient and frequent strategy of recovering one's balance from larger disturbances as noted in Chapter 2. The accurate prediction of recovery step locations and timings are hence essential for our balance recovery tool. In this chapter, we evaluate the adaptive stepping schemes previously proposed in the domains of biomechanics and robotics. Our focus will be on their ability to involve the stepping characteristics observed in humans.

Contents

3.1 Presentation of stepping reference points

Let us first recall the dynamic stability condition by Hof et al. (2005) from Chapter 2:

$$c_x + \frac{\dot{c}_x}{\omega_0} \leq p_x \tag{3.1}$$

where p_x defines the Base of Support (BoS), roughly equal to the size of the foot. The condition (3.1) requires the quantity $c_x + \frac{\dot{c}_x}{\omega_0}$ should be within the BoS in order to recover balance without stepping. For point feet, the quantity should be equal to zero.

If this condition is violated, a step must be placed at an appropriate location and timing to recover balance. Prediction of a stepping behavior involves the estimation of at least 2 parameters: Step length and Step duration (or contact time). There are few schemes which estimate one or both of these parameters using simple models of human-body and general physical principles. The usual approach is to calculate a reference point on the ground which, if stepped on, would dissipate the kinetic energy carried by the system and achieve a steady state final posture. In this section, we briefly present these formulations with a unified notation before evaluating their performance in the next section.

3.1.1 Capture Point Algorithm

Pratt et al. (2006) presented a simple velocity based formulation to solve for the required step position (or more precisely the required CoP position) once the equilibrium is disturbed. They used the Linear Inverted Pendulum (LIP) model with point feet to calculate the so-called Capture Point. The Capture Point is indeed the *effective CoP* position that if maintained *instantaneously* would render the CoM velocity to zero just over the CoP. The point is derived as follows:

The x-axis dynamics of the LIP system can simply be written as:

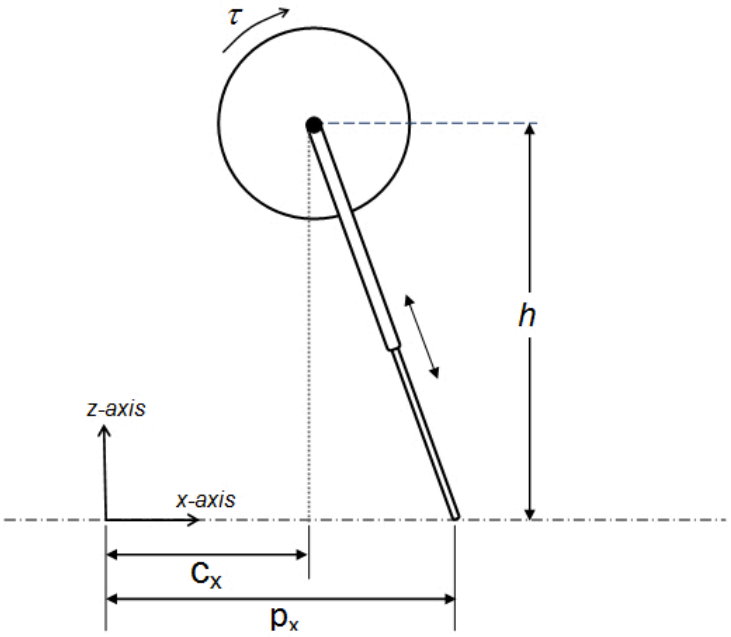

Figure 3.1: The Linear Inverted Pendulum (LIP) + Flywheel model with constant height CoM and telescopic legs

$$\ddot{c}_x = \omega^2(c_x - p_x) \tag{3.2}$$

where $\omega = \sqrt{g/h}$

This dynamic equation can be integrated to calculate a conserved quantity called Orbital Energy (Kajita and Tani, 1991; Kajita et al., 1992) which remains constant till foot impact on ground:

$$E_{LIP} = \frac{1}{2}\dot{c}_x^2 - \frac{g}{2h}(c_x - p_x)^2 \tag{3.3}$$

To calculate the Capture Point (CP), assuming no energy loss due to impact, the Equation (3.3) is put equal to zero resulting in the following expression:

$$\boxed{p_x = x_{capt} = c_x + \frac{\dot{c}_x}{\omega}} \tag{3.4}$$

which is the expression for the Capture Point. It is interesting to note that the Eq. 3.4 leads us essentially to the same condition (3.1) but the other way round. Instead of calculating a set of feasible CoM states by constraining the CoP within the support polygon (Figure 2.8), the Capture Point calculates the *effective CoP* position corresponding to a non-feasible state. Hence the Capture Point x_{capt} can be defined as a point on ground that the robot needs to cover, either with its stance foot or by stepping, and maintain its CoP at x_{capt} in order to end motion with a zero CoM velocity just above the CoP (Pratt et al., 2006). In other words, a biped can be stabilized if its CoP can be instantaneously shifted to x_{capt}.

Other variations of the capture point concept include the Foot Placement Estimator (FPE) of Wight et al. (2008) which uses the non-linear pendular dynamics and the Generalized Foot Placement Estimator (GFPE) (Yun and Goswami, 2011) extended to non-level ground walking. However, there fundamental principle remains the same.

Capture Region

Corresponding to an instantaneous state of the CoM, there exists a unique Capture Point to be be stepped on instantaneously. However, when an inertia wheel is made available to model upper-body inertial effects (Figure 3.1), the capture point expands to a Capture Region whose size depends upon the parameters and the level of inertia wheel usage. The torque profile which gives the most influence on CoM velocity is the Bang-Bang profile which accelerates as hard as possible in one direction and then decelerates similarly to respect the maximum joint angle constraint (Pratt et al., 2006). This results in an additional term in equation 3.4:

$$x_{capt} = c_x + \frac{\dot{c}_x}{\omega} \pm \frac{\tau_{max}}{mg}\left[\frac{e^{\omega T_{R2}} - 2e^{\omega(T_{R2}-T_{R1})} + 1}{e^{\omega T_{R2}}}\right] \tag{3.5}$$

where τ_{max} is the maximum flywheel torque in one direction, T_{R1} and T_{R2} are the acceleration and total times of the flywheel rotation, respectively. The sign of the flywheel term depends upon its direction of rotation (positive for counter-clockwise rotation and vice versa).

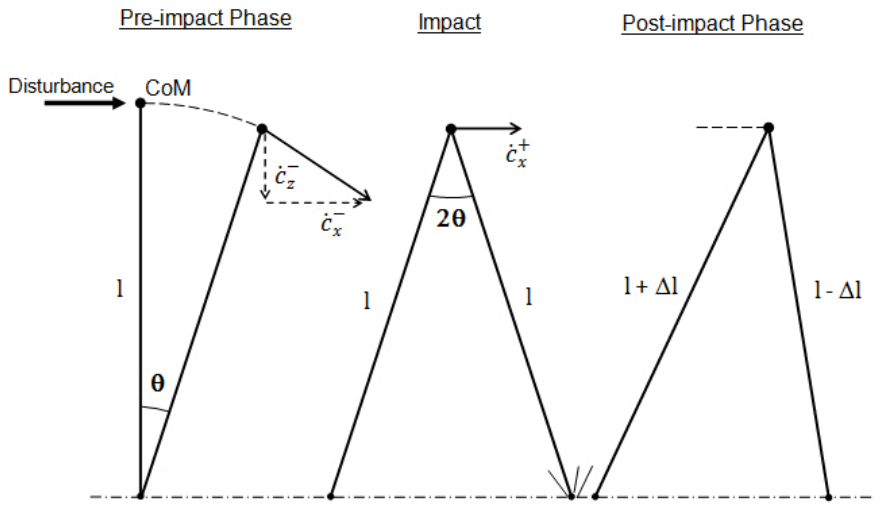

Figure 3.2: The stepping model proposed by Hofmann (2006) and extended by Stephens (2007). The system behaves like a simple inverted pendulum until impact with constant leg length l. After impact, the leg lengths are adjusted to move CoM at a constant height from ground.

3.1.2 Stepping model of Hofmann (2006) with Impact

Hofmann (2006) presented a sagittal plane model to analyze the effect of stepping on balance recovery. The calculations are done in two phases: During the pre-impact phase, the system is modeled using the simple inverted pendulum with fixed legs of length l (Figure 3.2). After the first step placement, the legs act like dampers and maintain a constant CoM height during the whole post-impact phase. The energy is absorbed during the impact and the post-impact double-support phase.

Under these assumptions, the required step length is derived by Stephens (2007) as follows:

Before impact, the horizontal and vertical velocities of the inverted pendulum system in polar coordinates can be written as:

$$\dot{c}_x = -l\ cos\theta\ \dot{\theta}, \qquad \dot{c}_z = -l\ sin\theta\ \dot{\theta} \tag{3.6}$$

At impact, there is a discontinuous change in these velocities given as:

$$\frac{\dot{c}_x^+ - \dot{c}_x^-}{\dot{c}_z^+ - \dot{c}_z^-} = tan\theta \tag{3.7}$$

where $\dot{c}_x^-$ and $\dot{c}_x^+$ are the horizontal CoM velocity just before and after impact respectively while $\dot{c}_z^-$ and $\dot{c}_z^+$ are the corresponding vertical velocities.

After impact, assuming that the vertical velocity of the system vanishes just after impact ($\dot{c}_z^+ = 0$, Figure 3.2), the change in the horizontal velocity can be represented as:

$$\dot{c}_x^+ = \dot{c}_x^- - \dot{c}_z^- \, tan\theta \tag{3.8}$$

In order to achieve system stability with point feet, the post-impact state of the system should obey the dynamic condition (3.1):

$$c_x + \frac{\dot{c}_x^+}{\omega_0} = 0 \tag{3.9}$$

Solving equations 3.8 and 3.9 together, and converting to polar coordinates for ease of calculations using relations (3.6), the following CoM angular position-velocity relationship just before impact is obtained:

$$\boxed{\dot{\theta} = \omega \frac{sin\theta cos^{1/2}\theta}{cos2\theta}} \tag{3.10}$$

where θ is the leg angle just before impact (Figure 3.2). Given the fixed pre-impact leg lengths, the step must be placed at a distance corresponding to the leg angle of 2θ.

To calculate the optimum step length, the perturbed state of the system can be extrapolated in time using the inverted pendulum dynamics till the optimal condition (3.10) is satisfied. This is shown graphically in Figure 3.3 where blue curves represent the extrapolation of pendulum state for different levels of initial perturbations while the black plot represents the optimal stepping condition (3.10). Each intersection

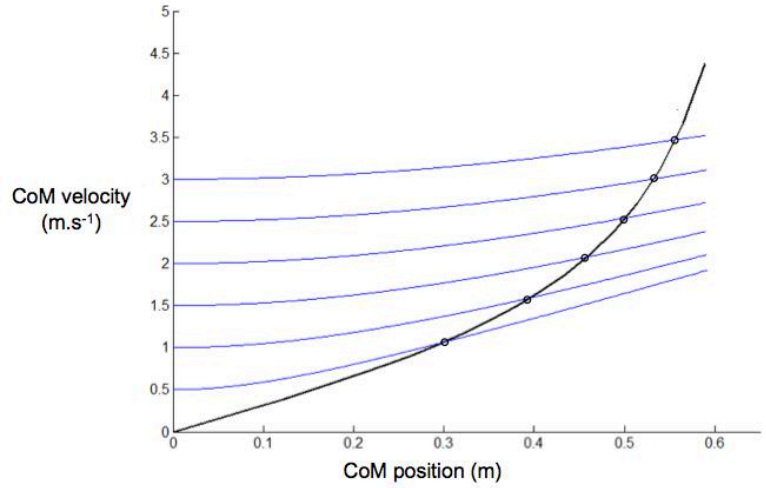

Figure 3.3: The trajectories under inverted pendulum model assumption from different levels of initial disturbance (blue curves) intersect the optimal step curve (black) at optimal step distance shown in Figure 3.4

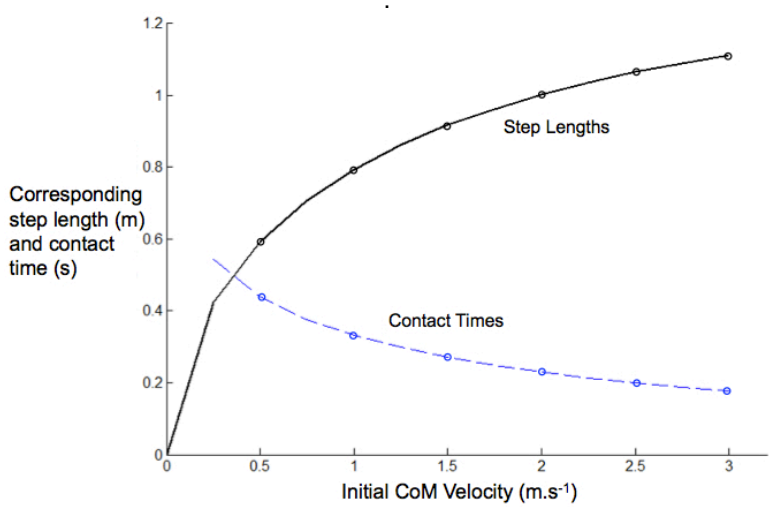

Figure 3.4: The optimum step lengths (black) and corresponding contact times (blue) for varying levels of initial velocity disturbances.

corresponds to a **unique step length-step duration combination**, shown in Figure 3.4, which stabilizes the system after disturbance.

3.1.3 Minimal step length model by Wu et al. (2007)

Wu et al. (2007) employed a non-linear optimization technique to calculate minimal step length for a single-step balance recovery response. Using the simple inverted pendulum + foot model and standard anthropomorphic values, the optimization routine chooses to step, if the ankle torque is not sufficient to restore balance. The resulting normalized step lengths in the CoM phase plane are shown in Figure 3.5. The "Feasible stability zone, F" indicates that the minimal step lengths are equal to zero, indicating that no forward step is needed. This region thus corresponds to the ankle strategy stability zone of Pai and Patton (1997) already presented in Chapter 2 (c.f. Figure 2.5). If the state of the system lies beyond this zone, a step must be placed instantaneously at the corresponding position.

3.1.4 Compliant leg Model of Hsiao and Robinovitch (1999)

An interesting stepping model was put forward by Hsiao and Robinovitch (1999) using an inverted pendulum model supplemented by massless linear and torsional springs in the stepping and stance feet respectively (Figure 3.6). The calculations are however limited to the predictions for lean-forward situations previously described (c.f. section 2.1). The model relates the body inclination with respect to vertical θ_c just before impact as a function of the initial inclination θ_0 and the foot contact time t_{cont} as follows:

$$\theta_c = \theta_0 cosh(\sqrt{\frac{3g}{2l} - \frac{3k_a}{ml^2}} t_{cont}) \tag{3.11}$$

Owing to the compliance in the stepping leg, it can be placed non-symmetrically with respect to the stance leg angle, also θ_c. However, the optimal step length is chosen on the basis of peak leg force F_{max} minimization which is achieved for step length corresponding to the leg angle, $\alpha = 2\theta_c$, for any value of input foot contact time t_{cont}.

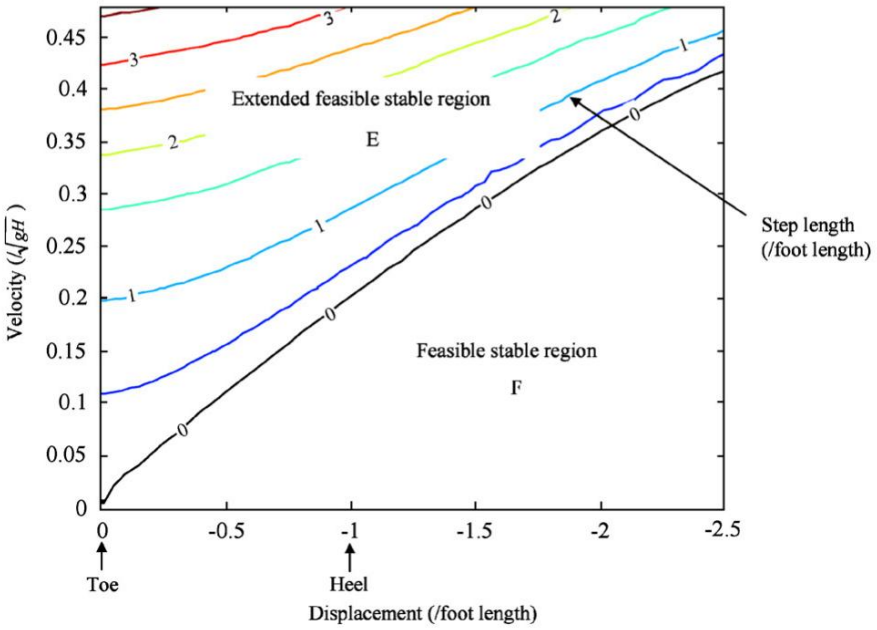

Figure 3.5: Minimal step length (normalized with the length of foot) needed for balance recovery of various initial displacements (normalized by the length of foot) and velocities (normalized by the $\sqrt{gH}$, where H is height of body and g is the acceleration due to gravity) of COM by (Wu et al., 2007)

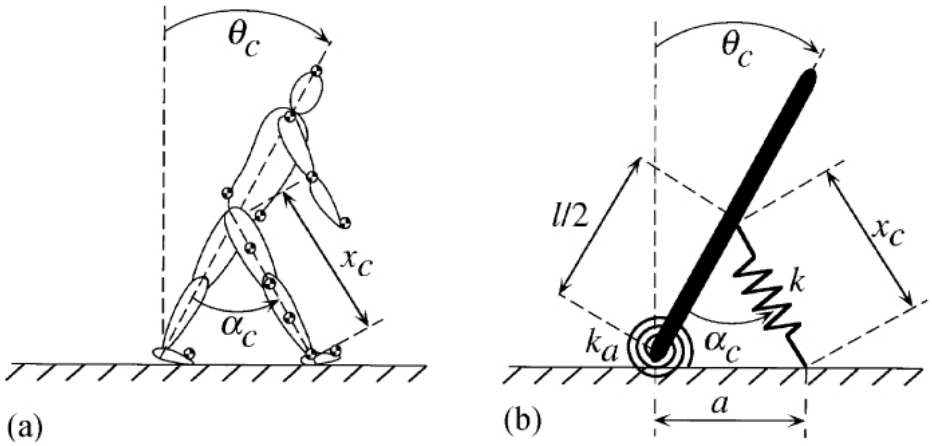

Figure 3.6: The stepping model of Hsiao and Robinovitch (1999) with torsional and linear springs in stance and stepping feet respectively

This model is unique in the sense that it chooses the step length based on a biomechanical criterion (peak leg force minimization) rather than on the system dynamics like the Capture point. However, the choice of the criterion is not completely validated with respect to experimental data.

3.2 Evaluation of stepping reference points

The stepping reference points presented in this section are a good starting point for the prediction of a human balance recovery response. They are based on simple criteria (e.g. dissipation of kinetic energy) and result in easy-to-implement algorithms. Let us now analyze these schemes in relation to the common features of a human recovery response presented in the Chapter 2.

Step delay

As we know from the experimental studies, there is a non-negligible delay between the stepping decision and its placement. This delay is composed of the step preparation time (during which the body weight is transferred to the non-stepping limb) and the legswing time. During this delay, the system continues to fall in the direction of the disturbance. Moreover, the legswing time is independently regulated in such a way that the step results in an effective balance recovery. However, these features are missing in all of the stepping reference schemes presented above.

Since the Capture Point/ region depends upon the instantaneous state of the system, the CoP must be maintained at the required point *instantaneously*. This is generally not possible if the Capture Point is located outside the stance foot and a step is required. Hence during the delay between step take-off and landing, the point would move away to a new location. Same is true for the model by Wu et al. (2007). Hence, for an accurate prediction and successful recovery, the **step duration** and the **system state at the time of impact** should be known.

This issue was addressed by Hofmann (2006) by modeling the pre-impact phase (c.f. Figure 3.2) and imposing a symmetrical stepping response. However, in the author's view, this constraint is not biologically realistic, as non-symmetrical stepping is common in human balance recovery responses (see for example, Hsiao and Robinovitch (1999), experimental results). An alternate solution is to impose a contact time and use one of the following 2 approaches:

(i) The instantaneous Capture Point can be calculated at regular sample periods and be used as a tracking reference over the course of the motion (Wight et al., 2008). In this case, one can imagine the continuous shift of the capture point in the direction of the motion and the leg trajectory has to be changed accordingly at each sample period till foot impact on ground.

(ii) or the position of the Capture Point at the time of impact can be estimated using the so-called capture point dynamics (Englsberger et al., 2011; Koolen et al., 2012). While this approach results in a quasi-static Capture Point, the choice of the model during the step time becomes a critical factor, especially in the context of human balance recovery prediction (Aftab et al., 2010).

Multiple strategies

Human employ multiple recovery strategies in parallel. For example, when a step is being executed to recover from a larger disturbance, the ankle strategy is active during this delay by maintaining the CoP at the border of the stance foot. This provide limited yet non-negligible braking effect on the accelerating CoM. Same is true for the hip strategy. On the other hand, none of the above schemes provide such a behavior. All schemes consider point feet, except Wu et al. (2007). Only Pratt et al. (2006) modeled the upper-body inertial effects using the inertia wheel model. However, only the maximum possible effect of its rotation was analyzed in terms of the size of the Capture Region.

Multiple steps

Multiple recovery steps are common in humans particularly for larger disturbances and for the elderly. One obvious reason for choosing a multiple step strategy is the actuation and geometric constraints which limit the length. However, this choice is also driven by task constraints and the subjects' desire to recover more comfortably (Robert, 2006, unpublished research). On the other hand, a common limitation of all of the above schemes is the consideration of single-step recoveries. At the best, multiple steps are considered only if the system is still unstable after having placed the previous step at the maximum length (Koolen et al., 2012).

Consideration of multiple criteria

Human's movement strategies are often based on multiple criteria such as minimum effort cost and/or metabolic energy demonstrated in several studies (e.g. Anderson and Pandy, 2001; Leboeuf et al., 2006). Hence, it is reasonable to assume that this is likely the case in human balance recovery tasks as well. However, most of the schemes calculate the step location based on a single criterion, that is, bringing kinetic energy of the system to zero in the most efficient way. While this might be the best strategy to avoid a fall, modeling a *human* behavior may require consideration of other criteria depending upon the task requirements.

To understand this, let us compare the stepping predictions from the Capture Point with actual human balance recovery data in two different balance recovery tasks.

3.3 Capture Point estimation for Human balance recovery

Capture Point is an easily-to-implement algorithm and can be directly calculated from the instantaneous CoM state. In this section, we calculate the Capture Point from the actual human balance recovery data and observe how the human subjects place their

recovery step in relation to the computed Capture Point to recover balance.

We use the balance recovery data acquired by subjecting young healthy volunteers to platform translations (Robert, 2006). The acceleration profile of the platform is shown in the Figure 3.7. Eight volunteers participated in a 1^{st} series of experiments where a large space was provided for the subjects in front of them to take several steps. Among them, four participated in a 2^{nd} series, where the space was limited to about 80 cm (the average stepping distance observed in the 1^{st} series). Ground reaction force and kinematics were recorded, body segments' inertial parameters were estimated using regression tables and the experimental whole body center of mass (CoM) position and velocity were computed.

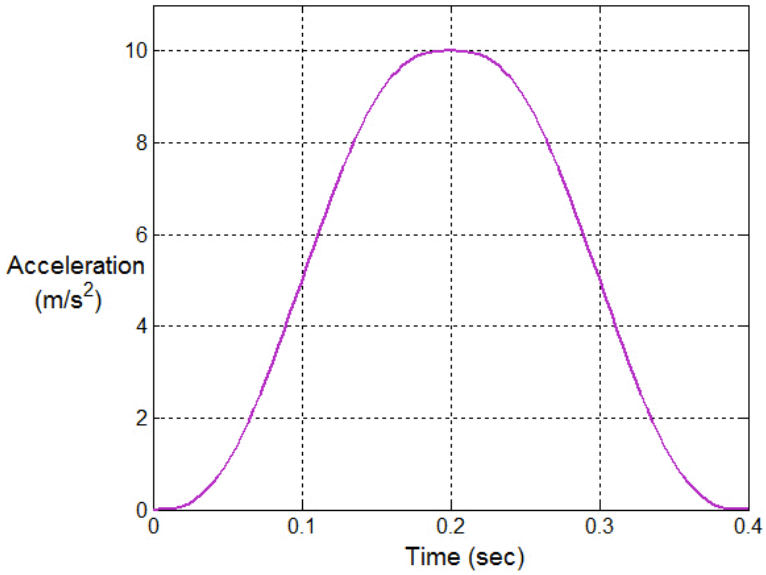

Figure 3.7: The platform disturbance profile

3.3.1 Comparison with the Capture Point

Subject-specific CoM data from the experiments is used to calculate the Capture Point using Eq. 3.4 at each instant after the disturbance onset till step placement. This way the contact time and the system's state at impact are directly available from the experimental data. The capture region is calculated using Eq. 3.5 for $\tau_{max} = 190N.m$ and maximum hip angle of 90° from vertical (Chaffin and Andersson, 1984) in both

directions. The inertial properties are estimated from regressions based on subject's anthropometry (Dumas et al., 2007). After the onset of disturbance, the evolution of the subjects' CoM state and the corresponding capture point/region in the direction of the motion is observed. When the first step is placed, the distance between the toe of the foot and the capture point (and capture region) are calculated.

3.3.2 Results

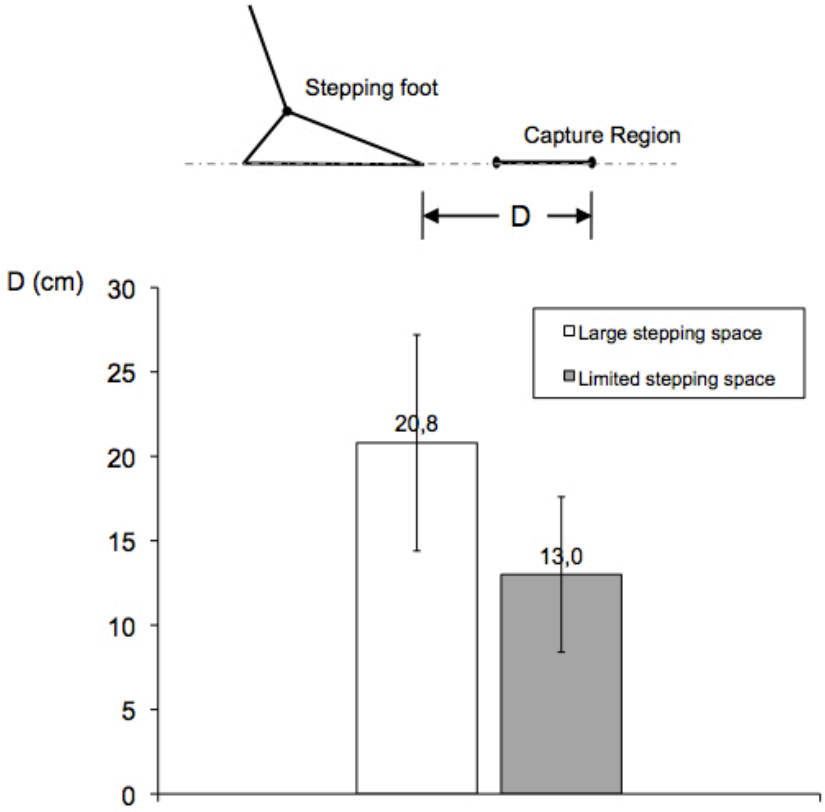

Figure 3.8: The distance D between the stepping foot and the capture point at impact. 1^{st} series subjects who stepped farther from the capture point (white bar) took several steps to recover balance.

For the subjects in the 1^{st} series, where a large space was provided, the gap between the actual foot placement and the capture point at impact is large $(20.8 \pm 6.4\ cm)$. These subjects were observed to take several (on average 3) steps to recover their

balance. However, when the same disturbance is applied with limited recovery space in the 2^{nd} series, subjects stepped relatively closer to the capture point (gap of $13 \pm 4.6\ cm$ at impact) (Figure 3.8). One subject intersected the base of support with the capture region (but not the capture point) and recovered absolutely in one step (Figure 3.9). Subjects who stepped close to the capture region (within 5cm), but not exactly on it, had to take another small step to retain balance (see Figure 3.10).

3.3.3 Discussion

These results give us a nice insight into the relation between the Capture Point location and human balance recovery. To start with, the capture point seems to be a valid reference point for recovery in a single step, provided the CoM velocity at the instant of step impact is known. This is somewhat in accordance with an earlier finding (Arampatzis et al., 2008), showing similar results in terms of the Extrapolated CoM (XCoM) concept (c.f. Chapter 2). But the most striking discovery of our comparison is that if the subjects are not bound to recover in one step (as in the 1^{st} series), they step far from the capture point/region and take several steps to recover. This points towards the existence of some other criteria during stepping decisions than just quickly minimizing the CoM velocity.

Moreover, the fact that one subject recovered balance in a single step by stepping on the capture region, and not on the capture point (see Figure 3.9), underlines the importance of upper-body inertia in the balance recovery process. However, the capture point algorithm only considers the maximum possible effect of this strategy in terms of the size of the capture region. Regulation of this strategy more systematically as a function of disturbance or situation would require a more comprehensive control scheme.

In short, the Capture Point (and other similar reference points) can be good mechanical references in situations where single step recoveries are emphasized and impact system state is available (known or model-based). However, their application to a more general balance recovery prediction tool, which includes multiple steps and upper-body

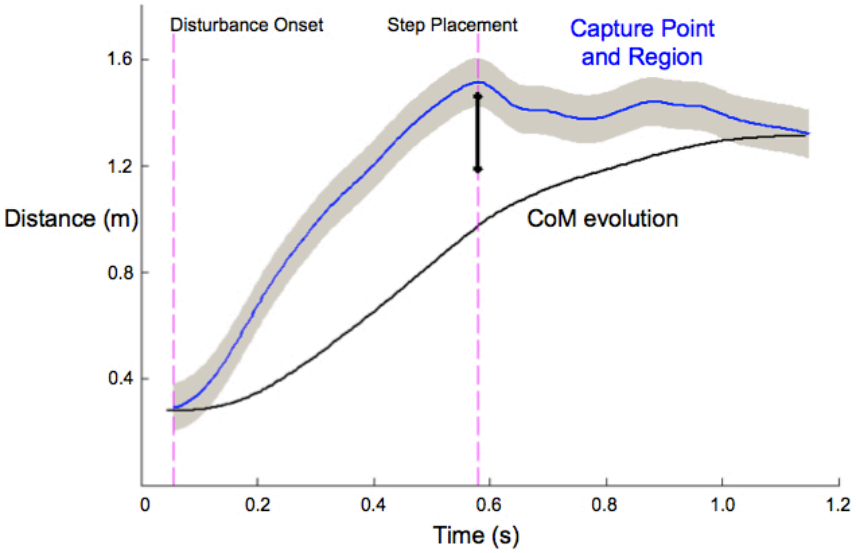

Figure 3.9: The evolution of the CoM (black) and Capture Point (blue) in time for one subject who stepped very close to the capture point, and on the capture region, and recovered balance in exactly one step. The grey area represents the capture region calculated using flywheel rotation with anthropomorphic parameters in both directions.

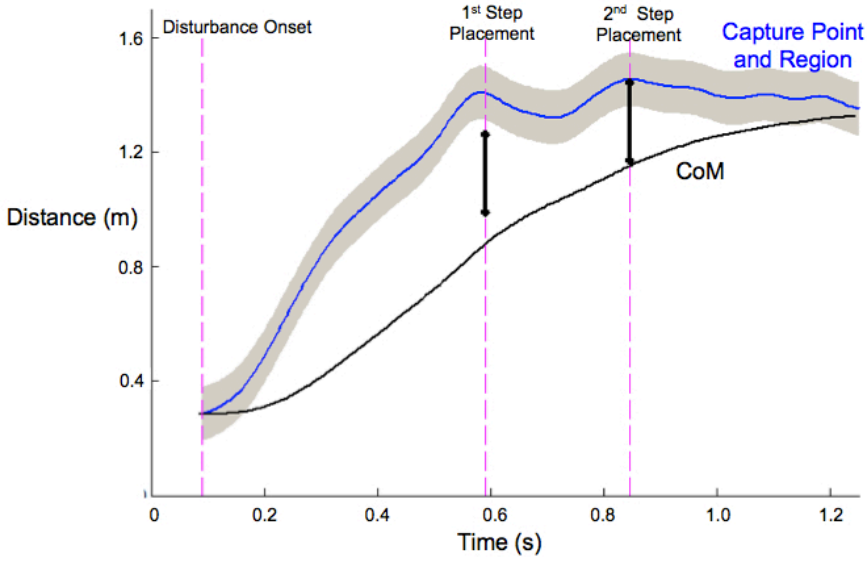

Figure 3.10: Example of a subject who did not step on the capture point / region in the first step and took a smaller second step to recover balance.

inertia regulation, is quite limited. We therefore turn our attention to a more comprehensive control approach called the Model Predictive Control. We will show in the coming sections that this approach naturally eliminates most of the limitations of the capture point and similar algorithms.

3.4 Model Predictive Control

Model Predictive Control (MPC) is a control technique which amounts to repeatedly solving online a series of Optimal Control problems, always taking into account the latest observation of the real state of the system. It usually takes the form of minimizing at every time t_k a cost function $\mathcal{L}$, considering a prediction of the dynamics of the system over a time horizon of length T :

$$\min \int_{t_k}^{t_k+T} \mathcal{L}(q(t), \dot{q}(t), \ddot{q}(t), u(t), \lambda(t))dt \tag{3.12}$$

The control $u(t)$ that results from this optimization is applied to the system until the next observation time t_{k+1} and the process is repeated.

Among the traditional advantages of this scheme is its flexibility in formulating the control objectives and its capacity to explicitly take into account the constraints of the dynamical systems (Wieber, 2008). In view of our objectives and following the discussion in the previous section, a major advantage of this approach is the calculation over a future time horizon which allows the consideration of multiple steps. Moreover, it has the capacity to consider a multi-objective cost function which again goes well with our earlier observation that a human stepping decisions might not be solely based on a single criterion. Last but not least, the dynamics of the system can be taken into account all along the process.

3.4.1 Biped MPC schemes

Several MPC schemes have been proposed for the locomotion of bipeds under disturbances (Azevedo et al., 2002; Diedam et al., 2008; Nishiwaki et al., 2002; Stephens

and Atkeson, 2010; Wieber, 2006). But all these schemes require pre-defined reference step positions, which are either fixed or are only slightly modified (e.g. Diedam et al. (2008)). Only recently, Herdt et al. (2010a) proposed a biped control scheme where future step locations are left completely free while stable motions are achieved mainly by regulating the CoM velocity to a reference value. This scheme is interesting in more than one way. It controls the CoM velocity of the system by means of 2 separate strategies, namely the ankle and the stepping. Moreover, thanks to a multi-objective cost function, the stepping decisions are also affected by other criteria (such as minimization of the jerk of CoM). Even though the scheme neglects the upper-body inertial effects at this stage, we see a strong incentive towards building our controller on the MPC formulation due to the advantages mentioned above. We briefly present this scheme here before evaluating its performance in the prediction of human balance recovery tasks in Section 3.5.

3.4.2 MPC controller with Variable Stepping

The schemes presented in Herdt et al. (2010a) and Herdt et al. (2010b) actually work on the principle of anticipating future motions on a prediction horizon initially proposed by Kajita et al. (2003). The horizon is composed of N time intervals of equal length T on which the motion is considered having a piecewise constant third derivative $\dddot{c}$ over each time interval. Considering the state

$$\hat{c}_k = \begin{bmatrix} c_k \\ \dot{c}_k \\ \ddot{c}_k \end{bmatrix}, \tag{3.13}$$

of the system at a time t_k, all it takes is a straightforward time integration to relate the position, speed and acceleration of the CoM over the whole prediction horizon

$$C_{k+1} = \begin{bmatrix} c_{k+1} \\ \vdots \\ c_{k+N} \end{bmatrix}, \dot{C}_{k+1} = \begin{bmatrix} \dot{c}_{k+1} \\ \vdots \\ \dot{c}_{k+N} \end{bmatrix}, \ddot{C}_{k+1} = \begin{bmatrix} \ddot{c}_{k+1} \\ \vdots \\ \ddot{c}_{k+N} \end{bmatrix} \tag{3.14}$$

to the piecewise constant third derivative

$$\dddot{C}_{k+1} = \begin{bmatrix} \dddot{c}_{k+1} \\ \vdots \\ \dddot{c}_{k+N} \end{bmatrix} \tag{3.15}$$

through simple matrices:

$$C_{k+1} = S_p \hat{c}_k + U_p \dddot{C}_k, \tag{3.16}$$

$$\dot{C}_{k+1} = S_v \hat{c}_k + U_v \dddot{C}_k, \tag{3.17}$$

$$\ddot{C}_{k+1} = S_a \hat{c}_k + U_a \dddot{C}_k. \tag{3.18}$$

Detailed formulas for these matrices can be found in Herdt et al. (2010a).

The x-axis motion of the CoP is approximated by the Linear Inverted Pendulum (LIP) model (c.f. Figure 3.1, without flywheel), which relates the position of the CoP to the motion of the CoM as:

$$z_x = c_x - \frac{h}{g} \ddot{c}_x \tag{3.19}$$

(Note the change of notation for CoP from p_x to z_x).

As before, we can easily relate the position of the CoP over the whole prediction horizon

$$Z_{k+1} = \begin{bmatrix} z_{k+1} \\ \vdots \\ z_{k+N} \end{bmatrix} \tag{3.20}$$

to the piecewise constant third derivative $\dddot{C}_k$ through simple matrices:

$$Z_{k+1} = S_z \hat{c}_k \ + U_z \dddot{C}_k, \tag{3.21}$$

with

$$S_z = S_p - \frac{h}{g} S_a, \tag{3.22}$$

$$U_z = U_p - \frac{h}{g} U_a. \tag{3.23}$$

Constraints and Controller Design

The dynamics (3.19) of human and humanoid balance is subject to kinematic and dynamic constraints. A highlight of MPC is its ability to explicitly take into account these constraints over the whole prediction horizon. This scheme introduces 2 explicit constraints. First, in order to ensure that the predicted foot placement(s) are within reachable limits in a given time, the horizontal velocity of the swing foot is bounded. If f_i' represents the horizontal position of the swing foot above the ground, this constraint can simply be represented as:

$$\|\dot{f}_i'\| \leq \dot{f}'_{max}. \tag{3.24}$$

Secondly, the CoP z_x is also constrained to stay within the boundaries of the support polygon, what can be expressed in the following way:

$$D(z_i - f_i) \leq b, \tag{3.25}$$

where D and b are a matrix and a vector encoding the shape of the foot with respect to the position f_i of the support foot on the ground (more details can be found in Herdt et al. (2010b)).

The controller is designed to regulate the biped's CoM speed $\dot{C}_{k+1}$ to a reference value $\dot{C}_{k+1}^{ref}$ over the prediction horizon while taking care of all the constraints listed earlier. However, weakly-weighted minimizations of the third derivatives $\dddot{C}_k$ of the motion and of the distance between the position Z_{k+1} of the CoP and the center F_{k+1} of the support foot are also introduced. The resulting multi-objective cost function is then :

$$\min \quad \frac{1}{c_1^2}\|\dot{C}_{k+1} - \dot{C}_{k+1}^{ref}\|^2 + \frac{1}{c_2^2}\|\dddot{C}_k\|^2 + \frac{1}{c_3^2}\|Z_{k+1} - F_{k+1}\|^2, \quad (3.26)$$

where c_1 , c_2 and c_3 are relative weight coefficients, while the control variables are represented as $u = \begin{bmatrix} \dddot{C}_k \\ \bar{F}_{k+1} \end{bmatrix}$, where the third derivative $\dddot{C}_k$ of the motion ends up controlling the CoP through Eq. (3.21) and $\bar{F}_{k+1}$ are the future feet positions. The number of steps previewed depend upon the length of the horizon and the step times fixed in advance.

3.5 MPC estimations for Experimental Situations

In this section, we adapt the MPC scheme presented above to predict the step location for real experimental situations. We start by modeling a simple balance recovery scenario for the famous tether-release situation (Figure 3.11) where the fall is uniquely driven under the gravitational force. Among numerous experimental studies which use this mechanism (c.f. section 2.1.1), we choose the following two studies which provide sufficient details about the perturbation, time delays and the resulting recovery steps:

1. the study from Hsiao-Wecksler and Robinovitch (2007) reports the maximum inclination angles for single-step recovery given a specific step length. Young subjects were inclined forward and asked to recover balance after release by taking a single step, no larger than a given target length. The maximum lean angle for four target lengths, averaged across subjects, were input to our model. The predicted step lengths are compared to the target lengths. For clarity in final results, step lengths expressed in % of body height are transformed into meters, based on the average body height of the subjects.

2. the study from Cyr and Smeesters (2009a) is to our knowledge the only study about the threshold of multiple steps balance recovery in which kinematics and timing of all recovery steps are reported. In this case, the subjects were asked to recover balance without any restriction on the maximum number of steps. The

lean angle was gradually increased until the subject failed to recover balance. For comparison, the reported average maximum lean angle value of 30.7 deg is used as the input to our simulation.

3.5.1 Mechanical and Internal Models

The mechanical model used for the prediction in the MPC scheme does not need to be the same as simulated mechanical model. This can help obtain more complex behaviors. We propose here to use two different human body models: One is the *mechanical* model which is used to represent the actual human body behavior. At this stage, the mechanical model is kept as simple as possible while still representing a correct overall kinematics for the tether-release scenario. This *mechanical* model is a sagittal plane inverted-pendulum-plus-foot model representing the support limb (see Figure 3.11). The trailing limb is not explicitly modeled and its influence on the system dynamics is neglected. The length of the pendulum is constant for each step but can change from one step to another. The resulting trajectories of the Center of Mass (CoM) are thus circles of possibly different diameters representing stride-to-stride knee flexion observed in these kinds of disturbances. However, this model can only experience instantaneous double support phases.

Other is the *prediction* or *internal* model used by the controller for predicting future control actions over a given time horizon. This is the classical Linear Inverted Pendulum (LIP) model which considers the CoM moving at a constant height. This model is chosen due its linear dynamics resulting in faster and more stable computations through Quadratic Programming algorithms.

3.5.2 Cost Function

For balance recovery scenarios, the cost function (3.26) is exploited by setting $\dot{C}^{ref}_{k+1} = 0$ i.e. the subjects try to be in a steady state posture. Future actions are predicted over a time horizon of duration $T_{horizon} = 1$ second, over which the constraints on the CoP with respect to the positions of the feet on the ground are checked every $T_{sampling} = 25$ ms. Incidentally, double support phases are assumed to coincide with such sampling intervals, and last therefore a mere 25 ms, staying close to the instantaneous double

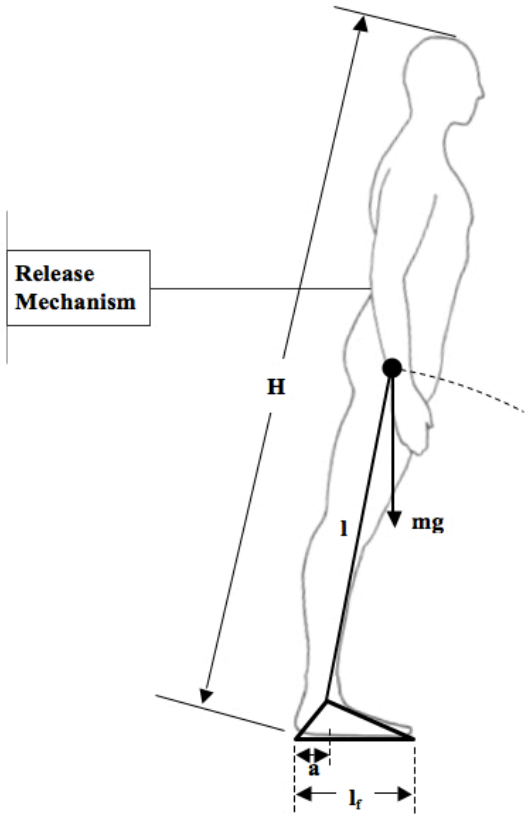

Figure 3.11: The representation of the human body used for the so-called *mechanical* model. It consists of a simple inverted pendulum + foot model, where the CoM follows a circular arc around the ankle joint.

support phases of the *mechanical* model. The total number m of steps considered within the time horizon is determined by these different timings of foot contacts.

3.5.3 Step Timings

In all the biped MPC schemes presented so far, the timing of the foot contacts (take-off and landing) has to be fixed in advance to conserve the linear nature of the algorithm. In context of the human balance recovery, the foot contact time is divided into (c.f. section 2.1.2) :

-- a reaction time, T_{reac}, between the onset of the perturbation and the beginning of the reaction (activation of the controller),

-- an additional delay, the step preparation time T_{prep}, considered before the initiation of the first step,

-- the durations of the further steps (delay between contra lateral feet landings) defined by the values of T_{step}.

For meaningful comparison between the step prediction of the MPC scheme and the experimental results at this stage, we use the same time values in our simulation as reported in the experimental study.

3.5.4 Selection of the Model Parameters

The model parameters can be broadly divided into 2 groups. The first group of parameters describes the experimental scenario considered. Values used for each simulated scenario are reported in Table 3.2. The subjects' stature are used to adjust the dimensions of the mechanical model (see Table 4.1 from (Winter, 1990)). The step timing are fixed based on the experimental values reported and rounded-off to the nearest multiple of the 25 ms sampling period. While Cyr and Smeesters (2009a) reported all values, Hsiao-Wecksler and Robinovitch (2007) only reported the first step landing time $T_{land} = T_{reac} + T_{prep} + T_{step}$. However, earlier reports suggested that T_{reac} and T_{prep} can be considered constant for these types of perturbations (Do et al., 1982; King et al., 2005). They are thus fixed respectively to 75 ms and 150 ms and T_{step} is defined as the difference between the reported T_{land} and the sum $T_{reac} + T_{prep}$.

Table 3.1: Anthropomorphic proportions used in the simulation (see also Figure 3.11).

Variable	Scaling
Body Height	H
Initial pendulum length, l	0.575 $\times$ H
Foot length, l_f	0.152 $\times$ H
Horizontal ankle-to-heel distance, a	0.19$\times$ l_f
Ankle height	0.039 $\times$ H

The remaining parameters are related to the controller and do not depend on the scenario. They are reported in Table 3.3. The maximal velocity of the swinging foot is

Table 3.2: Simulation parameters used as input for the five simulated scenarios: lean angles (θ), body height (H) reaction times (T_{reac}), step preparation times (T_{prep}) and leg swing times (T_{step}).

	H (m)	θ (deg)	T_{reac} (ms)	T_{prep}(ms)	T_{step} (ms)
Hsiao-Wecksler	1.63	12.5	75	150	100
et al. (2007)	1.63	17.5	75	150	125
	1.63	21.6	75	150	150
	1.63	27.5	75	150	225
Cyr et al. (2009)	1.73	30.7	75	150	175, 400, 275

set to 6 $m.s^{-1}$, i.e. slightly faster than during normal gait (Winter, 1992). The time horizon (1s) is chosen such that important events related to balance recovery, such as stepping, could arise during it. The simulation time (2s) is chosen large enough to allow complete convergence of CoM velocity to zero. In this first approach we consider an almost continuous control, i.e. the controller is called every sampling time (every 25 ms). The weight coefficients c_1 - c_3 are chosen such that minimization of CoM velocity remains the major balance recovery criterion, as the purpose of CoM jerk minimization and CoP centering in the foot just help obtain smooth contact forces and a comfortable final posture as noted in Herdt et al. (2010a). Hence, for $c_1 = 1\ m.s^{-1}$, c_2 and c_3 are set equal to 100 each.

Table 3.3: The controller parameters related to cost function and constraints

Parameter	Value
No of samples, N	40
Sampling Time, T	25 ms
Horizon length, N$\times$T	1 sec
Simulation Time	2 sec
Weight coefficient, c_1	1 m.s^{-1}
Weight coefficient, c_2	100 m.s^{-3}
Weight coefficient, c_2	100 m
Foot length, l_f	c.f. Table 4.1
Max foot velocity, v_{max}	6 m.s^{-1}

3.5.5 Implementation of the feedback loop

Consequently, the determination of the optimal foot placements and CoM trajectory boils down to minimizing a quadratic cost function under linear constraints, i.e. to solve a Quadratic Program (QP). Details can be found in Herdt et al. (2010a). Once this optimal control strategy has been determined, it is applied to the *mechanical* model of the human body during a whole sampling period $T_{sampling}$, after which the state of the system (altitude and horizontal position, velocity and acceleration of the CoM) is measured again and the whole MPC is recomputed on a new time horizon shifted accordingly (Figure 3.12).

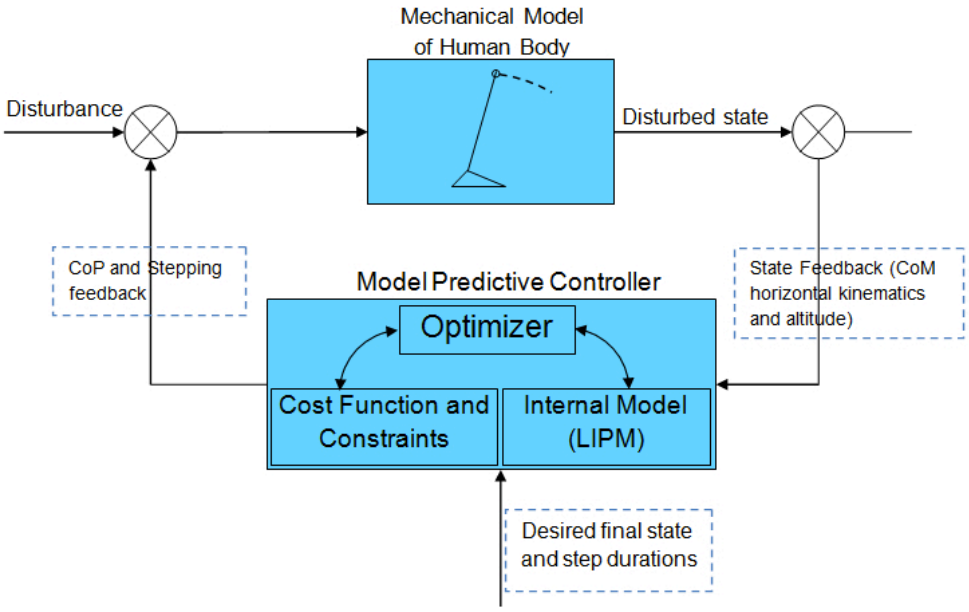

Figure 3.12: The feedback loop implemented to simulate the tether-release condition using the MPC controller

3.5.6 Results

Comparison between the experimental and simulated results are displayed in Figures 3.13 and 3.14. White plots show the experimental results (average $\pm$ s.d.) while the black plots represent the corresponding model predictions.

Figure 3.13 shows the results for the 4 inclination cases considered by Hsiao-Wecksler and Robinovitch (2007). It can be perceived that simulated and experimental step lengths match well, in particular for the smaller inclination angles.

Figure 3.14 shows the results for the extreme inclination case of Cyr and Smeesters (2009a) with no limit on number of steps. Stride lengths instead of step lengths are reported to be coherent with this study. Predicted and reported stride length are of the same order. Note that the third step, reported by Cyr and Smeesters (2009a) but not predicted by the model, was only observed for two out of 28 subjects.

Figure 3.15 shows the evolution of the *mechanical* model during the predicted recovery for the scenario of Cyr and Smeesters (2009). It can be seen that the CoM trajectory follows circular arcs of varying lengths.

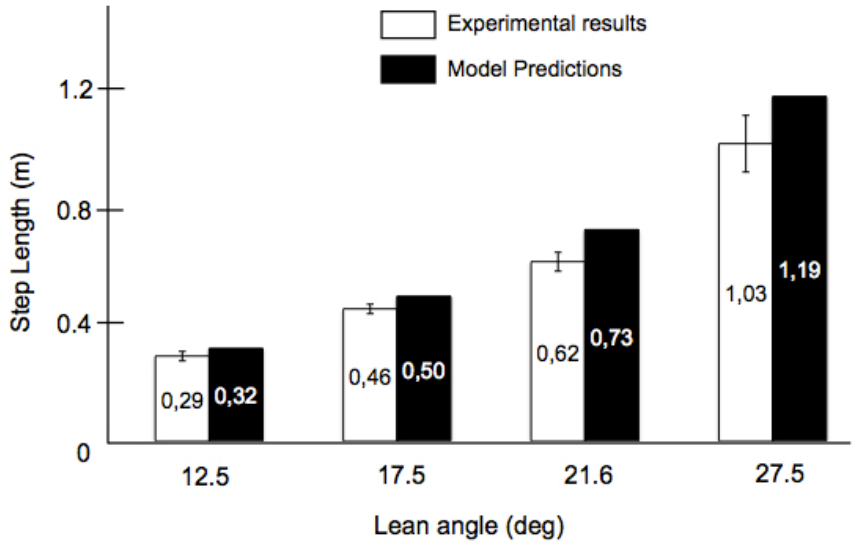

Figure 3.13: Step lengths for single step recovery scenarios from Hsiao-Wecksler and Robinovitch (2007): experimental (white bars, averaged across subjects $\pm$ one standard deviation) versus simulated (black bars) results.

3.5.7 Discussion

The comparison of predicted and reported results suggest that the model predictive control scheme (3.26) can predict the single as well as multiple step lengths with reasonable accuracy. However, the predicted step lengths are slightly larger than the

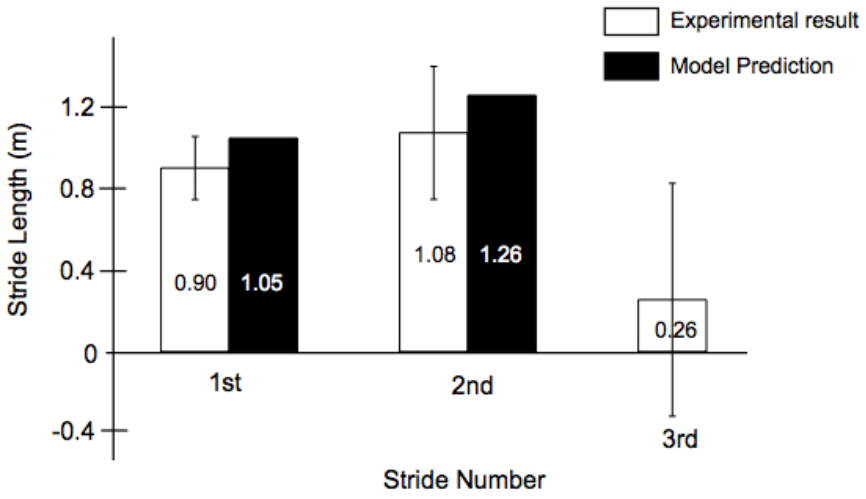

Figure 3.14: Stride length for multiple step recovery scenario from Cyr and Smeesters (2009a). Experimental (white bars, averaged across subjects $\pm$ one standard deviation) versus simulated (black bars) results.

experimental values in all cases. A closer look reveals that these differences scaled roughly with the inclination level. This could be attributed to the simplification of the human body model used, and in particular to the fact that rotations of the upper body are not considered in the current model. Indeed, it is known that upper body inertia plays a role in the balance recovery (e.g. Horak and Nashner, 1986; McIlroy and Maki, 1994; van der Burg et al., 2007), and can be used to limit the recovery step length. Moreover, Park et al. (2004) showed that upper body rotations scale positively with the level of perturbation. Taken together, these results tend to support our hypothesis: neglecting upper body rotations in the prediction model leads to over-estimate the recovery step length, and this bias increases with the perturbation level.

A further limitation of this scheme is the pre-allocation of the contact times. For the purpose of comparison in this section, we chose these timings to correspond to the reported experimental values. Even though the reaction and step preparation times could be considered almost constant for a given disturbance type, and sometimes disturbance level, the time of the legswing is an important variable and should be optimally adjusted according to the perturbation.

Despite these limitations, the real strength of this approach lies in its ability to predict

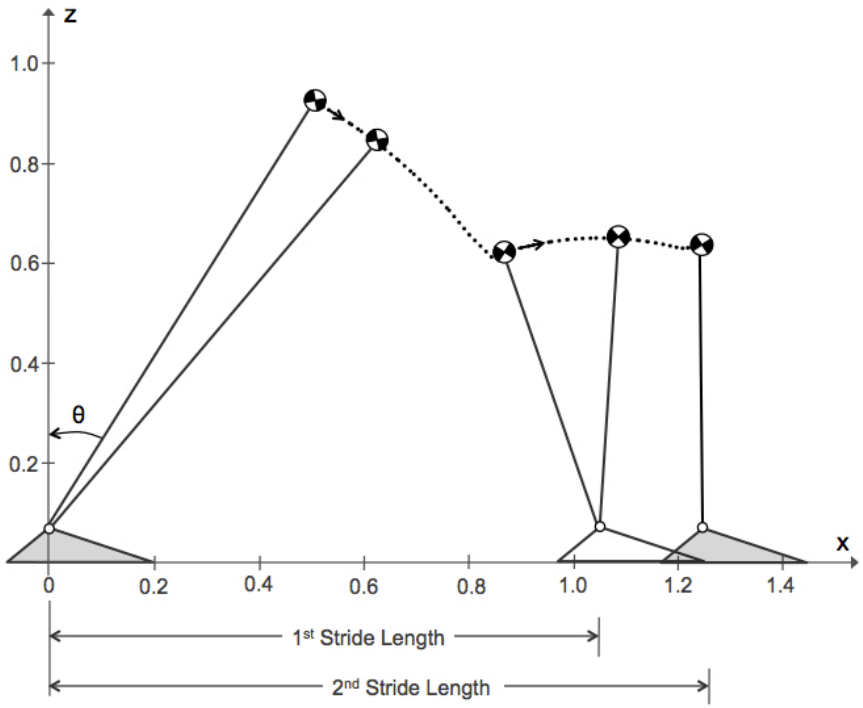

Figure 3.15: Evolution of the *mechanical* model during the predicted recovery for the scenario of Cyr and Smeesters (2009a) (snapshots every 200 ms).

multiple-step recoveries and its possible extension to include more complex behaviors, thanks to a multi-objective cost function. We therefore see a strong incentive to further continue on this approach and address its limitations.

3.6 Conclusion

Balance recovery by stepping is a common strategy in humans. Yet there are only a handful of studies which model this behavior. Most of these concepts come from the field of biped robotics. In the first part (Sections 3.1 and 3.2), we presented and evaluated some prominent formulations for estimating the location of a single recovery step and discussed their strong and weak points in the context of human balance recovery response. In general, the models consider the system's CoM state as input and predict the location of the recovery step. Only Hofmann (2006) additionally predicted the contact time, though it was merely a consequence of the inverted pendulum assump-

tion and a trivial constraint of symmetrical stepping. Similarly, only Pratt et al. (2006) modeled the effect of the upper-body rotation and quantified its maximum effect in terms of size of the capture region. However, the obligation of single-step recoveries, among other limitations, limit their practical usage for prediction of human recovery behavior.

On the other hand, the Model Predictive Control (MPC) approaches in general, and the scheme of Herdt et al. (2010b) in particular, proved to be quite capable of eliminating some key limitations of the above models. The MPC approach relies on a more general optimization-based approach to consider not only the multiple step recoveries but additionally the system's dynamics and its evolution all along the recovery process. Moreover, the predicted step lengths matched well with the experimental results for a simple balance recovery scenario considered in Section 3.5. We therefore build further on this approach by addressing its limitations of non-consideration of upper-body inertial effects and non-optimized contact times in the next chapter.

"Our experience hitherto justifies us in trusting that nature is the realization of the simplest that is mathematically conceivable." Albert Einstein, 1933

Chapter 4

A Multiple-Strategy Balance Recovery Model

The MPC scheme presented in the previous chapter (Herdt et al., 2010a) relies on a simplified LIP model and only considers the ankle and stepping strategies. A further limitation is the step durations fixed in advance. As we noted in chapter 2, the Upper-Body Inertia (UBI) has an important role in human balance recovery and the duration of a recovery step is also an important variable, just like its location. It is further observed that in humans, ankle and hip strategies often exist in parallel in balance recovery tasks (Maki and McIlroy, 1997) and the use of the hip strategy is positively scaled with the perturbation magnitude (Park et al., 2004).
In this chapter, we further build on the MPC scheme proposed by Herdt et al. (2010a) to implement an appropriate combination of ankle, hip and stepping strategies. Our goal is to develop a single MPC controller which can produce a balance recovery behavior as close as possible to the human behavior described above. Furthermore, we integrate a proper optimization of the step duration for improved efficiency.

Contents

4.1 Existing multiple-strategy controllers

To the author's knowledge, no MPC controller has integrated yet the upper-body inertial effects. However, there exist some other balance recovery schemes which model and control more than one balance strategies simultaneously. Some of these approaches are reviewed in this section.

The regulation of multiple strategies is a delicate issue from the control point of view. It globally amounts to deciding at what point the controller switches from one strategy to another. Most existing control schemes regulate only 2 fixed-support strategies and further suggest a sequential transition from ankle to hip strategy. For example Nenchev and Nishio (2007) used the sensor acceleration data and an arbitrary threshold to invoke the hip strategy. Kanamiya et al. (2010) proposed transition to hip strategy when the ankle strategy is saturated. Atkeson and Stephens (2007) proposed a non-linear controller using a single optimization criterion to switch between the two strategies. Takenaka et al. (2009) proposed a similar combination but with simple empirical rules without much explanation. Bonnet and colleagues in several works (Bonnet et al., 2009, 2007, 2011) used constrained optimization and a PD controller to simulate human tracking tasks while minimizing global joint torque variation. They observed transtions between the two strategies at the point of ankle torque saturation. Yin and van de Panne (2006) went a step further by including stepping and regulated three strategies at a time. However, the switching is based on heuristic principles which lack provable stability and effective implementation in a more general balance recovery model.

In the next section, we present in detail the complete development of our MPC scheme with the three balance recovery strategies. Later in the chapter we demonstrate how all three strategies are efficiently regulated in our controller without defining arbitrary thresholding or empirical rules.

4.2 Balance Recovery MPC scheme

4.2.1 System Dynamics

We employ the well-regarded LIP model and supplement it with a simple flywheel as in Pratt et al. (2006), leading to the simple linear dynamics:

$$mh\,\ddot{c}_x + j\,\ddot{\theta} = mg(c_x - z_x) \tag{4.1}$$

where c_x and z_x are the horizontal coordinates of the CoM and CoP, θ is the orientation of the trunk, j the inertia of the trunk and g the norm of the gravity force. The MPC controller in Herdt et al. (2010a) (c.f. Chapter 3) is based on anticipating future motions on a prediction horizon composed of N time intervals of equal length T. Keeping the same principle and extending it to the motion of the flywheel, we consider the motion of both CoM and the flywheel on the future time horizon having constant third derivatives $\dddot{c}$ and $\dddot{\theta}$ over each time interval. Hence just like the CoM, for the state

$$\hat{\theta}_k = \begin{bmatrix} \theta_k \\ \dot{\theta}_k \\ \ddot{\theta}_k \end{bmatrix} \tag{4.2}$$

of the flywheel at a time t_k, its position, speed and acceleration over the whole prediction horizon

$$\Theta_{k+1} = \begin{bmatrix} \theta_{k+1} \\ \vdots \\ \theta_{k+N} \end{bmatrix}, \dot{\Theta}_{k+1} = \begin{bmatrix} \dot{\theta}_{k+1} \\ \vdots \\ \dot{\theta}_{k+N} \end{bmatrix}, \ddot{\Theta}_{k+1} = \begin{bmatrix} \ddot{\theta}_{k+1} \\ \vdots \\ \ddot{\theta}_{k+N} \end{bmatrix} \tag{4.3}$$

is related to the piecewise constant third derivative

$$\dddot{\Theta}_{k+1} = \begin{bmatrix} \dddot{\theta}_{k+1} \\ \vdots \\ \dddot{\theta}_{k+N} \end{bmatrix} \tag{4.4}$$

through simple matrices:

$$\Theta_{k+1} = S_p\hat{\theta}_k + U_p\dddot{\Theta}_k, \tag{4.5}$$

$$\dot{\Theta}_{k+1} = S_v\hat{\theta}_k + U_v\dddot{\Theta}_k, \tag{4.6}$$

$$\ddot{\Theta}_{k+1} = S_a\hat{\theta}_k + U_a\dddot{\Theta}_k. \tag{4.7}$$

Note that identical relations hold for the CoM motion already derived in Section 3.4. The matrices S_p, U_p etc. follow directly from the recursive dynamics. Details can be found in (Herdt et al., 2010a,b).

The linear dynamics (4.1) can be reversed to compute the position of the CoP from the motion of the human or humanoid system:

$$z = c_x - \frac{h}{g}\,\ddot{c}_x - \frac{j}{mg}\,\ddot{\theta}. \tag{4.8}$$

As before, we can easily relate the position of the CoP over the whole prediction horizon

$$Z_{k+1} = \begin{bmatrix} z_{k+1} \\ \vdots \\ z_{k+N} \end{bmatrix} \tag{4.9}$$

to the piecewise constant third derivatives $\dddot{C}_k$ and $\dddot{\Theta}_k$ through simple matrices:

$$Z_{k+1} = S_z \begin{bmatrix} \hat{c}_k \\ \hat{\theta}_k \end{bmatrix} + U_z \begin{bmatrix} \dddot{C}_k \\ \dddot{\Theta}_k \end{bmatrix}, \tag{4.10}$$

with

$$S_z = \begin{bmatrix} S_p - \frac{h}{g}S_a & -\frac{j}{mg}S_a \end{bmatrix}, \tag{4.11}$$

$$U_z = \begin{bmatrix} U_p - \frac{h}{g}U_a & -\frac{j}{mg}U_a \end{bmatrix}. \tag{4.12}$$

4.2.2 Kinematic and dynamic constraints

Of course, the dynamics (4.1) of human and humanoid balance is subject to a series of kinematic and dynamic constraints that have to be satisfied over the whole prediction horizon, for all $i \in [k+1, \dots k+N]$. To start with, trunk rotation is limited by joint constraints. With such a simple model, it will be constrained by direct bounds

$$\theta_{min} \leq \theta_i \leq \theta_{max}. \tag{4.13}$$

The same concerning hip torques:

$$j|\ddot{\theta}_i| \leq \tau_{max} \tag{4.14}$$

If f_i represents the horizontal position of the support foot on the ground at time t_i, the maximum extension of the support leg can be simply enforced with the horizontal position of the CoM:

$$\|c_x^i - f_i\| \leq l_{max}. \tag{4.15}$$

However, instead of constraining the swing foot forward velocity as done in the previous chapter, we consider constraining its forward acceleration to be more biologically realistic. If f_i' represents the horizontal position of the swing foot above the ground, this constraint can simply be represented as:

$$\|\ddot{f}_i'\| \leq \ddot{f}_{max}' \tag{4.16}$$

The motion of the swing foot is interpolated with 5th degree polynomials between its current position, velocity and acceleration and the desired position on the ground with zero velocity and acceleration (no impact).

Finally, the CoP z_x is also constrained to stay within the boundaries of the support polygon, what can be expressed in the following way:

$$D(z_i - f_i) \leq b, \tag{4.17}$$

where D and b are a matrix and a vector encoding the shape of the foot with respect to the position f_i of the support foot on the ground. In order to express these constraints over the whole prediction horizon, we have to relate the position of the support foot over the whole prediction horizon

$$F_{k+1} = \begin{bmatrix} f_{k+1} \\ \vdots \\ f_{k+N} \end{bmatrix} \tag{4.18}$$

with the current support foot position f_k which is fixed on the ground and the positions $\bar{F}_{k+1}$ of the future steps which will have to be decided by the balance controller. If the step durations are fixed in advance, this can be done easily with matrices V_{k+1} and $\bar{V}_{k+1}$ filled with 0s and 1s simply indicating which sampling times t_i fall within which steps as done in Herdt et al. (2010b):

$$F_{k+1} = V_{k+1} f_k + \bar{V}_{k+1} \bar{F}_{k+1}. \tag{4.19}$$

with

$$V_{k+1} = \begin{bmatrix} 1 \\ \vdots \\ 1 \\ 0 \\ \vdots \\ 0 \\ 0 \\ \vdots \\ 0 \end{bmatrix}, \bar{V}_{k+1} = \begin{bmatrix} 0 & 0 & \\ \vdots & \vdots & \\ 0 & 0 & \\ 1 & 0 & \\ \vdots & \vdots & \\ 1 & 0 & \\ 0 & 1 & \\ \vdots & \vdots & \\ 0 & 1 & \ddots \end{bmatrix} \tag{4.20}$$

where rows correspond to sampling times and columns to steps.

However, when step duration is left as a free parameter, which is the objective of our controller, the filling of these matrices is not straightforward and the optimization problem becomes non-linear. This requires more complex numerical solvers such as the

one proposed in Diedam (2009). However, since this thesis is focused on the modeling of balance and analysis of different cost functions, a simpler multi-iterative process is used. At each sample time, multiple simulations are carried out testing different step durations and the corresponding values of the cost function are stored. The optimal step duration is then chosen as the one which results in the minimum value of the cost function.

4.2.3 Controller design

Since the basic objective of our controller is to regulate balance to a standstill posture, the MPC scheme should essentially minimize the speed $\dot{C}_{k+1}$ of the CoM and the rotation speed $\dot{\Theta}_{k+1}$ of the inertia wheel over the prediction horizon while taking care of all the constraints listed earlier. Moreover, as will be discussed in Section 4.3.3, minimizing the acceleration $\ddot{F}'_{k+1}$ of the swing foot over the whole prediction horizon helps to select the step durations. This leads us to a multi-objective controller minimizing a weighted sum

$$\min \ \frac{1}{c_1^2}\|\dot{C}_{k+1}\|^2 + \frac{1}{c_2^2}\|\dot{\Theta}_{k+1}\|^2 + \frac{1}{c_3^2}\|\ddot{F}'_{k+1}\|^2. \tag{4.21}$$

However, the resulting motions appear to be significantly improved when minimizing also the third derivatives $\dddot{C}_k$ and $\dddot{\Theta}_k$ of the motion and the distance between the position Z_{k+1} of the CoP and the center F_{k+1} of the support foot as done in the previous chapter. The final multi-objective controller looks therefore to minimize

$$\begin{aligned}\min \ \frac{1}{c_1^2}\|\dot{C}_{k+1}\|^2 + \frac{1}{c_2^2}\|\dot{\Theta}_{k+1}\|^2 + \frac{1}{c_3^2}\|\ddot{F}'_{k+1}\|^2 \\ + \frac{1}{c_4^2}\|\dddot{C}_k\|^2 + \frac{1}{c_5^2}\|\dddot{\Theta}_k\|^2 + \frac{1}{c_6^2}\|Z_{k+1} - F_{k+1}\|^2,\end{aligned} \tag{4.22}$$

with the control variables $u = \begin{bmatrix}\dddot{C}_k & \dddot{\Theta}_k & \bar{F}_{k+1}\end{bmatrix}^T$. The choice of the weights c_1 to c_6 will help tune the different strategies involved in the balance recovery process.

Table 4.1: Anthropomorphic proportions used in the simulation

Variable	Symbol	Value	Ref.
Body height	H	1.75 m	Chaffin and Andersson (1984)
Body mass	m	75 kg	Chaffin and Andersson (1984)
CoM height	$h = 0.575 \times H$	1.012 m	Winter (1990)
Foot length	$l_f = 0.152 \times H$	0.26 m	Winter (1990)
Ankle to toe distance	$0.81 \times l_f$	0.21 m	Winter (1990)
Ankle to heel distance	$0.19 \times l_f$	0.05 m	Winter (1990)
Max trunk rotation	θ_{max} (forward)	$\pi/2$ rad	
Min trunk rotation	θ_{min} (backward)	$-\pi/2$ rad	
Trunk inertia	j	8 kg.m^2	Winter (1990)
Max hip torque	τ_{max}	190 N.m	Chaffin and Andersson (1984)

4.3 Cost Function Analysis

Let's first analyze the cost function (4.22) step by step and explore the role of its different terms in the overall balance recovery. For this purpose, simple simulations are performed considering a human-sized model (c.f. Table 4.1) in the upright posture and experiencing sagittal plane perturbations of various amplitudes. The disturbance is characterized by a post-impact CoM velocity which is input to the controller for recovery action. Calculations are done over a prediction horizon of 1 s.

4.3.1 Stability using Fixed-support strategies

We start our analysis by considering only the fixed-support strategies. The stability of the system can be achieved by minimizing a cost function as simple as:

$$\min \ \frac{1}{c_1^2}\|\dot{C}_{k+1}\|^2 + \frac{1}{c_2^2}\|\dot{\Theta}_{k+1}\|^2. \tag{4.23}$$

with control variables, $u = \begin{bmatrix} \dddot{C}_k & \dddot{\Theta}_k \end{bmatrix}^T$ and under constraints (4.13), (4.14) and (4.17).

The amount of disturbance that can be dealt with depends upon maximum ankle torque and inertia wheel parameters. Ankle torque is limited by the size of the base

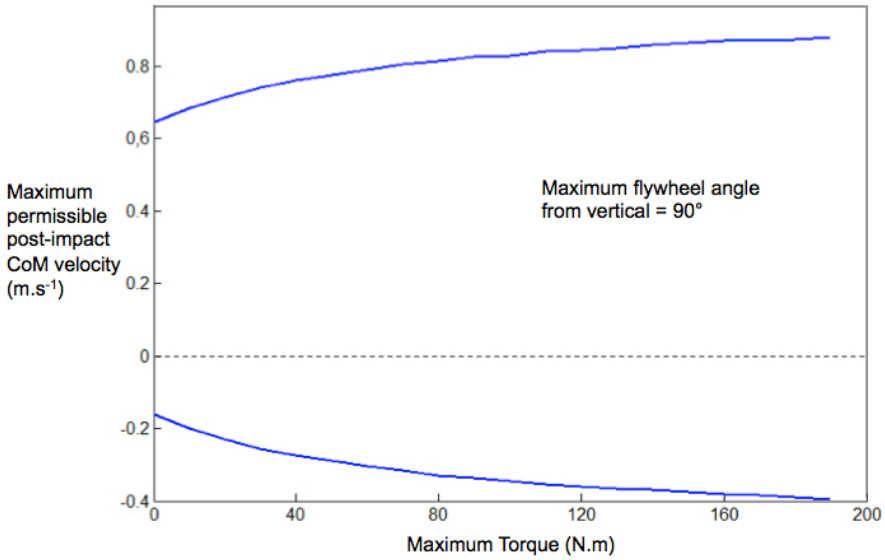

Figure 4.1: Effect of inertia wheel torque limit on the maximum disturbance that can be sustained without stepping. The maximum rotation angle is fixed to $\frac{\pi}{2}$

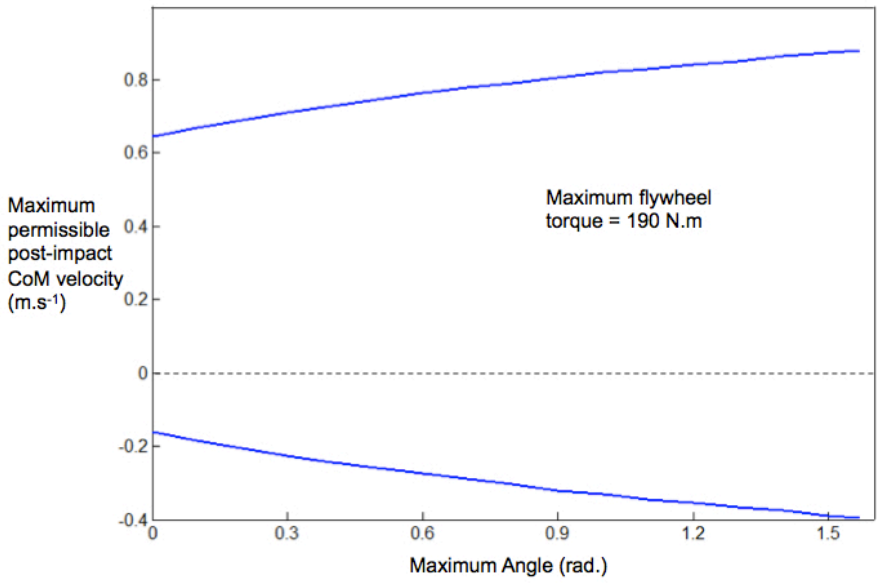

Figure 4.2: Effect of inertia wheel angle limit on the maximum disturbance that can be sustained without stepping. The maximum torque is limited to 190 $N.m$

of support (the length of foot in sagittal plane) which is indirectly taken care of by the CoP constraint (4.17). The inertia wheel has to run within the maximum angle and torque limits (constraints (4.13) and (4.14)). The effect of τ_{max} and θ_{max} on the maximum permissible post-impact velocity is shown in the Figures 4.1 and 4.2 separately. We can see that if the ankle strategy is used alone (corresponding to zero hip torque), a stability limit is reached for a post-impact velocity of 0.64 m.s^{-1} in the forward direction and 0.16 m.s^{-1} in the backward direction. This directional difference is due to the non-symmetric stretch of foot around the reference equilibrium position i.e. the ankle (c.f. Table 4.1). In presence of the inertia wheel, and with anthropomorphic limits of $\tau_{max} = 190N.m$ and $\theta_{max} = \frac{\pi}{2}$, the post-impact velocities of upto 0.88 m.s^{-1} in the forward direction and 0.40 m.s^{-1} in the backward direction can be managed without stepping from a standstill initial posture.

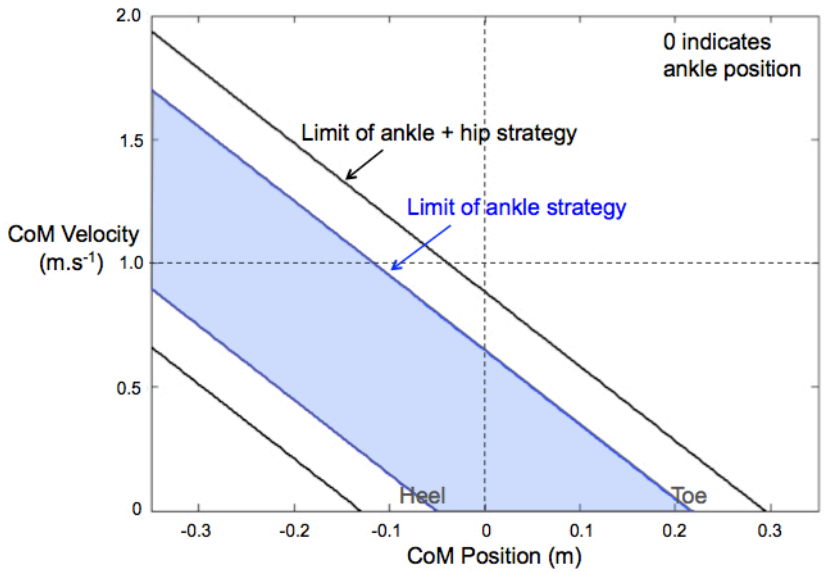

Figure 4.3: The fixed-support stability region in CoM state space with our MPC controller (4.23) using anthropometric parameters. Zero indicates the position of ankle in sagittal plane. It is evident that the disposition of upper-body allows recovering from much larger disturbances than with ankle strategy alone without stepping

This analysis can further be extended to non-upright postures in terms of a stability region (see Figure 4.3). The inner blue area corresponds to the ankle strategy stability zone similar to one proposed by Hof et al. (2005) (c.f. Section 2.2.2). Outer lines

represent the limits of the ankle and hip strategies working together obtained by minimizing the cost function (4.23) using anthropomorphic parameters listed in Table 4.1. It shows that the disposition of upper-body inertia enhances the fixed-support stability area by about 50%. This matches well with the increase of around 30% reported by Koolen et al. (2012) given that they used a relatively low peak hip torque value (100 N.m). Interestingly, the torque profile predicted by our controller at the limit of combined ankle+hip strategy (along the outer black line in Figure 4.3) is also very similar to the bang-bang profile used in Koolen et al. (2012) to exert maximum effect on the CoM velocity. (For a quick reference, the reader may refer to the Figure 4.9 in Section 4.4 which shows time profiles of hip torque corresponding to disturbances of varying level).

4.3.2 Smoothing of motion trajectories

Though the basic fixed-support stability can be achieved by minimizing the cost function (4.23), the resulting motions are not very smooth. For example, Figure 4.4 shows profiles of CoM forward acceleration (top) and hip angular acceleration (bottom) while recovering from a post-impact velocity of 0.7 m.s^{-1} using the cost function (4.23). As a whole, a mean zero acceleration is maintained towards the end of the motion for both CoM and the flywheel. However, not only abrupt acceleration changes are observed during the initial phase of the motion, the absolute acceleration value is never converging to zero.

Minimizing a weakly-weighted CoM jerk term $\|\dddot{C}_k\|^2$ helps smoothing the motion to much extent (Figure 4.5, left) but the oscillations of the inertia wheel still disturb the system. Finally, the minimization of both CoM and flywheel jerks (Figure 4.5, right) results in a much smoother trajectory and results in a steady state posture.

However, this trajectory smoothing is not without a cost. Penalizing the jerks of motion can reduce the stability margins in Figure 4.3 by 1-2 cm.s^{-1}, even for weak penalizations c_4 and c_5 (both c_4 and c_5 equal 300 m.s^{-3} and rad.s^{-3} respectively in this case). It is therefore judicious to penalize them as faintly as possible. The issue of control weight values will be discussed more thoroughly in Section 4.3.4.

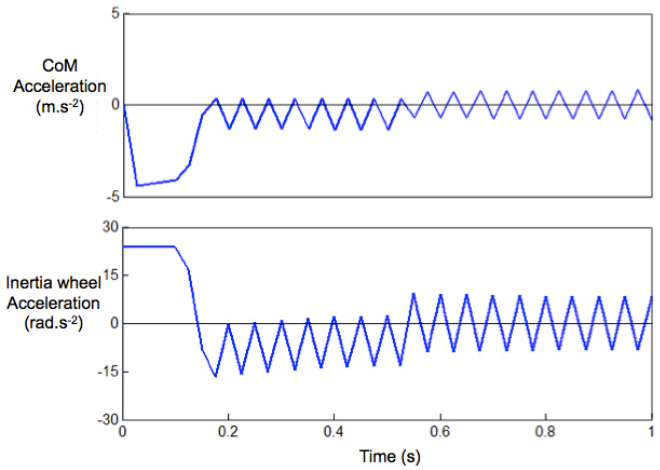

Figure 4.4: Time profiles of CoM and inertia wheel accelerations following a given disturbance obtained by minimizing cost function (4.23). Note the resulting fluctuations due to the absence of their third derivative penalization

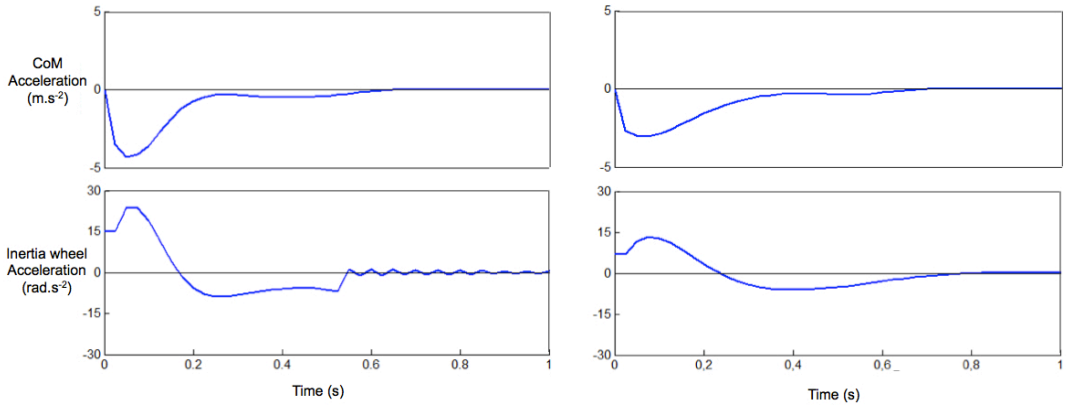

Figure 4.5: Time profiles of CoM and inertia wheel accelerations when only CoM jerk (left) and both CoM and inertia wheel jerks (right) are penalized.

4.3.3 Stepping and Contact time optimization

Let's now observe the role of minimizing the swing foot acceleration term in optimizing step durations. Allowing the duration of the steps to vary in an MPC scheme has been tried in Diedam (2009), but the steps ended up being always chosen the quickest possible: if no explicit lower limit was set on their duration, they were chosen to be infinitely quick!

The reason for this ill behavior lies in the objective function which is essentially

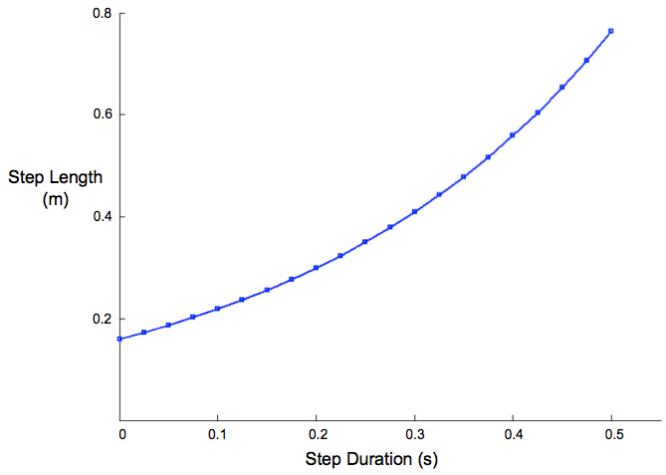

Figure 4.6: Single recovery step lengths for a given perturbation as function of step durations

based on the CoM regulation. To understand this, let's take a simple case of a single-step recovery response for a post-impact CoM velocity of 0.5 m.s^{-1}. For the system without inertia wheel, minimizing a cost function as simple as $\|\dot{C}_{k+1}\|^2$ would result in a basic stabilization of the system with different step lengths depending on the imposed step duration (see Figure 4.6). However, if the value of this cost function is plotted against the step durations (c.f. Figure 4.7, left), we can observe that the objective function decreases continuously with shorter step durations: quicker steps always allow minimizing the CoM speed more and more efficiently. This behavior is unaffected by the inclusion or not of the third-derivative of motion or the centering of the CoP within the foot as done in Herdt et al. (2010a).

However this behavior is understandable given our simplified model and control scheme. Quicker steps incur a mechanical and energetic cost (Doke and Kuo, 2007; Zarrugh et al., 1974) in human stepping due to the fact that legs are not massless entities. Consequently, humans choose a reasonable stepping frequency during walking or balance recovery. On the other hand, this cost is generally neglected by almost all control schemes, MPC or otherwise.

In this regard, we propose to introduce a simple model of this mechanical cost in the objective function by penalizing the acceleration $\ddot{F}'_{k+1}$ of the swing foot. Figure 4.7 (right) shows the value of the new cost $\|\ddot{F}'_{k+1}\|^2$ against step durations for the

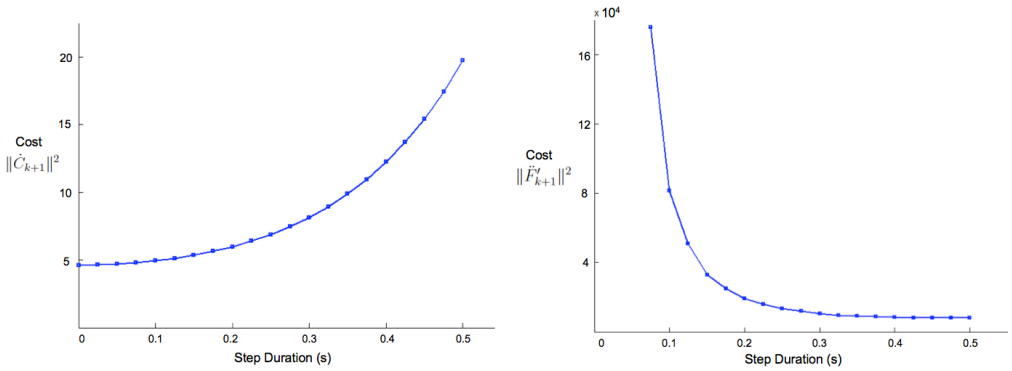

Figure 4.7: The CoM velocity cost (left) and swing foot acceleration cost (right) against varying step durations and for step lengths plotted in Figure 4.6. Note that both the costs show completely opposite trend against step duration

same disturbance. Clearly, this new cost rises steeply for quick steps and is minimized for larger step durations.

If these two mutually opposing costs are combined together in a single objective function, and given appropriate relative weight coefficients values, an intermediate value can be obtained for the optimal step duration. Depending upon the order of magnitude of these two terms (see Figure 4.7, y-axis values), it can be deduced that the foot acceleration term should be penalized more. For example, minimizing the combined objective function $\frac{1}{c_1^2}\|\dot{C}_{k+1}\|^2 + \frac{1}{c_3^2}\|\ddot{F}'_{k+1}\|^2$ with a coefficient ratio of $\frac{c_3}{c_1}$ equal to 100 m.s^{-2} selects a step duration of 0.2 s (c.f. Figure 4.8) for which the corresponding step length is 0.3 m from the Figure 4.6. This example demonstrates the validity of our idea for optimizing the step duration. Later, in the next section, we will show its role in the strategy regulation.

4.3.4 A note on the relative control weights

In a multi-objective function like (4.22), it is important to carefully select the relative control weight values for a reasonable model behavior. This is not quite straightforward as each coefficient is multiplied by a different term of different magnitude. Moreover, the weight value should also take into account the relative importance of a given variable in the overall balance recovery task. In this section, we try to develop a general guideline for the selection of these control weights values.

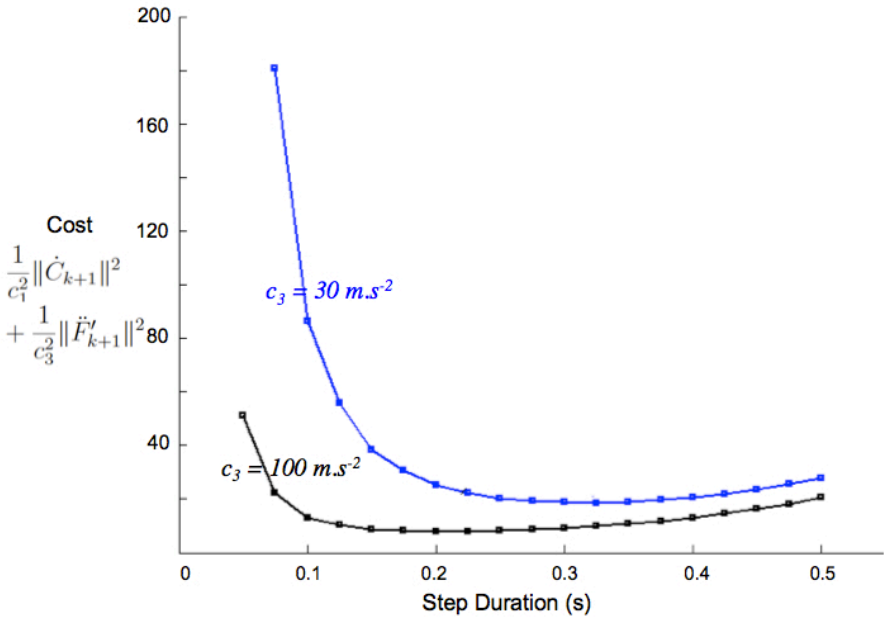

Figure 4.8: Minimal values of the cost function for different penalization coefficients c_3

Starting from the third derivatives of motion, as noted in section 4.3.2, only weak penalizations (i.e. high weights c_4 and c_5) are necessary to smooth the resulting motion. For a reference weight c_1 equal to 1 m.s^{-1}, typical values of c_4 (in m.s^{-3}) and c_5 (in rad.s^{-3}) are of the order of 100-1000, without much effect on the final recovery behavior. The same principle applies to the final term which makes the CoP roughly converge under the ankle position to attain a comfortable final posture. Typical values are noted in Table 4.2.

The most important penalizations in this cost function are that of trunk rotation speed (c_2) and foot acceleration (c_3). Regarding c_2, its value considerably affects the level of use of the inertia wheel as we will see in Section 4.4. Based on simulations, typical values of c_2 around 3 to 30 rad.s^{-1} are found to be reasonable. The penalization c_3 is important for an effective step time optimization. As we saw in section 4.3.3 that the value of its associated foot acceleration term $\|\ddot{F}'_{k+1}\|^2$ is roughly 10^3 to 10^4 times higher than the corresponding velocity norm $\|\dot{C}_{k+1}\|^2$, for a given perturbation. One can imagine that if the disturbance level is increased or decreased, the two costs vary

Table 4.2: A general guideline for selecting control weight values

Control Weight	Reasonable Range
c_1	1 m.s^{-1}
c_2	3-30 rad.s^{-1}
c_3	300-1000 m.s^{-2}
c_4	100-1000 m.s^{-3}
c_5	100-1000 rad.s^{-3}
c_6	10-100 m

in the same direction, following the above empirical relation as a whole. Hence for a unit value of c_1, the corresponding equivalent value of c_3 would be $\approx$ 100 m.s^{-2}. We will further show in the following section how this penalization helps regulate different strategies.

4.4 Regulation of strategies

While the disposition of multiple balance strategies greatly enhances the recovery ability, their effective regulation can be a tedious task from the control point of view. In this section, we show how various strategies are regulated with a single cost function in our controller by simply adjusting the relative control weight values. We start our analysis by first fixing the feet to their positions and see how the ankle and hip strategies combine together. Next, the feet will be freed and all three strategies will be regulated simultaneously.

4.4.1 Ankle and Hip strategies

Let's recall our cost function (4.22):

$$\min \ \frac{1}{c_1^2}\|\dot{C}_{k+1}\|^2 + \frac{1}{c_2^2}\|\dot{\Theta}_{k+1}\|^2 + \frac{1}{c_3^2}\|\ddot{F}'_{k+1}\|^2 + \frac{1}{c_4^2}\|\dddot{C}_k\|^2 + \frac{1}{c_5^2}\|\dddot{\Theta}_k\|^2 + \frac{1}{c_6^2}\|Z_{k+1} - F_{k+1}\|^2$$

In order to simulate only the ankle and hip strategies, we minimize this cost function without the foot acceleration penalization cost and fix the steps to their initial

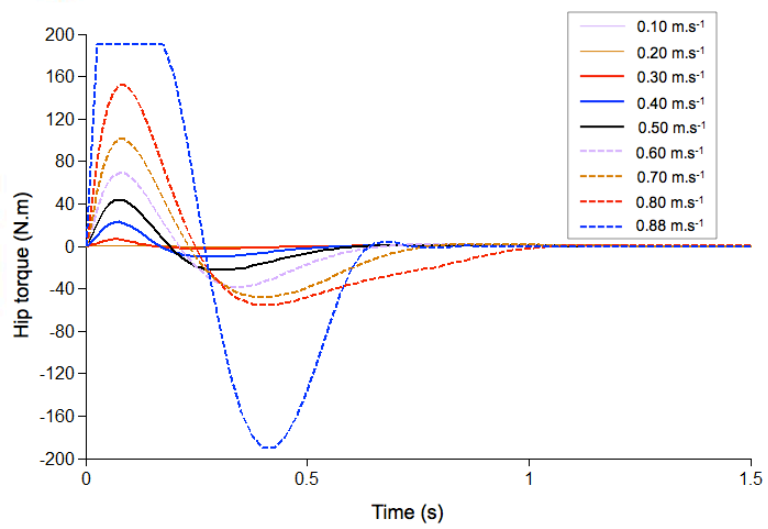

Figure 4.9: Time plots of resulting hip torque after the system is exposed to disturbances of increasing magnitudes till the limit of the combined ankle+hip strategies

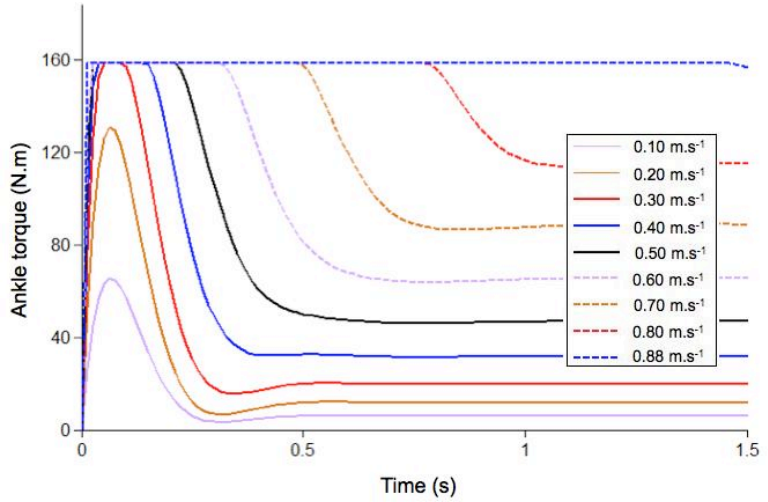

Figure 4.10: Time plots of resulting ankle torque after the system is exposed to disturbances of increasing magnitudes till the limit of the combined ankle+hip strategies

positions. The system is then exposed to impacts of increasing magnitudes in the forward direction characterized by the post-impact CoM velocity. Time profiles of resulting ankle and hip torque values are shown for various perturbations obtained using c_2=10 rad.s^{-1} and c_5=1000 rad.s^{-3} (c.f. Figures 4.9 and 4.10). Other parameters are set according to the guidelines in Table 4.2. Overall, the plots show a well scaled use

of both strategies in parallel which is consistent with the biomechanical observations as noted in Chapter 2. However, the final recovery posture is not completely upright, as evident from the ankle torque plots, indicating a constant CoP deviation from the ankle position towards the end of the motion. This highlights one of the traits of our controller in which the objective of the balance recovery (quick convergence of CoM velocity to zero) is privileged over the other objectives.

Moreover, for the smaller perturbations (0.1 and 0.2 m.s^{-1}) the hip torque values are too small to be visible in Figure 4.9. To understand the reason of this behavior, let's observe the coexistence of the two strategies in detail by varying the control weights c_2 and c_5 (c.f. Figure 4.11). Only the peak values of the ankle and hip torque values (black and blue plots respectively) are plotted against the disturbances of various magnitudes till combined ankle and hip strategies limit for the upright posture. The control weight c_2 varies between 3-30 rad.s^{-1} between plots while c_5 is varied on each plot between 300 and 1000 rad.s^{-3}.

In all cases, ankle strategy is used increasingly for small disturbances until it reaches its limit torque of around 160 N.m in the forward direction. Till this point, the use of inertia wheel is negligibly small (though not completely zero), independent of control weights c_2 and c_5. Once the limit of the ankle torque is reached, the controller then switches to combined ankle+hip strategy to apply sufficient deceleration to the system. This phenomenon is consistent with the observation by Bonnet et al. (2011) who designed a controller for a human tracking task and showed minimal hip use until the ankle torque saturation.

The level of usage of the upper-body inertia beyond this 'transition' point depends upon its control weight values. For example, a strong penalization of inertia wheel angular jerk reduces its overall usage in all cases. Similarly, for a strong angular velocity penalization ($c_2 = 3$ rad.s^{-1}, Figure 4.11), the use of hip strategy is minimal until the ankle strategy limit of around 0.64 m.s^{-1} is reached. Note also that the flywheel angle limit of 90° is reached (indicated by white circles on peak hip torque plots) at different

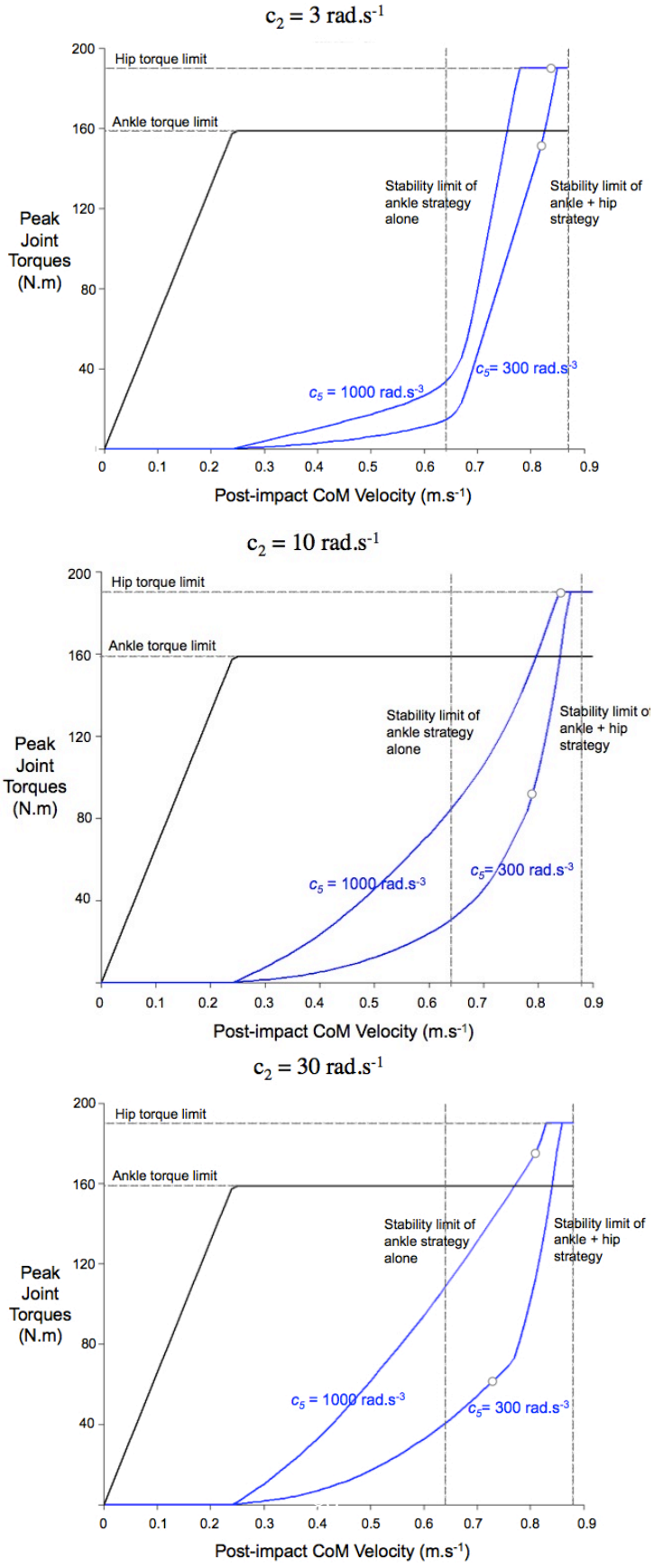

Figure 4.11: The relative level of use of ankle and hip strategies. Peak ankle (black) and hip (blue) torques are plotted against varying perturbations. White dot indicates the point where upper-body angle limit of 90° is reached

instants depending upon c_2 and c_5 values. The weaker the c_2 penalization, the earlier the angle is saturated (compare white circles' location on corresponding plots) and vice versa. Hence, by appropriate tuning of these control weights, different balance recovery behaviors can be obtained.

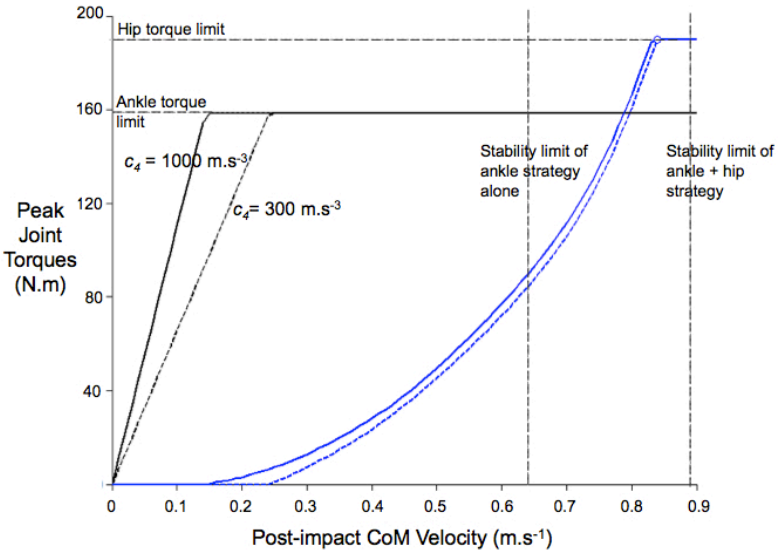

Figure 4.12: Effect of varying CoM jerk penalization c_4 on relative contribution of ankle and hip torques.

Apart from the control weights of the inertia wheel, other coefficients also play interesting roles in the strategy regulation. With $c_6 = 10$ m, the CoM jerk penalization c_4 strongly influences the point of ankle torque saturation. The weaker the CoM jerk penalization ($c_4 = 1000\ m.s^{-2}$ continuous plots in Figure 4.12), the earlier the ankle torque is saturated and vice versa. This is consistent with our earlier observation in section 4.3.2 about abrupt motions for weak or no penalization of higher motion derivatives. Interestingly, the transition from ankle to combined ankle+hip strategy again coincides with this new point of ankle torque saturation confirming our earlier finding. However, if the CoP divergence is more strongly penalized (e.g. $c_6 = 3$ m, Figure 4.13), the use of ankle torque (which is proportional to this divergence) is naturally reduced and this loss is compensated by an increased use of upper-body inertia even for smallest disturbances. However, even in this case, the ankle torque

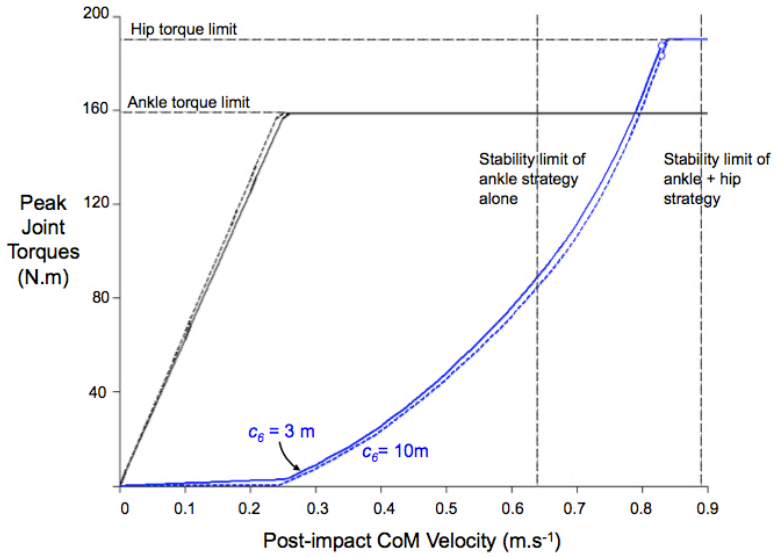

Figure 4.13: Effect of varying CoP divergence coefficient c_6 on relative contribution of ankle and hip torques.

remains the major contributor against smaller disturbances.

Remarks

Overall, these results show a reasonable behavior of the system against varying perturbations and control weights. The coexistence of ankle and hip strategies before reaching the ankle strategy limit has been reported in the biomechanics literature (Park et al., 2004). By minimizing a single cost function under linear constraints, we are able to reproduce this phenomenon. Moreover, the extent of use of the hip strategy is also tuned in our controller by adjusting the control weights c_2 to c_6.

We now move on to free up the feet and show the regulation of 3 strategies at a time.

4.4.2 Regulation of 3 strategies

Let's complete now the balance recovery behavior with the stepping strategy. In order to analyze how the three strategies combine, let's consider a situation where the step duration is fixed to 0.3 s. We can see in Figure 4.14 that if the acceleration $\ddot{F}''_{k+1}$ of

the swing foot is not penalized, the stepping strategy is initiated even for the smallest perturbations. This parallels the discussion we already had in Section 4.3.3: if the stepping strategy incurs no cost, then there's no reason not to put it at work, even when it's absolutely not necessary nor even particularly helpful.

Depending on how much this acceleration is penalized, the stepping strategy will be activated at different levels of perturbations, as shown in Figure 4.14. For a small penalization (c_3 =300 m.s^{-2}), the stepping strategy is initiated before even reaching the stability limit of the ankle strategy alone. This behavior has been observed in human balance recovery experiments when the subjects are not instructed to avoid stepping (Maki and McIlroy, 1997). For a strong penalization (c_3 =3 m.s^{-2}), it is initiated only when reaching the stability limit of the ankle and hip strategies working together. We can tune therefore very easily when the decision is taken to use the stepping strategy, and how much.

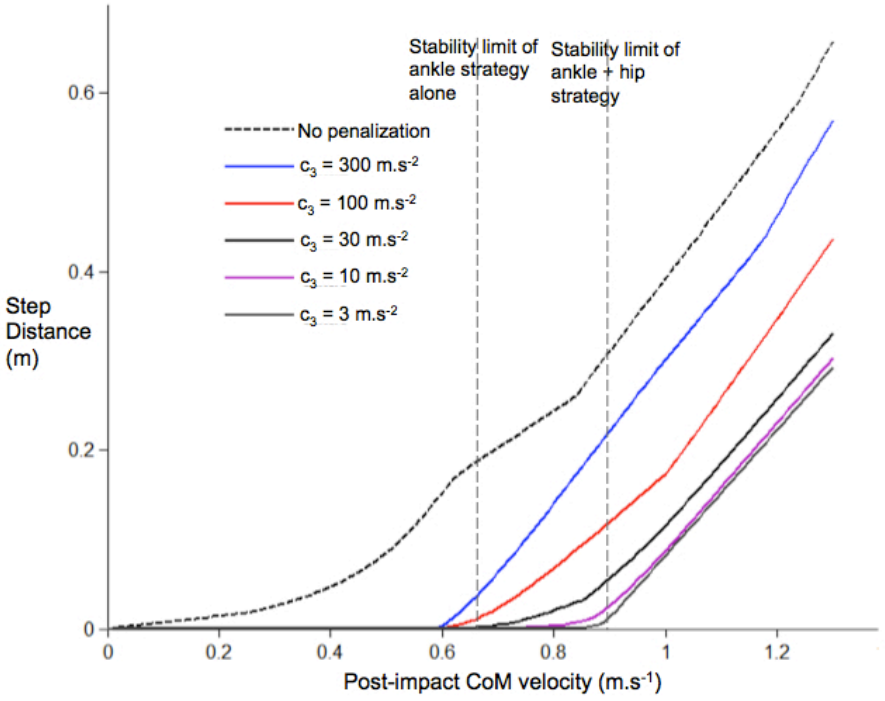

Figure 4.14: Step length when reacting to varying post-impact CoM velocities for different penalization coefficients c_3, or for no penalization at all of the swing foot acceleration $\ddot{F}'_{k+1}$

4.5 Comparison with Experimental Data

In order to validate our new MPC scheme, let us compare its predictions against experimental results like we did in Chapter 3 (c.f. Section 3.5). The basic approach is the same where a mechanical model of human body (here the simple inverted pendulum + inertia wheel model) is perturbed and its state is fed to the MPC controller in a feedback loop. The output of the controller (mainly the CoP location and upper-body state) is then applied to the model during the whole sampling period $T_{sampling}$.

4.5.1 Model Parameters

The majority of the simulation parameters are kept the same. The reaction and step preparation times (T_{reac}, T_{prep}) values are taken either from the study or from the literature. The duration of this swing phase T_{step} is automatically chosen by the scheme unless otherwise indicated. The values of control weights are set according to the guidelines developed in section 4.3.4. These values are reproduced in Table 4.3 and are kept the same throughout. The simulations are performed over a time horizon of 1 s.

4.5.2 Results

In the following subsections, we present the comparison between model predictions and experimental results for 3 different studies:

i) Single-step recovery results from Hsiao-Wecksler and Robinovitch (2007) for 4 inclination scenarios

ii) Multiple-step recovery result from Cyr and Smeesters (2009a) for a forward inclination of 30.7°

iii) Single-step recovery results from Moglo and Smeesters (2005) for the combined inclination and pull force experiments

Table 4.3: The controller parameters related to simulation and constraints

Parameter	Value
No of samples, N	40
Sampling Time, T	25 ms
Horizon length, N×T	1 sec
Simulation Time	2 sec
Foot length, l_f	c.f. Table 4.1
Max foot acceleration, $\ddot{f}'_{max}$	180 m.s^{-2}
Max CoM-support foot divergence	0.85 m
Max trunk rotation, θ_{max}	$\pi/2$ rad
Max hip torque, τ_{max}	190 N.m
Control weight, c_1	1 m.s^{-1}
Control weight, c_2	10 rad.s^{-1}
Control weight, c_3	1000 m.s^{-2}
Control weight, c_4	300 m.s^{-3}
Control weight, c_5	300 rad.s^{-3}
Control weight, c_6	30 m

In all cases, the considered perturbations correspond to the average maximum permissible disturbances sustained by the subjects while obeying the stepping instructions. To be coherent with the studies, the comparison is made for the variables reported in each particular study. The studies from Hsiao-Wecksler and Robinovitch (2007) and Moglo and Smeesters (2005) report the *step* distances while the study from Cyr and Smeesters (2009a) reports the *stride* lengths. The difference between a step and a stride is shown in Figure 4.15, taken from Cyr and Smeesters (2009a). The step length is defined as the distance between successive foot placements while a stride length is measured from the starting position of the individual foot. Hence, for the feet initially aligned in the sagittal plane, step and stride lengths are the same only for first step but are different for successive steps (c.f. Figure 4.15).

Similarly, Hsiao-Wecksler and Robinovitch (2007) report the step landing time (T_{land}) which is the total time interval between the tether-release and step impact on ground. This time is composed of reaction, step preparation and legswing times ($T_{land} = T_{reac} + T_{prep} + T_{step}$, c.f. Chapter 2). For the other two studies (Cyr and Smeesters, 2009a; Moglo and Smeesters, 2005), the reported timings correspond to

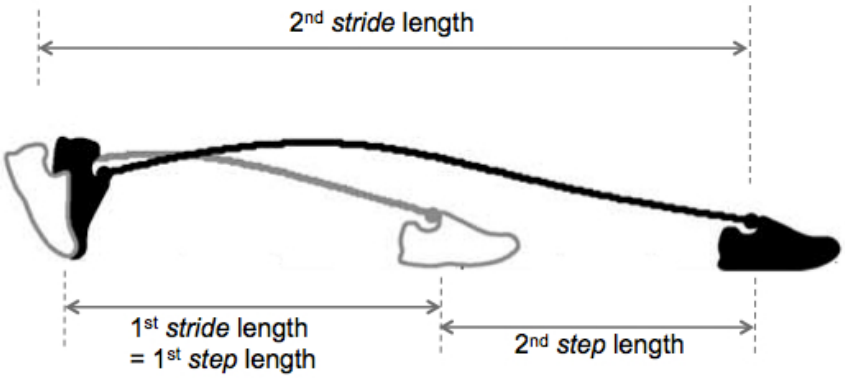

Figure 4.15: Difference between a step and a stride length. For the feet initially aligned the sagittal plane, both step and stride lengths are the same for the first step

T_{step}.

4.5.3 Stepping predictions with upper-body inertia

Let us start by considering the effect of upper-body inertia on the balance recovery behavior. At the first place, the step durations are fixed according to the respective studies as done in Chapter 3 (c.f. Table 3.2). The cost function (4.22) is minimized *without the swing foot acceleration term* to be able to analyze independently the effect of the upper-body inertia on the recovery step length. Figure 4.16 shows the comparison between experimental results (average $\pm$ s.d.) and model predictions for the 4 inclination scenarios of Hsiao-Wecksler and Robinovitch (2007). Black bars represent the results without upper-body inertial (UBI) considerations (as already presented in Chapter 3, with slight modification due to new constraints (4.15) and (4.16)). Grey bars represent model predictions with UBI. Clearly the predicted step lengths with UBI are reduced by 3-11%. More importantly, the results become closer to the average reported experimental values particularly for larger inclinations. This reinforces our hypothesis that UBI has a non-negligible role in these balance recovery tasks and its inclusion in the balance recovery model is imperative for accurate predictions.

Figure 4.17 shows the peak hip torque values used by our controller for the four scenarios alongwith a schematic representation of the final recovery posture. The con-

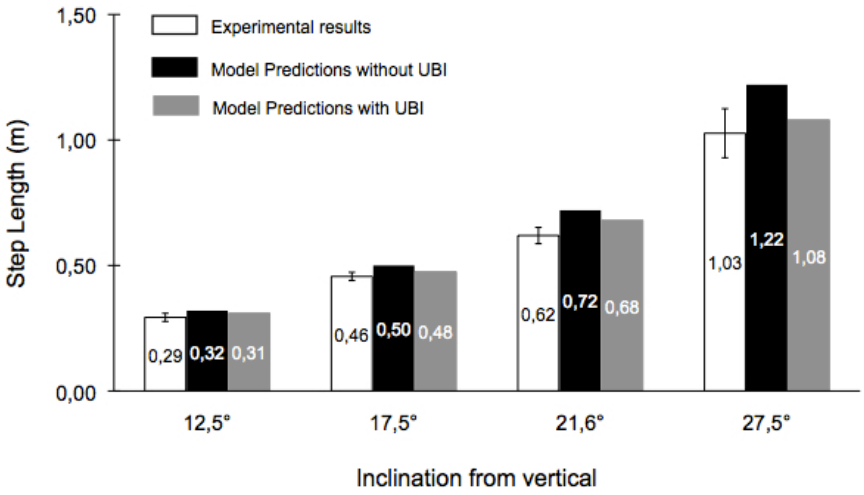

Figure 4.16: Step lengths for single step recovery scenarios from Hsiao-Wecksler and Robinovitch (2007): experimental (white bars, averaged across subjects $\pm$ one standard deviation) versus simulated (with and without UBI) results. The step timings are fixed in advance according to the reported values in the study.

troller produces a scaled use of UBI with the perturbation level both in terms of the peak hip torque and the upper-body rotation angle. Note that the knee joint is added for better visual comparison and is not the part of our prediction model.

Figure 4.18 shows the stride length comparison for the multiple-step recovery scenario of Cyr and Smeesters (2009a). In this case, the extensive use of UBI (peak hip torque of 176 N.m) results in a significant reduction of 2nd stride length. Interestingly though, the length of 1st stride (1 m) is unchanged even though the inertia wheel starts rotating as soon as the controller is activated. This points towards the importance of a larger first step to recover balance more effectively.

Figure 4.19 compares the snapshots of predicted balance recovery with that of an example subject reported by Cyr and Smeesters (2009a) at 3 key instants (before release and at the instants of first and second step impacts on ground). The comparison shows close resemblance between real and simulated recovery behavior. It is particularly interesting to observe the important knee flexion (equivalent to the reduction of pendulum length) during the 2^{nd} stride in experimental as well as simulated recovery

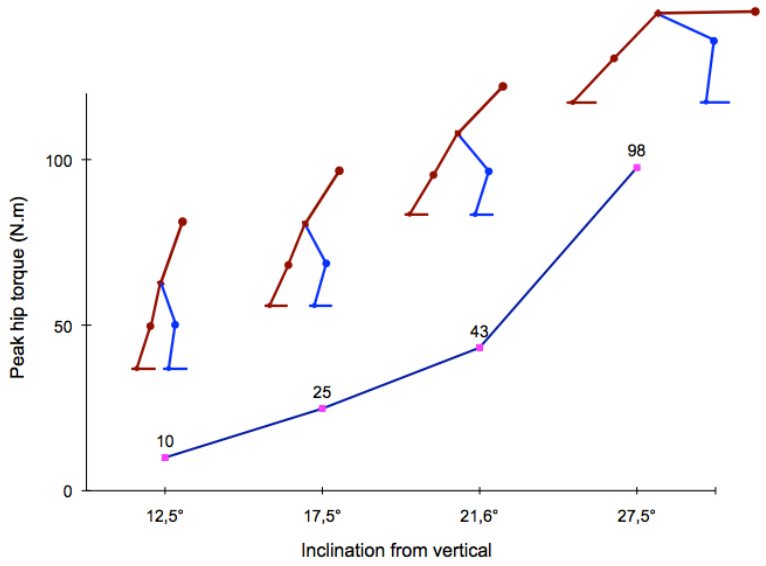

Figure 4.17: The peak hip torque values achieved during the 4 recovery scenarios from Hsiao-Wecksler and Robinovitch (2007) and corresponding final recovery postures of the mechanical model. Note that the peak hip torque and upper-body rotation angle are positively scaled with the perturbation level.

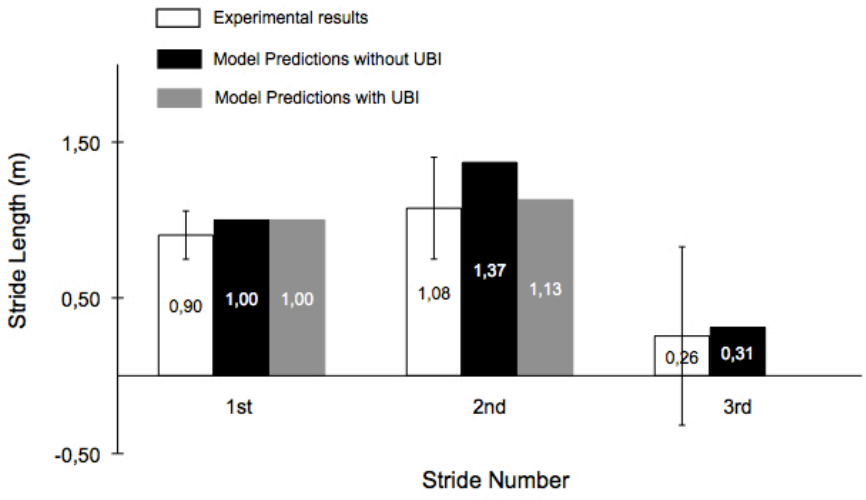

Figure 4.18: Stride length for multiple step recovery scenario from Cyr and Smeesters (2009a). Experimental (white bars, averaged across subjects $\pm$ one standard deviation) versus simulated (with and without UBI) results. Stride times are fixed in advance.

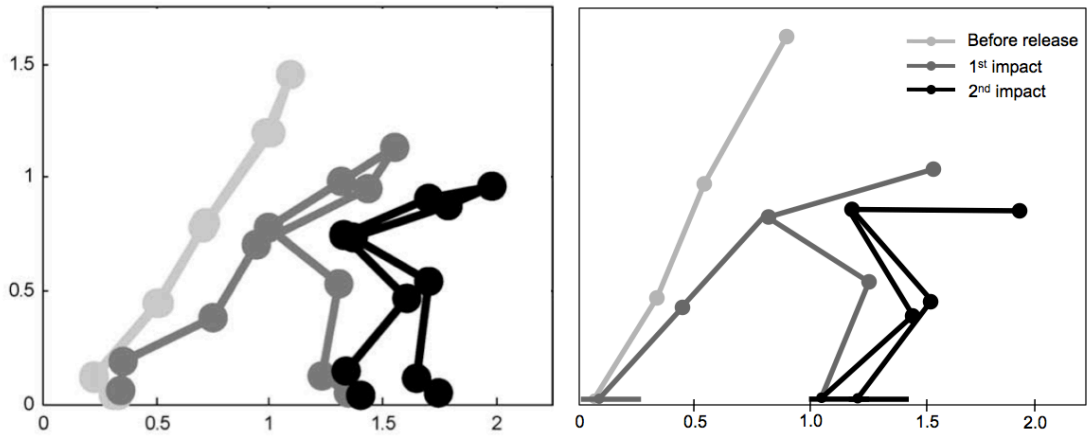

Figure 4.19: Evolution of the *mechanical* model during the predicted recovery for the scenario of Cyr and Smeesters (2009a). Note that the knee joint has been added for better visual comparison and is not the part of the model.

response. This justifies our choice of simple inverted pendulum as the human-body representation for these scenarios where the length of pendulum changes from one step to another.

4.5.4 Stepping predictions with step time optimization

Now we minimize our complete cost function (4.22) and introduce the automatic step time selection. The reaction and step preparation times are set to 75 ms and 150 ms respectively as before while the legswing time T_{step} is optimized between 50-400 ms with 25 ms increment. The control weight c_3 is set to 1000 m.s^{-2}. Figures 4.20 and 4.21 show the optimized step length and step landing time results for Hsiao-Wecksler and Robinovitch (2007). The comparison is made with UBI (grey plots) as well as without (black plots). Overall, the predicted step lengths and step landing times show reasonable accuracy with respect to the experimental values. However, for the smallest inclination of 12.5°, the predicted step length is significantly reduced against an overestimated step landing time. This points towards a two-way effect of penalizing the swing foot acceleration for smaller disturbances: the cost function is minimized for larger step duration while simultaneously reducing the step size, if the disturbance is not too large.

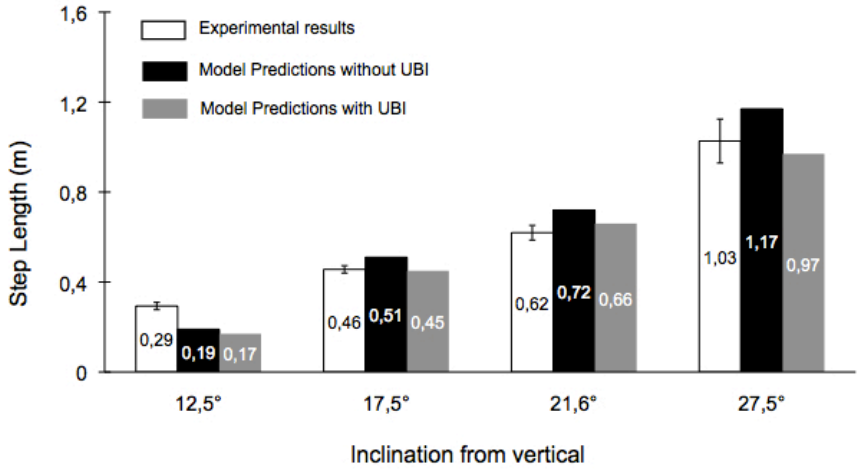

Figure 4.20: Step lengths for single step recovery scenarios from Hsiao-Wecksler and Robinovitch (2007) with optimization of step landing times: experimental (white bars, averaged across subjects $\pm$ one standard deviation) versus simulated (with and without UBI) results.

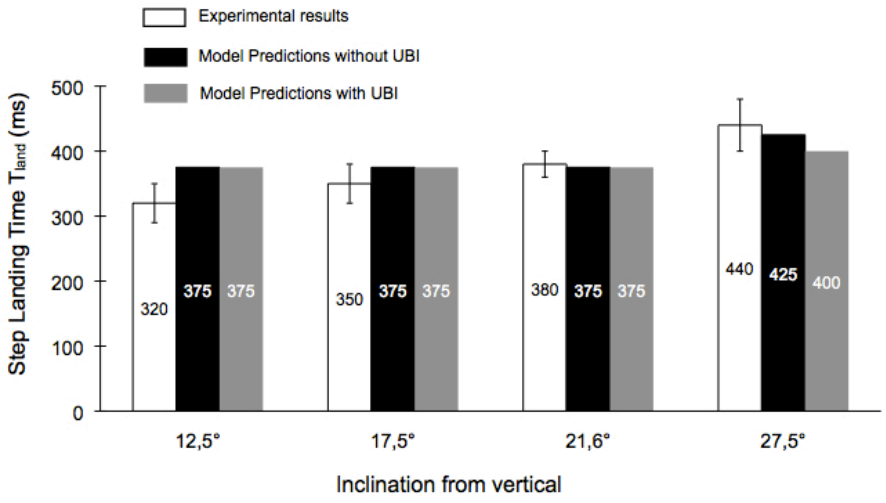

Figure 4.21: The predicted step landing times T_{land} for the 4 perturbation scenarios of Hsiao-Wecksler and Robinovitch (2007), with and without UBI considerations compared against experimental values (white bars)

The peak hip torque again scales well with the inclination level (c.f. Figure 4.22). The use of UBI did not affect the landing time optimization results, except for the largest inclination where it was reduced by 25 ms.

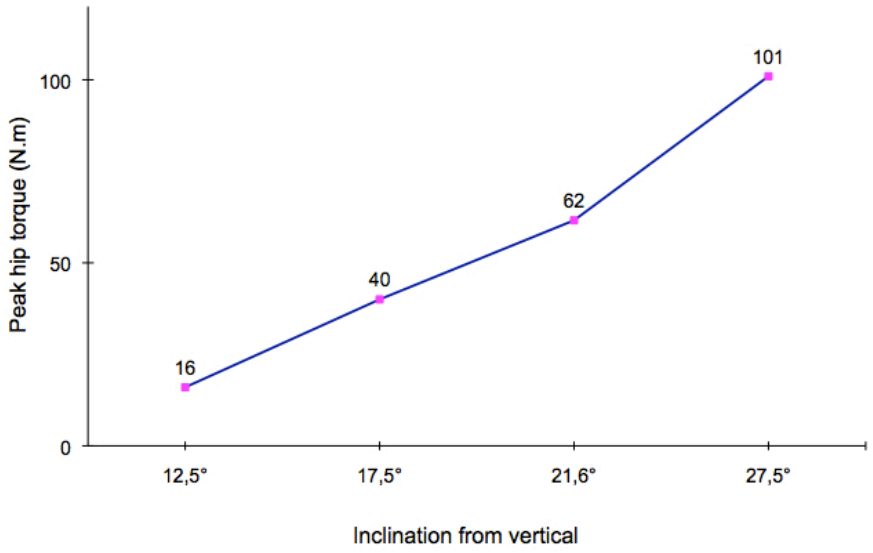

Figure 4.22: The peak hip torque values achieved during the 4 recovery scenarios from Hsiao-Wecksler and Robinovitch (2007) when T_{step} is also optimized.

Figures 4.23 and 4.24 show the multiple step recovery results for Cyr and Smeesters (2009a). With or without UBI, the predicted stride times match well (within 1 s.d. of experimental data) with the reported average values. However, with UBI, a larger stride time (200 ms) results in an even larger first stride length. Note that the third step, reported by Cyr and Smeesters (2009a) but not predicted by the model, was only observed for two out of 28 subjects.

Lastly we simulate the single-step recovery scenario from Moglo and Smeesters (2005) where the subjects are inclined as well as are pulled forward at the waist level. The study reports two different combinations of lean angle and pull forces beyond which recovery is not possible using a single forward step. For simulations, average values of lean angles and forces are taken as inputs while the step length and the swing time T_{step} are predicted. The force is applied horizontally at the CoM level. Other parameters are kept the same as in Table 4.3.

Comparison between experimental and simulated results is shown in Figures 4.25 and 4.26. Being at the single-step recovery limit, almost identical step lengths and timings are reported in the study for both perturbations, which match well with our

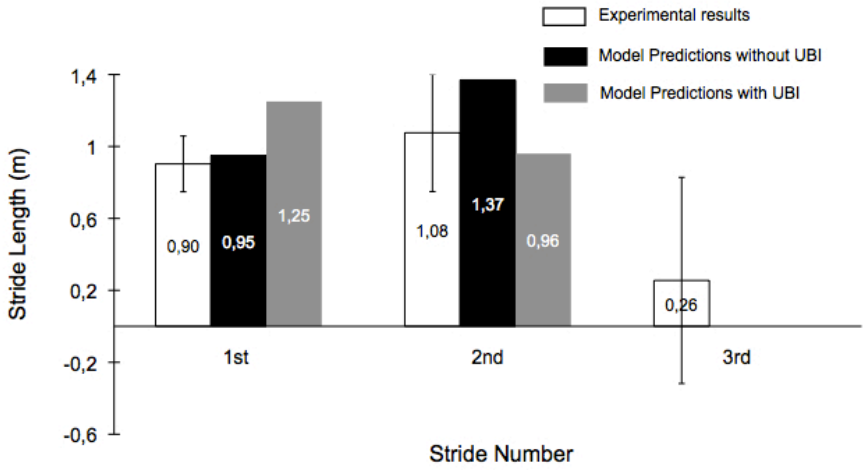

Figure 4.23: Stride length results for multiple step recovery scenario from Cyr and Smeesters (2009a) where stride times are also optimized. Experimental (white bars, averaged across subjects ± one standard deviation) versus simulated (with and without UBI) results.

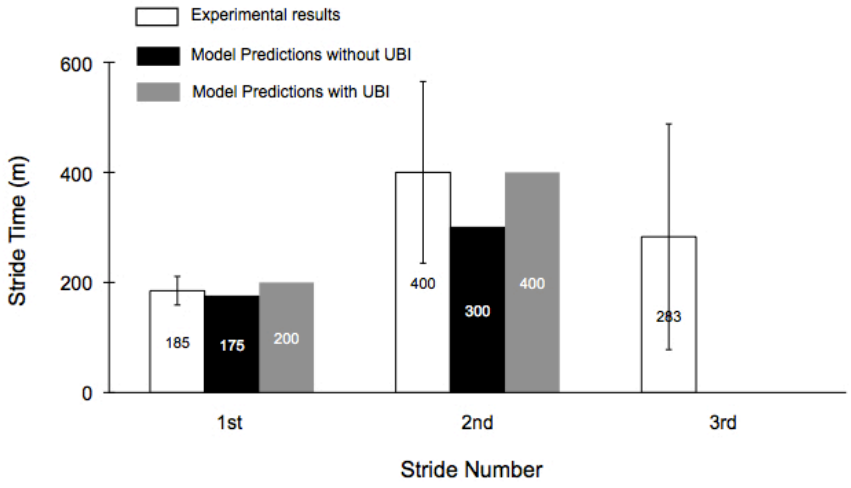

Figure 4.24: The optimized stride timings, with and without UBI, compared against experimental values for multiple step recovery scenario from Cyr and Smeesters (2009a).

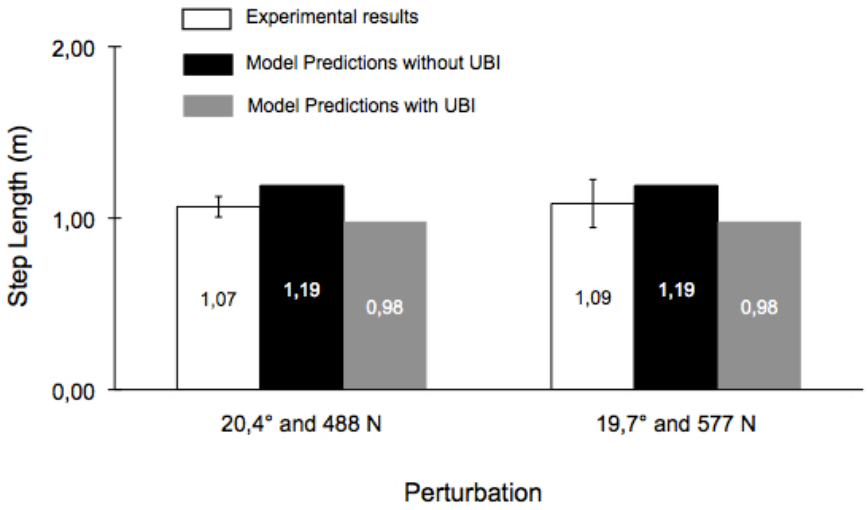

Figure 4.25: The single step recovery predictions for 2 recovery scenarios from Moglo and Smeesters (2005), with and without UBI compared against experimental results (white bars).

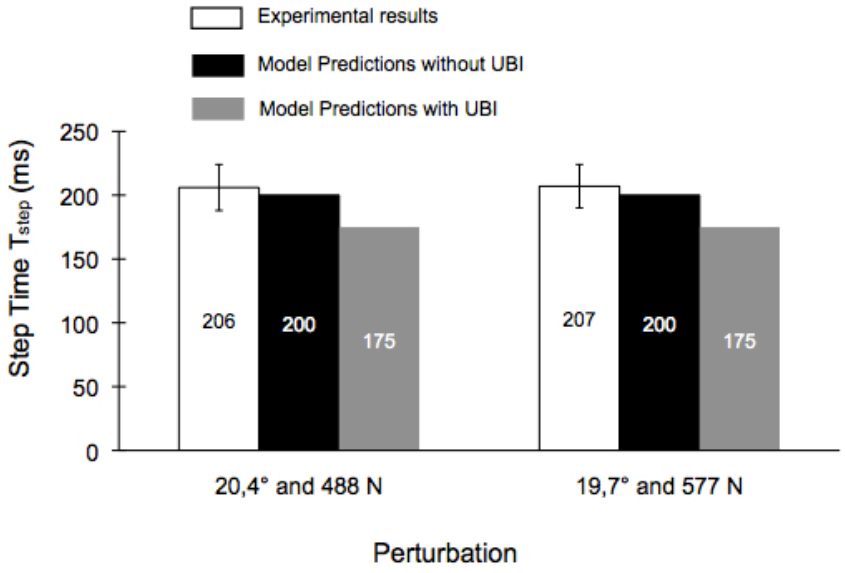

Figure 4.26: Optimized step durations for 2 recovery scenarios from Moglo and Smeesters (2005).

predicted results. When predicted with the upper-body inertia (grey bars), the step length is reduced by 21 cm (c.f. Figure). This reduction is a combined result of UBI usage (peak hip torque = 80 N.m) and the selection of a smaller swing phase (175 ms with UBI against 200 ms without, c.f. Figure 4.26). Overall in both cases, the predicted step characteristics are within reasonable range of reported average experimental results.

4.6 Conclusion

In this chapter, we presented a comprehensive balance recovery scheme based on the Model Predictive Control (MPC). While employing a simple prediction model (linear inverted pendulum + inertia wheel), the MPC scheme demonstrated the capacity to predict an adaptive stepping response to external postural disturbances while simultaneously regulating the ankle, hip and stepping strategies. In the last section, the model predictions were also compared against the experimental data and were shown to match well, both in terms of step lengths and timings. The use of upper-body inertia scaled with the perturbation level which is consistent with the experimental observations while the controller parameters (control weights, length of horizon, constraints) were kept the same in all cases.

In the next chapter, we will further test this tool for different and slightly complex disturbance scenarios such as for platform type disturbances.

Chapter 5

Simulating More Complex Behaviors

In the previous chapter, we developed a comprehensive model predictive control scheme capable of producing realistic results when compared to human balance recovery data. However, the simulated disturbance scenarios were relatively simple in at least two ways:

1. The disturbances (forward inclinations and pull forces) were *constant* in the sense that their properties did not change during the course of balance recovery. The pull forces were applied instantaneously while the forward inclinations triggered a fall purely under the effect of gravity, which is already taken into account in the predictive system dynamics.

2. The balance was disturbed to the *maximum* recoverable limits of the subjects for a given stepping condition. This required the subjects to exert their best effort to recover balance by minimizing the forward speed as quickly as possible.

On the other hand, the disturbances observed in the public transportation vehicles are of a different nature. These disturbances are far from being instantaneous, which necessitates particular attention to its varying profile and appropriate adjustment of the recovery strategy. In addition, typical real-life disturbances do not necessarily challenge the balance to its maximum limits. The recovery strategies in these so-called

sub-maximal scenarios may be significantly affected by different biomechanical criteria such as economy of motion and/or minimum effort.

In this chapter, we will explore such scenarios. We will simulate the disturbances of translating platform type which are the most common means of replicating the public transport scenarios. We will also explore how our relatively simple balance recovery model can be tuned to obtain sub-maximal recovery behaviors. In the last section, we will conduct a preliminary study on the effect of age-related parameters on the predicted recovery response.

We start by simulating the balance recovery cases from Robert (2006) which is one of the rare studies to report the acceleration profile of the platform and the complete kinematics of multiple step recoveries.

Contents

5.1 Simulating platform disturbances

5.1.1 Experimental data

Let us recall the disturbance scenario discussed in Chapter 3 (Section 3.3) where the Capture Point predictions were compared against first step experimental results for two different scenarios from Robert (2006). In this section, we present the detailed experimental results along-with multiple step lengths and timings before trying to predict these results with our MPC controller.

The study from Robert (2006) designed 2 different recovery tasks for the same disturbance level. Subjects stood on a platform which was accelerated backward unexpectedly (c.f. Figure 5.1 for platform acceleration profile). 8 volunteers participated in a 1^{st} series of experiments where a large space was provided for the subjects in front of them to take several steps. Among them, 4 participated in a 2^{nd} series, where the space was limited to less than 1 m by means of an obstacle (Figure 5.2). Ground reaction force and kinematics were recorded, body segments' inertial parameters were estimated using regression tables and the experimental whole body center of mass (CoM) position and velocity were computed.

Experimental Results

The experimental results for the main kinematic parameters are summarized in Table 5.1. It can be perceived that there is a marked difference between the behavior of the subjects in the two scenarios, despite being subjected to the same level of disturbance. In the 1^{st} series, where a large space is provided to the subjects, they take, on average, 3 steps to recover balance and cover a large distance (1.85 m on average). On the other hand, in the 2^{nd} series, balance is achieved using a single forward step, followed sometimes by a very small second step. However in this case, 1 out of 4 subjects could not avoid the obstacle and was not included in the analysis.

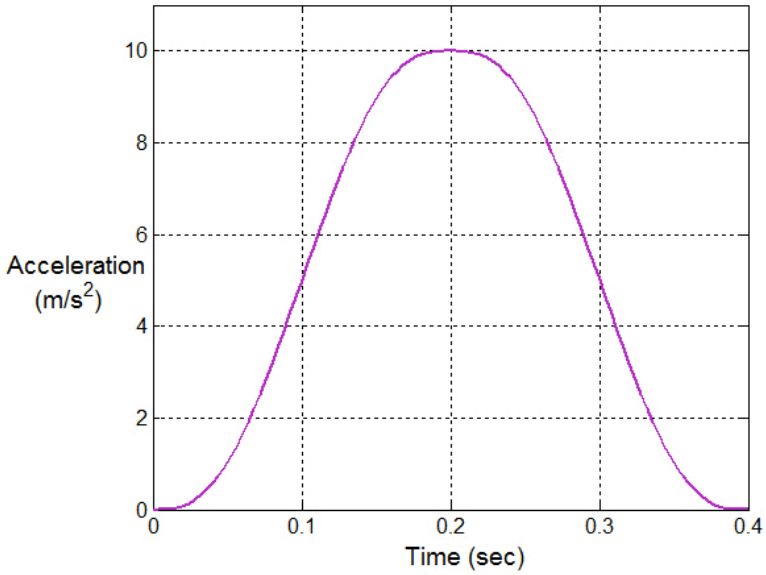

Figure 5.1: The platform disturbance profile used to destabilize the subjects by (Robert, 2006).

Figure 5.2: The two recovery tasks given to the subjects against the same level of disturbance; large available space (left) vs. limited space (right).

Table 5.1: Complete step kinematics, previously unpublished, for the two balance recovery scenarios considered in Robert (2006)

Scenario	Reaction time, T_{reac}	Step preparation time, T_{prep}	Leg swing time(s), T_{step}	Step lengths
Large space	94 ± 10 ms	258 ± 43 ms	209 ± 45 ms, 364 ± 80 ms, 384 ± 77 ms	0.79 ± 0.08 m 0.60 ± 0.15 m 0.44 ± 0.13 m
Limited space	113 ± 12 ms	227 ± 44 ms	188 ± 18 ms 168 ± 146 ms,	0.88 ± 0.11 m 0.09 ± 0.09 m

Remarks

These experimental results underline the importance of the instructions or task constraints on the balance recovery strategy observed in some previous studies (Adkin et al., 2000; McIlroy and Maki, 1993). However, little has been reflected about the biomechanical criteria which govern this difference. In the author's view, this difference can possibly be explained in terms of the optimization principles. It is generally accepted that human movement tasks (such as reaching a target, walking, sit-to-stand etc) tend to fulfill some sort of optimality criterion. Several performance criteria have been proposed and validated against the experimental data. For example, it has been demonstrated that in hand-reaching motions, humans tend to minimize the jerk of motion to produce smooth trajectories (Flash and Hogan, 1985; Hogan, 1984). In more complex motions such as walking or gymnastics, minimum energy and/or effort cost produce realistic motion trajectories (Anderson and Pandy, 2001; Leboeuf et al., 2006). Other performance criteria include minimum torque change (Kuzelicki et al., 2005; Uno et al., 1989) and time derivative of muscle forces (Pandy et al., 1995).

Though the above studies primarily considered voluntary motions as opposed to reactive motions in case of balance recovery, it is reasonable to assume that the stepping decisions in a balance recovery tasks are also influenced by similar biomechanical factors when not subjected to extreme situations. However, the relative predominance of these criteria may change from one recovery task to another. In case of *maximal* performance (e.g. limited recovery space), the primary objective is to recover balance

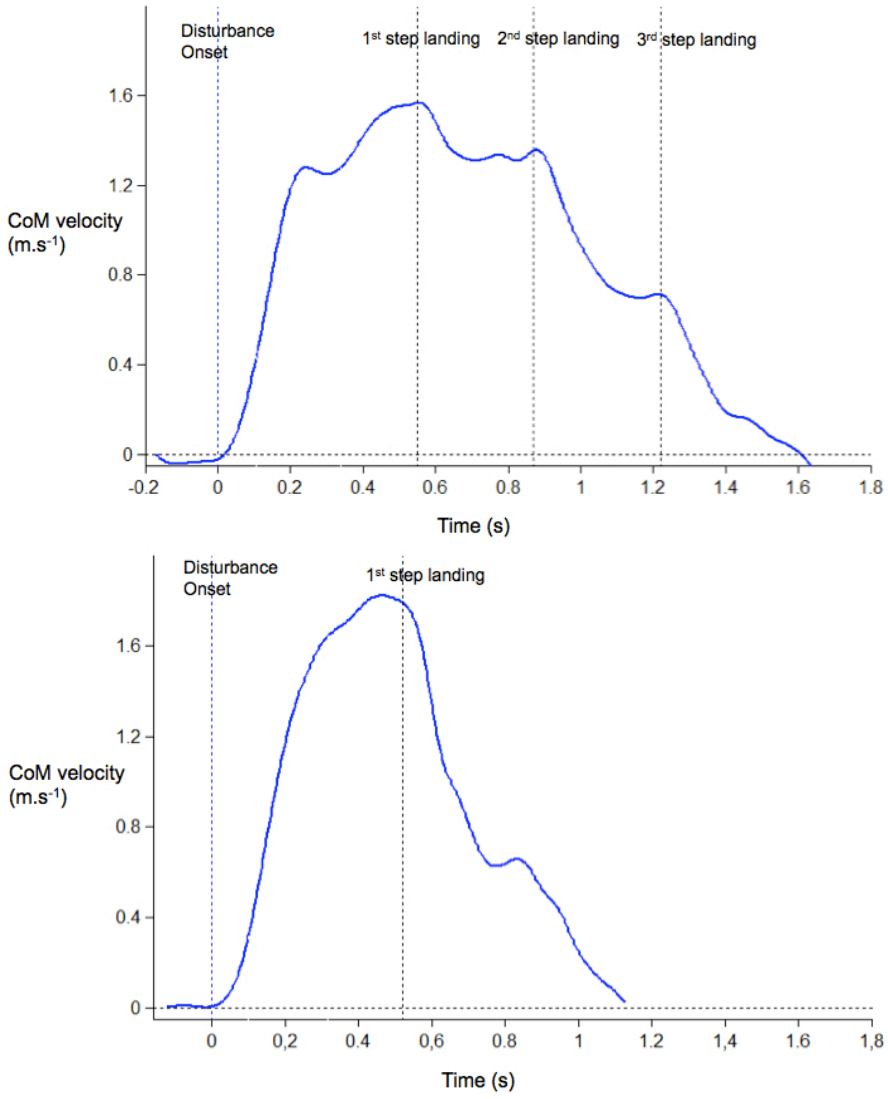

Figure 5.3: Time profiles of CoM velocity of an example subject in both recovery tasks; large available space (top) vs. limited space (bottom).

by minimizing the speed of motion as quickly as possible. However, in case of sub-maximal situations (such as the large space scenarios), the objective may evolve to include the trajectory smoothness and/or stepping effort minimization. The difference between the two behaviors can clearly be seen in the time profiles of the subjects' CoM velocities (c.f. Figure 5.3). In case of a large available space, the velocity is smoothly brought back to zero over a larger period of time.

We now simulate these recovery scenarios with our MPC controller and test its ability to predict the stepping characteristics in both scenarios.

5.1.2 Simulations

To simulate the translating platform scenario, the mechanical model is considered mounted on a moving cart (Figure 5.4). The cart is given a backward acceleration similar to the one applied during the experiments (c.f. Figure 5.1). The standard dynamics of the inverted pendulum-on-cart system is solved and the resulting pendular state is fed to the MPC controller. The resulting feedback is then applied back to the system. The cost function used in the controller is the same as in Chapter 4 and is reproduced here:

$$\min \ \frac{1}{c_1^2}\|\dot{C}_{k+1}\|^2+\frac{1}{c_2^2}\|\dot{\Theta}_{k+1}\|^2+\frac{1}{c_3^2}\|\ddot{F}'_{k+1}\|^2+\frac{1}{c_4^2}\|\dddot{C}_k\|^2+\frac{1}{c_5^2}\|\dddot{\Theta}_k\|^2+\frac{1}{c_6^2}\|Z_{k+1}-F_{k+1}\|^2 \tag{5.1}$$

Using the parameters listed in Tables 5.1 and 5.2, the predicted step length results for the two scenarios are shown in Figure 5.5. The control weights c_1 to c_6 are chosen in the same way as in Chapter 4 where the cost function terms other than the CoM velocity are weakly penalized. It can be seen that the controller predicts a single forward step in both cases. This prediction is somewhat closer to the limited-space scenario (Figure 5.5, right) confirming our earlier hypothesis that in such situations, subjects aim to minimize the CoM velocity as quickly as possible. However, such a setting is far from predicting the sub-maximal situation (Figure 5.5, left) where several steps are observed during the experiments.

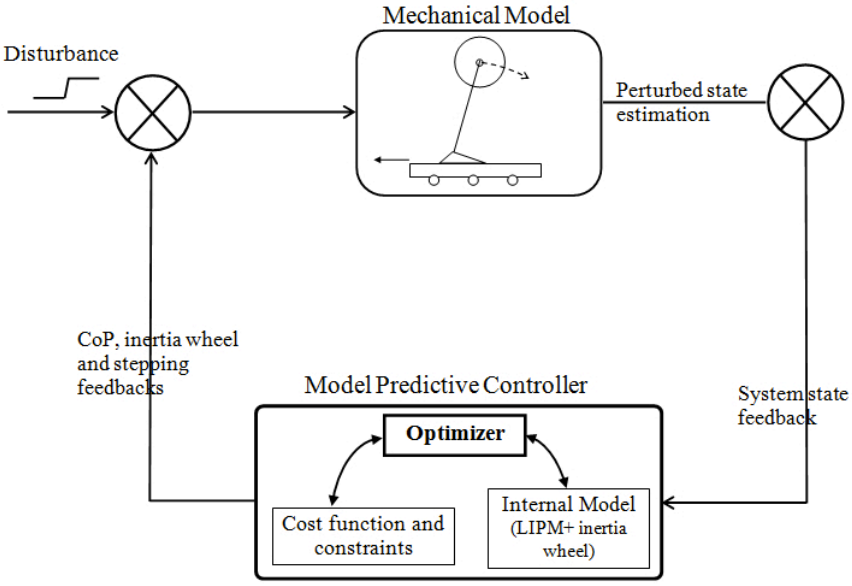

Figure 5.4: The implemented feedback loop with MPC controller in the loop.

Table 5.2: Controller parameters

Parameter	Value
Reaction time, T_{reac}	100 ms
Step preparation time, T_{prep}	250 ms for the 1^{st} series, 225 ms for the 2^{nd} series
Leg swing time, T_{step}	Chosen by the controller
No of samples, N	40
Sampling Time, T	25 ms
Horizon length, N×T	1 sec
Simulation Time	2 sec
Max foot acceleration, $\ddot{f}'_{max}$	180 m.s^{-2}
Max CoM-support foot divergence	0.85 m
Max trunk rotation, θ_{max}	$\pi/2$ rad
Max hip torque, τ_{max}	190 N.m
Control weight, c_1	1 m.s^{-1}
Control weight, c_2	10 rad.s^{-1}
Control weight, c_3	1000 m.s^{-2}
Control weight, c_4	300 m.s^{-3}
Control weight, c_5	100 rad.s^{-3}
Control weight, c_6	30 m

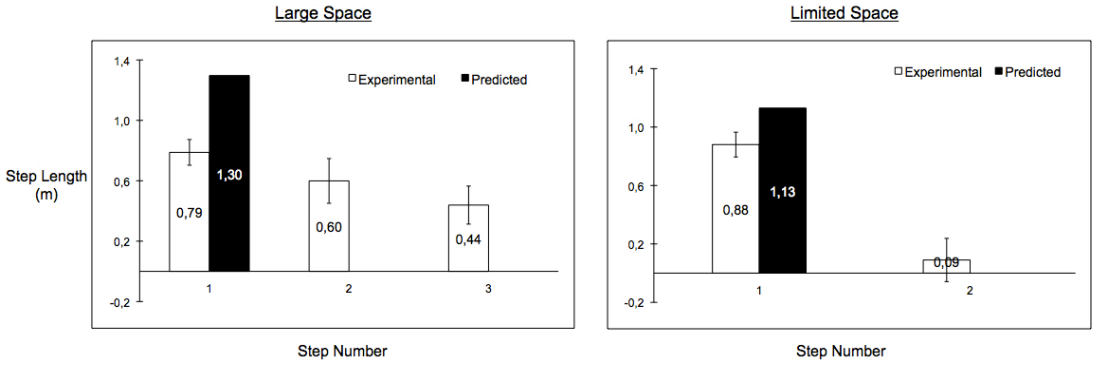

Figure 5.5: The simulation of two balance recovery tasks (large space vs. limited space) using the same controller parameters (c.f. Table 5.2.) The predicted stepping behavior is closer to the limited space experimental scenario (right) than with the large space.

Simulating the sub-maximal behaviors

To simulate the large space scenario, more emphasis on biomechanical performance criteria may be needed in our cost function. This is not quite straightforward as most of such criteria involve *dynamic* variables (joint torques, muscle forces etc) as opposed to the *kinematic* variables on which our simple model is based (i.e. motion and its derivatives). However, conceptually the acceleration and joint torques can be regarded as equivalent terms in that minimizing one variable directly results in regulating the other. Hence, the stepping effort minimization can be introduced by penalizing more strongly the swing foot acceleration term $\|\ddot{F}'_{k+1}\|^2$ in our cost function (5.1). Similarly, the desire to generate smoother motion trajectories can be directly represented by strongly penalizing the jerk of the CoM term $\|\dddot{C}_k\|^2$ in our cost function. The effect of varying their corresponding control weights c_3 and c_4 on the first step length are shown in Figure 5.6. The resulting number of forward steps is also noted at the bottom of each plot.

It is evident in Figure 5.6 that the more we penalize the CoM jerk and foot acceleration terms (smaller c_3 and c_4 values), the more the first step lengths are reduced and multiple steps preferred. Using $c_3 = 200$ m.s^{-2} and $c_4 = 30$ m.s^{-3}, exactly 3 forward steps are predicted by our controller whose lengths are compared against the experimental data in Figure 5.7. The comparison shows close agreement between

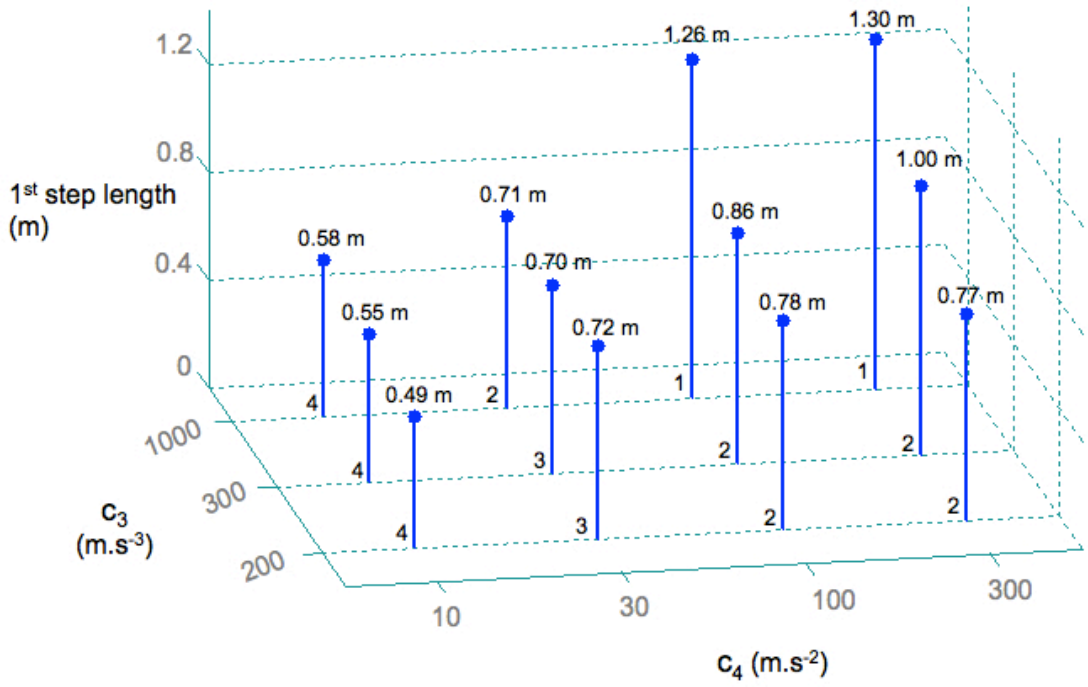

Figure 5.6: The lengths of predicted first step against varying values of control weights c_3 and c_4, which penalize the CoM jerk and swing foot acceleration terms respectively. The number at the bottom of each plot represent the total number of predicted forward steps. It can be seen that the smaller control weight values (implying stronger penalization of corresponding cost function terms) result in shorter step lengths and more steps.

experimental and predicted results where the model predictions are within the single standard deviation of the experimental data for all steps. The corresponding step times (not shown) are 200, 300 and 500 ms respectively for 3 steps which again match well with the experimental data (c.f. Table 5.1).

Figure 5.8 compares the corresponding evolution of the predicted CoM velocity (continuous plot) with that of a real subject (dotted plot). In both cases, the velocity of the CoM is smoothly brought to zero over a longer period of time. Based on this result, we can speculate that maximizing smoothness and/or minimizing stepping effort are important criteria to consider while simulating sub-maximal scenarios.

5.1.3 Conclusion

The purpose of this section was to demonstrate the ability of our MPC controller to generate different balance recovery behaviors by modifying the relative penalizations of the cost function terms. It turns out that in the maximum performance scenarios, minimizing the CoM speed should be the major criterion ($c_1 \ll c_3,\ c_4$) while in the sub-maximal situations, other performance criteria such as motion smoothness and effort minimization become equally important.

Note that in this section, the control weights were manually adjusted to simplify our analysis. However a more sophisticated approach is sought in the future which would involve a more systematic definition of the task constraint (e.g. maximum recoverable distance). The controller would then perform the necessary tuning to generate the recovery reaction, resulting in a unified scheme for all situations. Moreover, this study only explored two possible performance criteria to generate distinct recovery patterns. However, other biomechanical criteria (e.g. energy optimization), different post-step recovery behaviors (e.g. pendular vs. free-fall evolution) or cognitive aspects may also influence these recovery behaviors and would be investigated in the future.

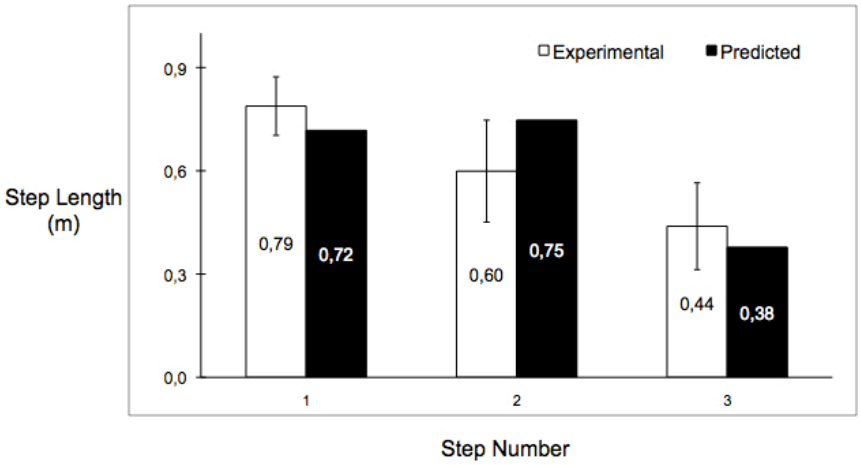

Figure 5.7: Comparison of average experimental step lengths with predicted lengths with $c_3 = 200$ m.s^{-2} and $c_4 = 30$ m.s^{-3}.

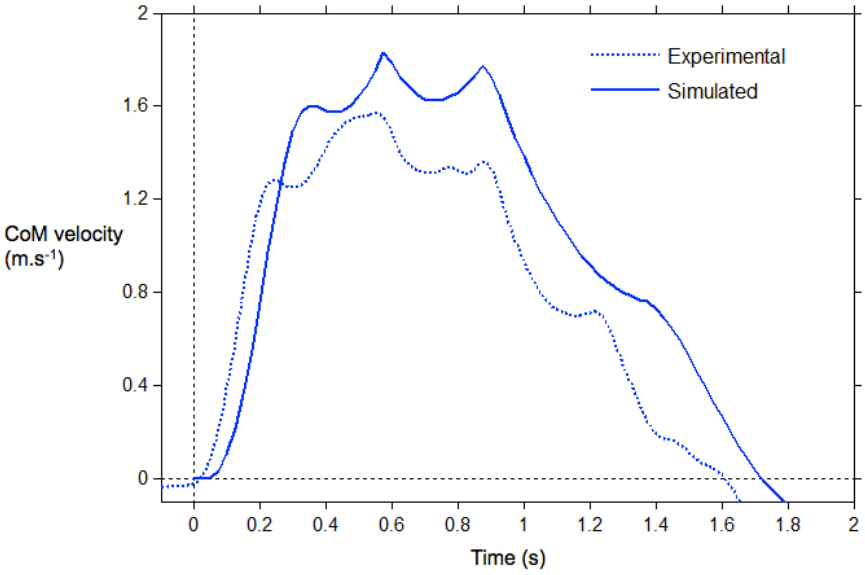

Figure 5.8: Comparison between the CoM velocity for a real subject (dotted plot, large space scenario) and the simulation (continuous plot) with $c_3 = 200$ m.s^{-2}, $c_4 = 30$ m.s^{-3}.

5.2 Simulating longer disturbances with Forecasting

As mentioned in the introduction, the daily-life disturbances observed in the public transport vehicles persist for longer periods of time (actually for several seconds). Under these conditions, maintaining or recovering one's balance involve two important properties. First is a rough estimation of the future evolution of the disturbance (disturbance forecasting) which helps to plan necessary recovery actions in advance. Second is the frequency at which this recovery action is/can be re-planned for possible variations in the disturbance level. It is reasonable to hypothesize that a higher re-planning frequency and a more accurate disturbance forecasting would improve recovery response to longer disturbances.

On the other hand, we previously tested our balance recovery (BR) tool against either the constant or instantaneous disturbance situations (Chapter 3 and 4) or against short platform disturbances (Section 5.1.2, disturbance duration $=$ 400 ms). The controller was run in a continuous feedback manner and its internal model (LIP model $+$ inertia wheel) estimated the system's evolution over a future time horizon purely under the effect of gravity. Arguing that the prediction of the external disturbance plays an important role in tackling longer disturbances, we further develop our BR tool in this section to include appropriate disturbance forecasting. Our objective will be to explore how the recovery action is affected by the presence or absence of this property. Moreover, we will also explore the effect of re-planning frequency on the recovery action, which can be an important factor for variable disturbance levels. Given that these two properties are also closely related to the cognitive aspects of balance recovery, their inclusion will also allow to study the effects of cognitive factors on the balance recovery performance.

5.2.1 Disturbance forecasting

We take a familiar situation experienced by the standing passengers during an emergency braking situation in urban trams and railway vehicles. The disturbance profile is shown in Figure 5.9 which has been exploited in an experimental setup by Verriest et al.

(2010). The total duration of the disturbance is 2s divided equally into a constant jerk (4 m.s^{-3}) phase followed by a constant acceleration (4 m.s^{-2}) phase.

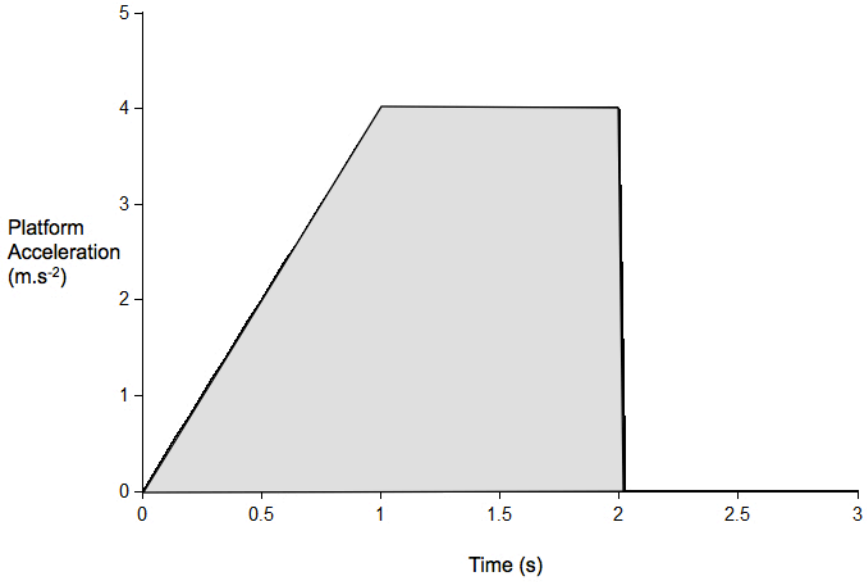

Figure 5.9: The typical acceleration profile of the emergency braking condition in urban guided vehicles.

In the context of our model, the disturbance forecasting can be defined as the estimation of the future disturbance magnitude and duration made by the controller as soon as the disturbance starts and is refreshed until the disturbance disappears. Similarly, the frequency of re-planning can be defined in terms of the Controller Sampling Time (CST) which is the time delay between each call of the controller. The control is considered continuous if the controller is called at each time step T (= 25 ms) of the simulation, while intermittent if CST = nT, where 'n' is any integer greater than 1.

Simulations are performed for 4 different forecast scenarios:

(a) No disturbance forecasting, where no information is given to the controller about the future evolution of the platform acceleration profile.

(b) Mean acceleration forecasting, where the controller makes its own estimation of the future disturbance profile based on the previous time history of the actual

disturbance. In this case, the controller takes the mean platform acceleration experienced over the last 1s and projects it the to the next 1s as the future expectation (c.f. Figure 5.10, left).

(c) Instantaneous acceleration forecasting, where at each instant, the controller estimates the current real platform acceleration to continue during the next 1s (c.f. Figure 5.10, right).

(d) Perfect forecasting, where the controller is informed about the exact future platform acceleration profile at each sampling time.

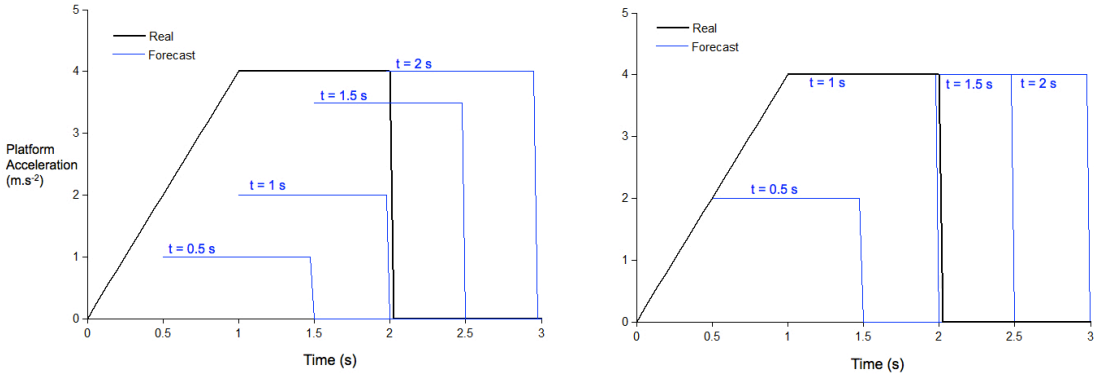

Figure 5.10: The forecasted platform disturbance profiles (dotted blue) are shown with respect to the actual profile (black plot) at four sample instants (t = 0.5, 1.0, 1.5, 2 s) after the disturbance onset. At each instant, the controller forecasts the disturbance to continue for the next 1s: Left: With an acceleration equal to the average of past 1s (scenario b), or Right: With the same instantaneous acceleration (scenario c). When the actual disturbance disappears at t= 2s, the forecast is also made to zero.

5.2.2 Implementation

The information about the platform disturbance is integrated in the internal model of the MPC controller. Lets recall the basic dynamic equation of the LIP model with inertia wheel from Chapter 4:

$$\ddot{c}_x = \frac{g}{h}(c_x - z_x) - \frac{j}{mh}\ddot{\theta} \tag{5.2}$$

The disturbance information is integrated in terms of the platform acceleration resulting in the following dynamics equation:

$$\ddot{c}_x = \frac{g}{h}(c_x - z_x) - \frac{j}{mh}\ddot{\theta} \pm \ddot{x}^{pf}_{Fcast} \tag{5.3}$$

where $\ddot{x}^{pf}_{Fcast}$ is the controller's estimation of the platform acceleration.

The feedback loop is implemented as before (c.f. Figure 5.4) using the controller parameters given in Table 5.2. The efficiency of a recovery action is measured in terms of the net distance traveled by the CoM before coming to a complete halt. The step timings are fixed in advance to 0.3 s to simplify post-simulation analysis.

5.2.3 Results

Let's first consider the results with the continuous control mode (CST = 25 ms) in Figure 5.11. Plots on the left show the time profiles of CoM position (black) along with the ankle positions of the corresponding foot placements (blue dots). The plots on the right show the corresponding evolution of the CoM velocity. t=0 indicates the onset of disturbance.

It can be seen that there are marked differences between the foot placements and the resulting distance traveled by the system depending upon the accuracy of forecasting. In the first scenario, where the disturbance forecasting is absent, the resulting reaction is much slower during 1s following the disturbance onset. During this phase, the relatively small disturbance level together with the absence of any forecasting results in negligibly small initial steps. However, as the disturbance peaks to 4 m.s^{-2} at t = 1s onward, larger steps are required to compensate for the earlier latent response resulting in a large overall CoM distance (1.76 m).

The second row of the figure shows the result for the scenario (b) where the controller makes its own estimation of the future acceleration profile based on the previous 1s time history of the actual platform acceleration. Even though the forecasted evolution is far from being accurate (see Figure 5.10), the resulting recovery response

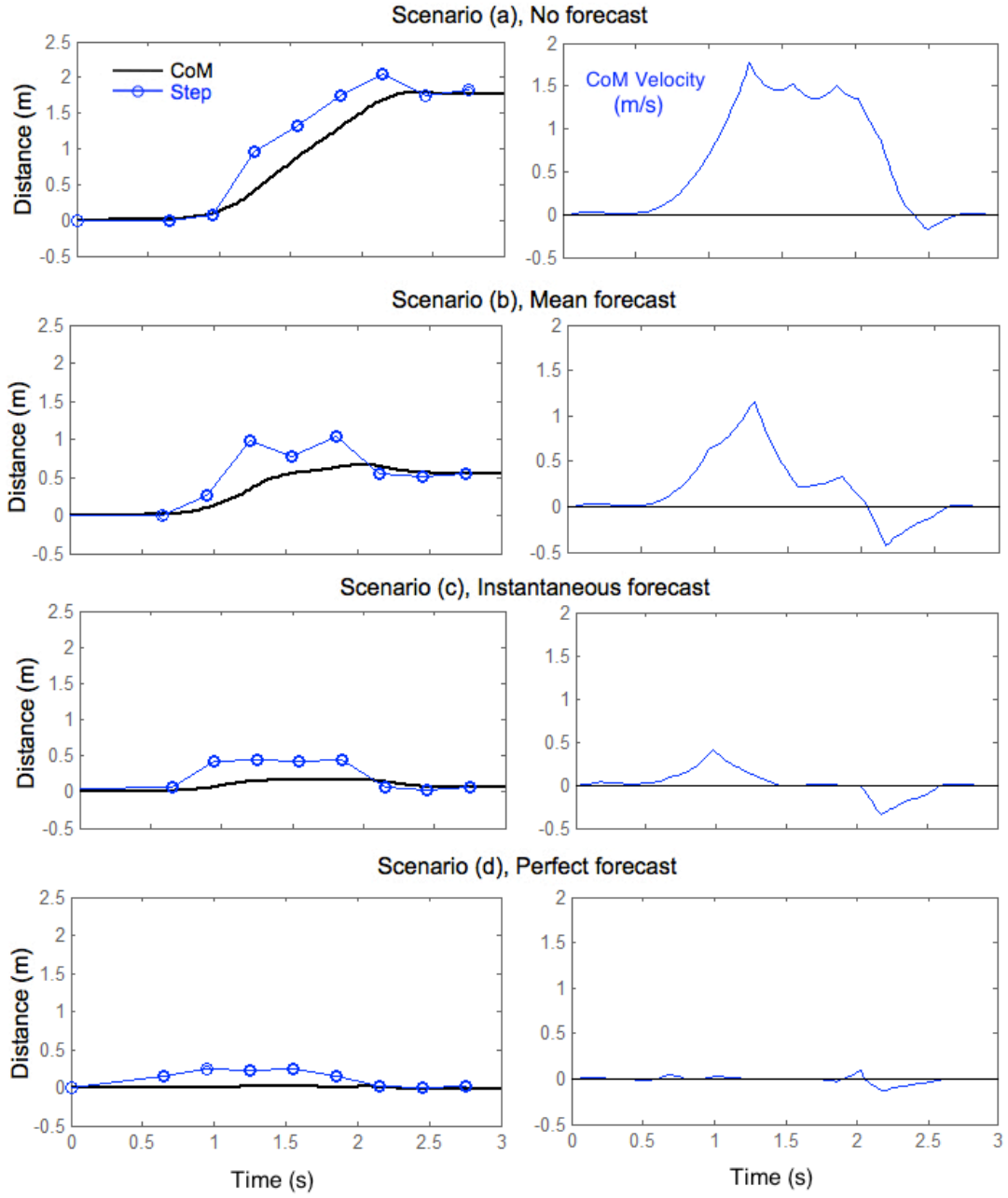

Figure 5.11: The predicted recovery behavior under the emergency braking scenario (c.f. Figure 5.9) with no or varying levels of disturbance forecasting. Time profiles of CoM position (left, black plot) and velocity (right) are plotted. The step positions are indicated with blue dots.

is much improved in this case. The second step is placed at a relatively larger distance while the maximum CoM excursion is limited to around 0.66 m. Also note that after the actual disturbance vanishes after t = 2s, the CoM velocity slightly slides to the negative side before being brought to zero again. This phenomenon is typical of an over-estimated disturbance forecast, since the controller still expects the disturbance to continue for another 1s (c.f. Figure 5.10, t=2 s). A back step is actually taken to restabilize the system.

The third row shows the result for the scenario (c) where at each instant, the controller assumes the platform to move with the current acceleration during the next 1s. In this case, the 2^{nd} step is placed even farther due to the expectation of relatively larger platform disturbance and the resulting recovery distance is even more reduced. Interestingly, during the later part of the peak acceleration phase (t = 1-2 s), the velocity is completely converged to zero as the controller expectation matches well with the actual disturbance in this phase. This phenomenon is even more pronounced throughout the scenario (d) where the controller is fed with the exact future platform motion profile. In this case, the steps are placed in such a way that the upcoming disturbance is completely mitigated producing minimal deviation of CoM velocity from its reference zero value.

In short, the results show good agreement with our hypothesis about the positive correlation between the disturbance forecast accuracy and the efficiency of the recovery action.

Frequency of re-planning

In the above results, the controller is run in a continuous manner (CST = T) meaning that any variation in the system's state is readily detected by the controller and the recovery strategy is re-planned. Now lets observe how the recovery action, in terms of maximum recovery distance, is affected if the controller action is refreshed intermittently. For this purpose, we simulate the above scenarios with different values of the controller sampling times (CST = 50, 100, 150, 200 ms) and plot the resulting recovery distances in Figure 5.12. Clearly, the recovery distance increases with the CST

value in all cases, except where the exact disturbance is fed to the controller (scenario (d)). Also observe that the better the forecasting accuracy, the lesser is the effect of the CST on the recovery distance. Overall this result shows the importance of quick motion re-planning in case of longer disturbances, suggesting a particular attention to its varying profile for effective recovery.

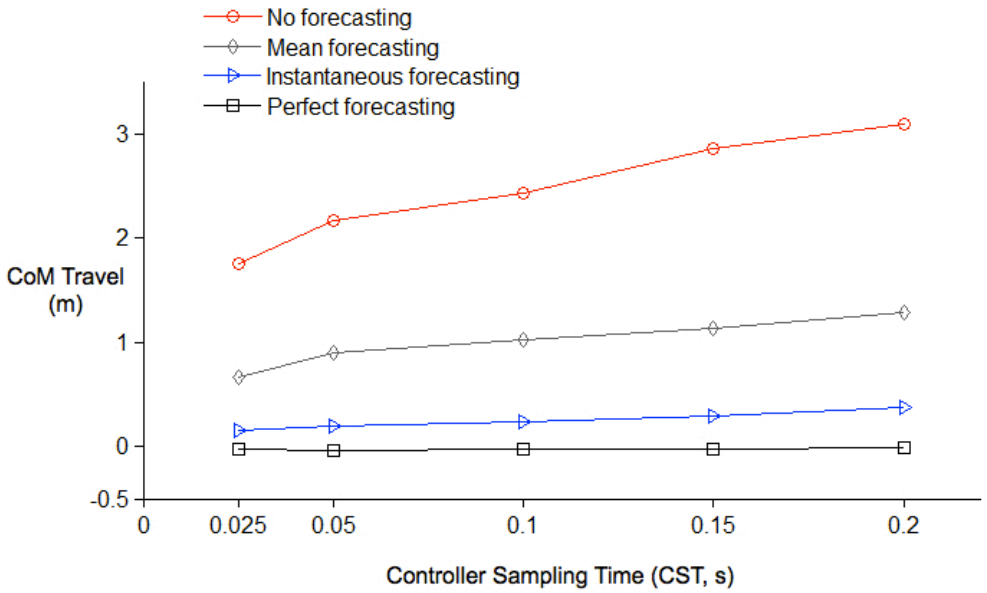

Figure 5.12: The total CoM travel as function of controller sampling time values for different levels of disturbance forecasting, under the platform disturbance profile given in Figure 5.9.

5.2.4 Remarks

The purpose of this section was to extend our balance recovery tool beyond transitory disturbance scenarios and simulate longer disturbances with their associated phenomena. The tool showed an expected recovery behavior depending upon varying levels of disturbance forecasting and the re-planning frequency. The results suggest that the recovery ability is significantly affected by the accuracy of the disturbance forecasting and the frequency of re-planning in case of longer disturbances. Hence further investigation should focus on defining appropriate parameters of these properties to evolve realistic recovery behaviors. Finally, these two properties have a strong correlation with

the cognitive processing capacities in humans which are known to degrade with age. Hence, a degraded BR response due to an inaccurate disturbance forecasting and a low re-planning frequency also characterizes one of the age-related deficiencies. More age-related effects and their simulation is the subject of next section.

5.3 Simulating the situation of elder population

Falls resulting from the loss of balance are a major health concern in the elderly. These are a leading cause of injury related hospitalizations in person aged 65 years and over in many countries (Lord et al., 2001). This has led to numerous studies which investigate the reasons of the elder's vulnerability in terms of balance. In this section, we briefly review and synthesize some major elderly characteristics which can be simulated with our BR tool. We take an exploratory approach and focus more on the qualitative, rather than quantitative, assessment of the predicted results.

5.3.1 Characteristics of an elderly response

It is a well-established fact that the balance recovery ability reduces significantly with age. The reasons of this degraded response have been investigated at different levels. Starting from the musculoskeletal system, experiments show a strong correlation between muscle weakness in lower limbs and the postural instability in the elderly (Carty et al., 2012; Lord et al., 1991b). Moreover, the rate at which force can be produced in muscles is reduced with age (Thelen et al., 1996). At the functional level, this leads to a decrease in the maximum speed with which legs could be moved in balance recovery tasks (Thelen et al., 1997; Wojcik et al., 1999), resulting in large contact times for the elderly with respect to the younger adults for the same step length (Hsiao-Wecksler and Robinovitch, 2007). This lower-limb weakness can be represented in our model by a reduced peak acceleration of the swing foot in our model. Similarly reduced joint flexibility and the reduced functional BoS in the elderly (Lee and Deming, 1988) can also be taken into account in terms of model constraints.

Other major age-related phenomena appear as the deterioration of the sensori-

motor functions. Poor leg proprioception properties originating from poor tactile sensation below feet has been associated with increased falls (Lord et al., 1991a,b) and step initiation times (Maki et al., 2003) in the elderly. This reduced sensitivity together with slow neural processing/conduction result in longer reaction times in the elderly (Maki and McIlroy, 1997) and has been shown to be a major determinant of a successful or a failed recovery response (Owings et al., 2001; Van den Bogert et al., 2002).

Finally, it has been established that recovering balance from external disturbances requires considerable cognitive resources and processing capacity (Brown et al., 1999; Maki and McIlroy, 2007). This mainly involves the ability to rapidly plan and execute the recovery strategy and is known to degenerate with age. The effects of some of the cognitive factors are already shown in the previous section in terms of forecasting accuracy and the frequency of re-planning and therefore will not be studied in this section. Below, we modify other aforementioned age-related parameters in our model and explore how the predicted balance recovery action is organized.

5.3.2 Simulation of age effects

Let's consider again the balance recovery scenario from Hsiao-Wecksler and Robinovitch (2007) where young and elderly subjects were inclined forward and asked to recover balance after release by taking a single step, no larger than a given target length. The comparison for young subjects was made in the Chapter 3 and 4 of this thesis. Here, keeping the same principle, we simulate our model by inputting maximum lean angle for the elderly and calculate the corresponding step lengths and timings. Simulations are performed using the parameters given in Table 5.3. The age-related parameters are modified as follows:

– The lower limb weakness in the elderly is simulated by reducing the maximum forward acceleration of the swing foot from 180 m.s^{-2} to smaller values of 60, 80, 100 and 140 m.s^{-2}. Similarly, upper-body peak torque is reduced from 190 to 100 N.m. To represent reduced joint flexibility, maximum upper-body rotation angle is also reduced from $\pi/2$ to $\pi/3$ rad.

Table 5.3: Controller parameters for the elderly reaction

Parameter	Value
Body Height, H	1.57 m
Body Mass	65 kg
Foot length, l_f	0.152 $\times$ H
Step preparation time, T_{prep}	150 ms (fixed)
Reaction time, T_{reac}	Varied between 75 and 150 ms
Leg swing time, T_{step}	Chosen by the controller
Max foot acceleration, $\ddot{f}'_{max}$	Varied between 60 and 180 m.s^{-2}
Max trunk rotation, θ_{max}	$\pi/3$ rad
Max hip torque, τ_{max}	100 N.m

– To simulate the sensori-motor degradation, increased reaction time values of 100 and 150 ms are tested, apart from the previously used value of 75 ms.

– Finally, following the analysis from Lee and Deming (1988) and Pai and Patton (1997), the reduced functional CoP range in the elderly is simulated by reducing the effective size of the base of support. The simulations are performed with the full effective BoS equal to the full foot length as well as with 55% reduction in its size (an extreme case used by (Pai and Patton, 1997)).

Control weights c_1 to c_6 and other parameters are kept the same and are given in Table 5.2. The step time T_{step} is optimized between 50 and 500 ms.

5.3.3 Results and discussion

The results for all four inclination scenarios are shown in Figures 5.13 and 5.14. For each inclination, predicted step length and step time results are shown for two cases: Left hand side plots assemble results where effective BoS is reduced by 55% while right hand side plots show the results with full BoS. The peak swing foot acceleration is varied along the x-axis on individual plots. Reaction time is varied between 75, 100 and 150 ms.

As a whole, the prediction results tend to confirm earlier experimental findings. For each inclination scenario, reducing the effective BoS size significantly increases the required step length to recover balance in all cases. This shows the important role of the ankle torque (which is proportional to the size of BoS in our model) applied during the delay when the step is being prepared and executed. Given the important difference between the results with full and reduced effective BoS length even for smaller inclinations, this parameter may need particular attention while simulating an elderly reaction.

Following a postural disturbance, the system has a limited amount of time to place the recovery step to avoid a fall. Within this time, the step should be placed at a sufficient distance to be mechanically effective. When the ability to step far in the given time is reduced (either by muscle weakness in the elderly or by limiting the swing foot acceleration in our simulation), the step times are bound to increase. This increase, experimentally observed in the elderly (e.g. Hsiao-Wecksler and Robinovitch, 2007), is confirmed in our simulations. For example, at larger inclinations and reduced BoS, a more stringent foot acceleration constraint frequently results in larger step times, for all reaction time values (c.f. Figure 5.14, red plots). However, at smaller inclinations, this constraint plays almost no role since the required recovery step lengths are small and the swing foot is not accelerated to its maximum limit.

Similarly, step lengths are positively correlated with the reaction time in all cases. This is coherent with the observation that the elderly require larger recovery distances to stabilize themselves, in part, due to larger reaction times. Moreover, at larger inclinations, step times are also increased with increasing reaction time which is consistent with the above observation that larger step lengths require larger step times. When the reaction time becomes too large and the step cannot be placed far enough, recovery may not be possible using a single step at larger inclinations. This is what can be observed in Figure 5.14 for the peak inclination of 16.8° with reaction time of 150 ms (represented by a star ($\star$)). Interestingly, the same phenomenon was observed in the experimental studies (e.g. Pavol et al., 2001) where elderly subjects who failed to recover balance following a disturbance had slower response times and smaller step lengths than those who were successful in recovering balance.

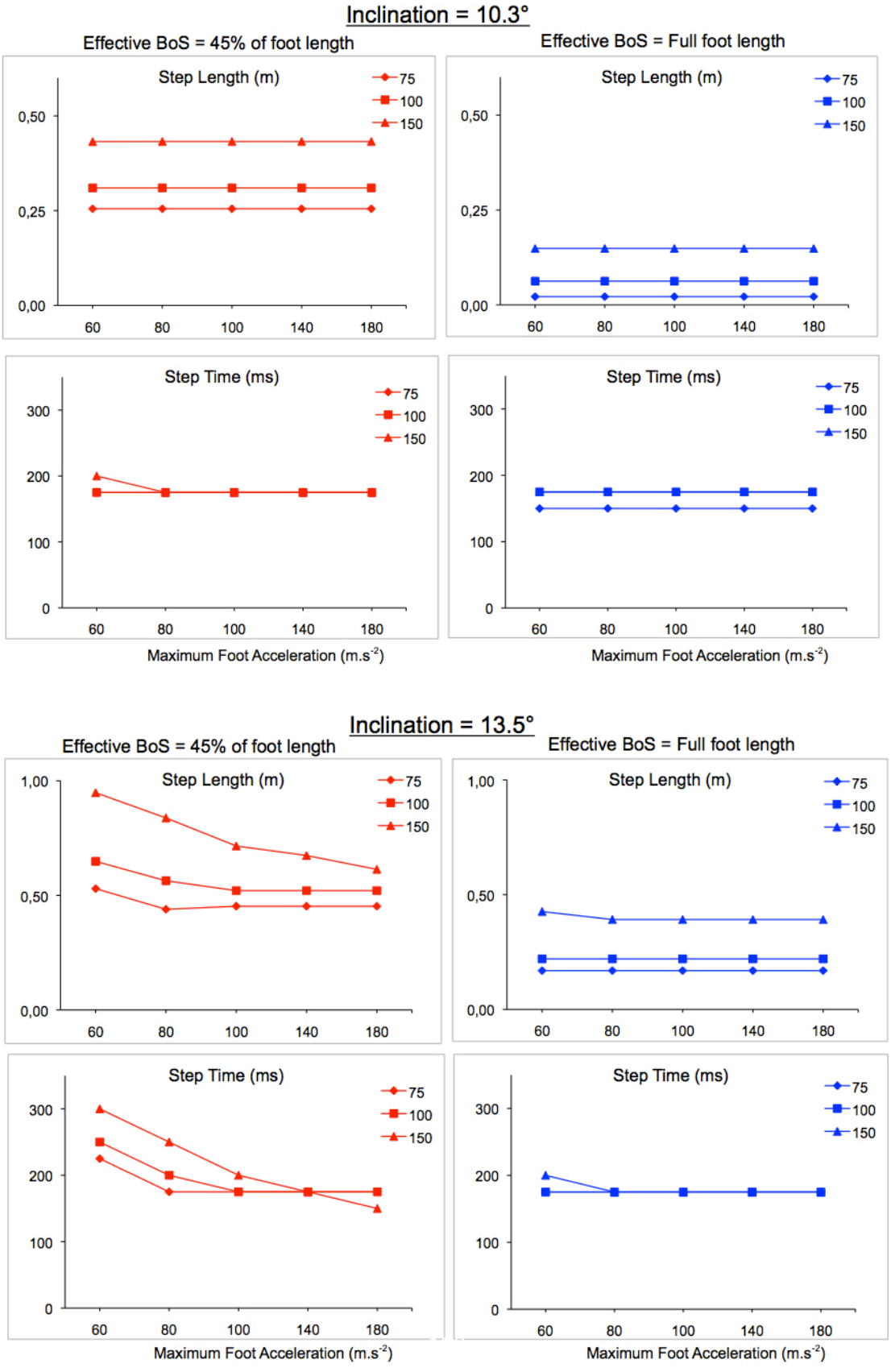

Figure 5.13: Optimized step lengths and timings against forward inclinations scenario for elderly from Hsiao-Wecksler and Robinovitch (2007) against maximum foot acceleration values (varied along x-axis) for 3 different reaction time values (75, 100 and 150 ms) and 2 different effective BoS lengths: (left red plots for reduced BoS vs. right blue plots for full BoS).

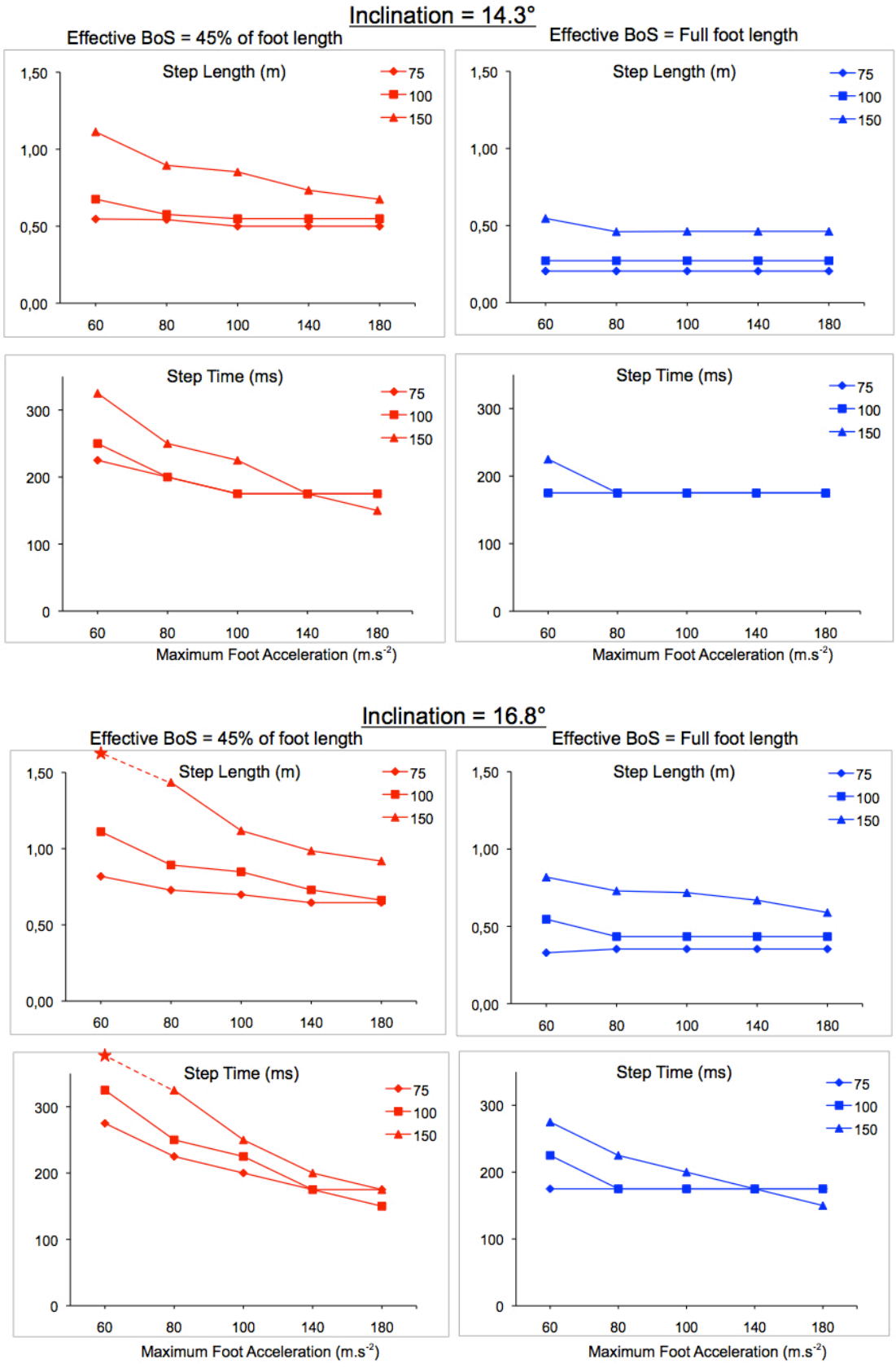

Figure 5.14: Optimized step lengths and timings against forward inclinations scenario for elderly from Hsiao-Wecksler and Robinovitch (2007) against maximum foot acceleration values (varied along x-axis) for 3 different reaction time values (75, 100 and 150 ms) and 2 different effective BoS lengths: (left red plots for reduced BoS vs. right blue plots for full BoS). Starred value ($\star$) represents a fall.

All in all, this brief study shows the capacity of our BR tool to evolve similar trends as observed in the elderly when the age-related parameters are modified. The effective BoS size, reaction time, lower-limb strength, all seem to be important parameters particularly under large inclinations. Further investigation should focus on identifying realistic values of these parameters along with the integration of other age-related properties.

5.4 Conclusion

This chapter was aimed at simulating the scenarios of platform disturbance type which closely resemble to the perturbations observed in the public transportation vehicles. To start with, the balance recovery tool was tested against transient platform disturbances. The controller generated reasonable recovery responses to both maximal and sub-maximal recovery situations by adjustment of appropriate cost function parameters. We then introduced the notion of disturbance forecasting in the controller to tackle longer disturbances and showed how the recovery ability is affected by the accuracy of forecasting. While different forecast profiles were tested, the question of a realistic estimated profile chosen by a human subject remains open. In the end, the effect of some age-related parameters on the predicted recovery response was explored. The qualitative analysis of the results showed the capacity of our controller to produce similar trends as observed in the experimental studies against relevant parameter variation.

"Remember that all models are wrong; the practical question is how wrong do they have to be to not be useful."
Empirical model-building and response surfaces by George E. P. Box, Wiley, 1987

Chapter 6

The Last Word

The objective of this work was to develop a mathematical model of human balance recovery following strong external disturbances. The main motivation of this work came from the abundance of balance-related casualties in public transport, though the ideas and the model developed are not limited to this particular scenario. Using general physical principles, some control ideas from the field of robotics and focused development inspired from the human balance recovery, we developed a balance recovery (BR) model which showed close resemblance to an actual human response.

6.1 Summary and contributions

To start with, a brief literature review was conducted in Chapter 2 to find out some fundamental human BR characteristics. It turned out that humans employ different recovery strategies in parallel, including mainly the so-called ankle, hip and stepping strategies. Single and multiple steps were particularly predominant in natural conditions with step placements and timings being meticulously regulated to generate an efficient recovery response. These properties served as a reference for the rest of the development of our BR controller.

We evaluated some existing BR schemes in the fields of biomechanics and robotics in Chapter 3 and concluded that none of them offered such a versatile recovery response

as humans. We could nevertheless identify that Model Predictive Control (MPC) is a promising technique. A particular characteristic of this approach in view of our objective of simulating human behavior is the calculations over a future time horizon using a simpler internal representation of the actual system. Hence building our controller on the MPC approach, we developed it further in Chapter 4 and 5 to include human-like versatility. The main contributions of this thesis can be summarized as follows:

Modeling of human balance under strong disturbances

The first main contribution of this work is to the field of human balance. Unlike existing models which only consider postural balance, this work specifically targeted the balance recovery from large external disturbances including recovery steps. Anthropomorphic balance properties such as **co-existence and regulation** of different strategies were reproduced within a single optimization routine.

A multi-strategy MPC scheme for biped robots

The second contribution of this work is to the field of biped robots. These machines are conceived to possess similar skills as humans but are still much less versatile in BR tasks than their human counterparts. The complex biped dynamics leads researchers to make several simplifying assumptions such as neglecting the regulation of upper-body inertia (UBI) and/or fixing the step timings in advance to simplify the calculation process. However, our controller addresses both these issues and integrates the **UBI and an effective step time optimization in an MPC scheme** for the first time.

Application to vehicle design and operating practices

From the application point of view, our BR tool is a step forward towards the **assessment of risks** to the standing passengers in the public transport. The 'passive' safety of these vehicles, which deals with the post-incident safety of its occupants, is an important research field. To design an injury-free internal structure as well as defining good operating practices of these vehicles, the estimation of passenger kinematics following a disturbance is essential. The current model can be exploited to evaluate

passenger behavior under varying disturbance scenarios which is hitherto studied using experiments. This can thus help reduce/eliminate the need of expensive experimental procedures.

From prediction to new research questions

Though *prediction* remains the chief goal of mathematical modeling in biomechanics, the process also provides insights into the real physical phenomena and can guide future research direction. Testing model behavior by varying assumptions (e.g. what we did in Section 5.1 regarding environmental conditions) or by modifying model parameters (as we did in Section 5.3 for the elder reaction) is an intellectually fruitful practice.

6.2 Perspectives

Though our BR tool simulates well a human BR reaction, it still has room for improvements. We discuss some of the possible future research tracks in this section.

More realistic human-body representations

Two separate but very similar human-body models are used in our BR tool. A *mechanical* model with fixed leg lengths (inverted pendulum assumption) represents the system to be controlled while the MPC controller itself employs an *internal* model with constant CoM height (LIP assumption). This small modeling error is compensated by the feedback type control. This approach is comparable to what has been suggested in the 'internal model hypothesis' for human tasks in the field of neurosciences (see e.g. the reviews from Desmurget and Grafton, 2000; Kawato, 1999). This theory proposes that, in order to execute a task, the human brain employs neural mechanisms in the form of inverse internal models to calculate the required motor command in advance. The command could then be applied in a feedforward manner to achieve that task, but the modeling and perception errors require its fine-tuning during its execution based on the most recent sensory feedback.

However, the choice and structure of these simplified internal representations for a given task remains an open question. Different internal models may lead to different solutions and hence varying responses. In this regard, further development should focus on testing different internal body representations in our MPC controller and evaluating their effect on the balance recovery. For example, a free fall CoM evolution could be envisaged during the step execution (Aftab et al., 2010) where the CoM follows a parabolic path with constant forward CoM velocity.

On the other hand, the controlled *mechanical* model can be further improved to include more realistic functions. The current model (inverted pendulum with the inertia wheel) is not compatible with the double support (DS) phases between steps, nor can it account for the possible energy dissipation in the leg after a step. Moreover, the so-called hip strategy is only characterized by the upper-body inertial (UBI) effects while its kinematic aspects are neglected (i.e. the anti-phase rotation of upper- and lower-body, see illustration in Figure 2.2). To address these limitations, two more realistic alternatives may be explored: First, the DS phase and the post-step leg compliance can be modeled using a spring model such as the one proposed by Geyer et al. (2006) (c.f. Figure 6.1). Second, a double-inverted pendulum (DIP) model can be used to represent more realistically the single-support phase where lower and upper body are represented by two segments connected at the hip level. It is expected that, despite the resulting non-linear system dynamics, it could still be correctly operated by our 'linear' MPC controller, which is one of the strong points of this approach.

Human sensory systems

In the current model, it is assumed that the disturbed state of the system is accurately known by the controller, neglecting any measurement and perception errors that may be present in humans. In this context, an interesting future direction would be to model the human sensory systems and to explore their effect on the balance recovery simulation.

It is well known that humans rely on several sensory systems to detect a balance

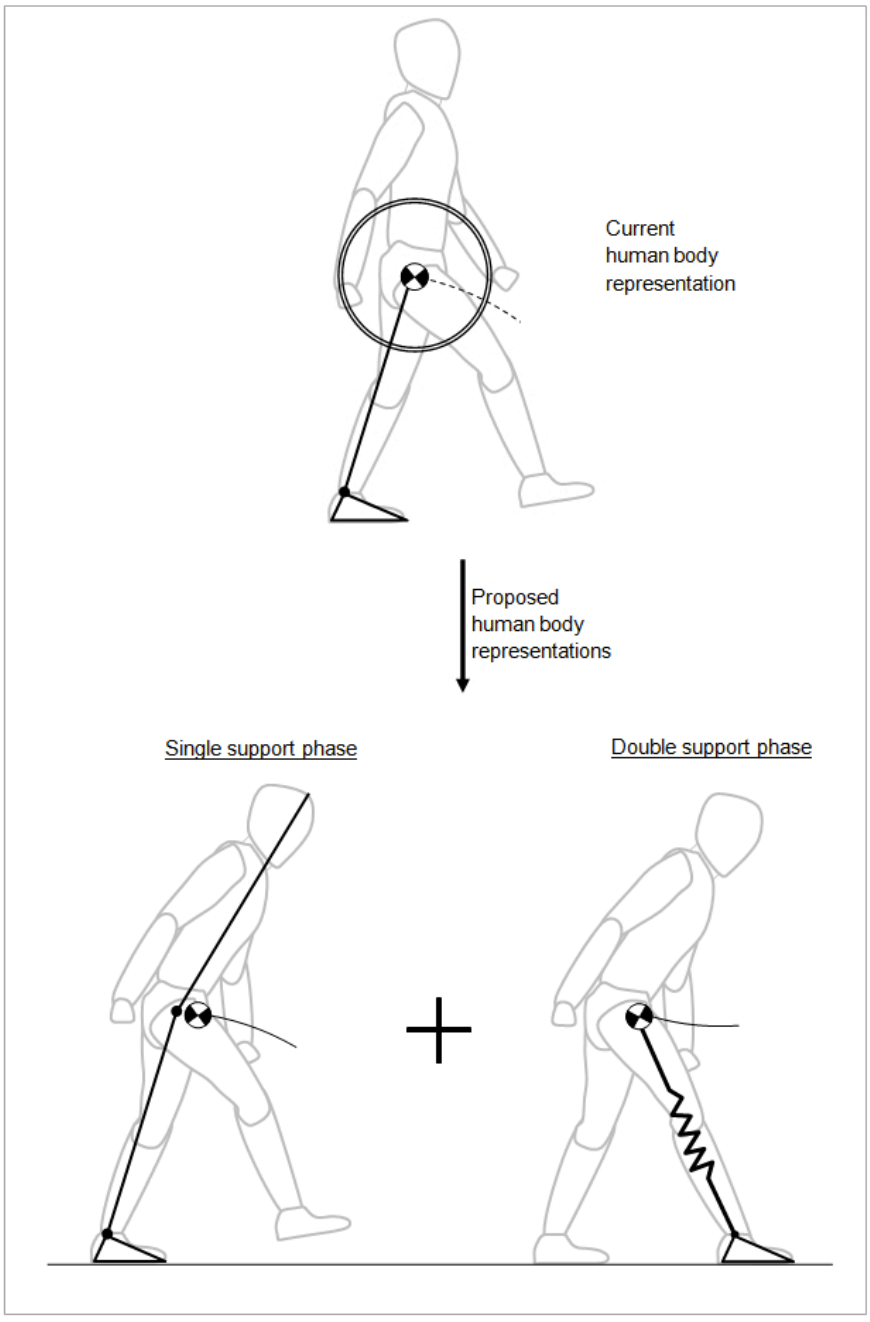

Figure 6.1: The current human-body representation (top) can be replaced by more realistic models such as a double-inverted pendulum (DIP) model during the single-support phase and a spring model during the double-support phase.

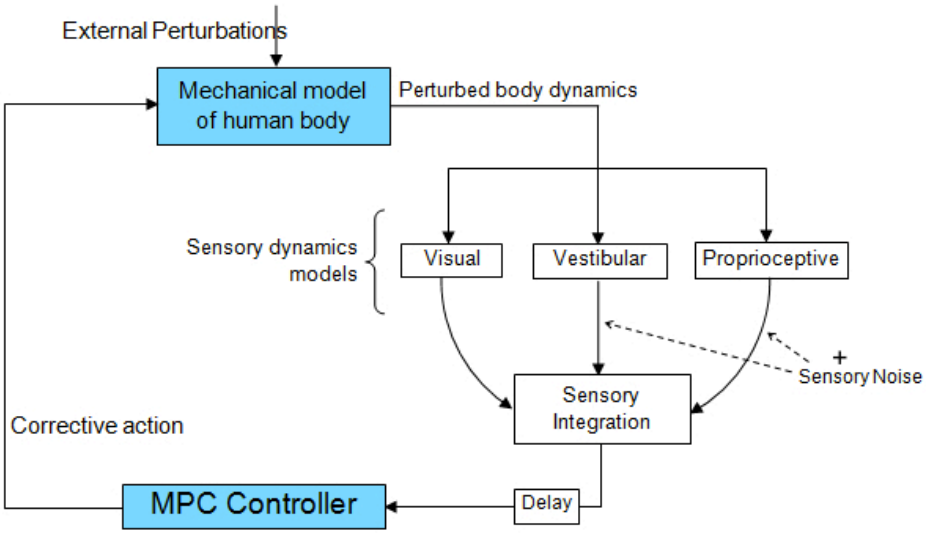

Figure 6.2: A possible integration of human sensory systems in the BR tool would involve a separate sensor dynamic model of each sensory modality ((e.g. Borah et al., 1988)) and a sensory integration center.

perturbation. The three systems mainly contributing to balance are the visual, vestibular and the somatosensory (tactile and proprioceptive) systems, each of which make an estimation of instability in its own frame of reference. Contribution of each of the sensory systems is considered necessary for a best estimation of system state in humans. In the author's view, integration of these sensory systems, with their associated inaccuracies and signal noise, would allow studying more complex BR phenomena. For example, since aging adversely affects the sensory acuity in the elderly, their reactions can be better simulated and understood by this inclusion. Similarly, the effects of upper-body rotation, especially of the head where the vestibular system is located, on the balance perception and performance can be analyzed.

A schematic diagram of the possible integration of the sensory models is shown in the Figure 6.2. The method is inspired from the works from Borah et al. (1988) and van der Kooij et al. (1999) which were briefly discussed in Chapter 2 of this thesis. The system dynamics is calculated as usual by a mechanical representation of the human body and the relevant dynamic variable is transmitted to separate sensory dynamic

systems. For example, head accelerations are input to the vestibular systems, ankle angle to the proprioceptive system, etc. Estimations from each sensory model are then integrated together in a sensory integration center to make an overall estimation of the system state. All the processing or transmission delays are represented by a single delay in the loop. This seems to be a promising approach, which to-date have only been exploited for simulating the postural human balance.

Different application scenarios

On the application side, the current tool can be extended to different initial postures. Lateral perturbation as well as perturbations during walking are also common in the public transport and should be considered in the future. Similarly, the effect of extra non-coplanar supports (such as handrails) on the balance recovery would also increase the versatility of the prediction tool.

Résumé en Français

Contexte et Motivation

Contexte : le problème de la stabilité des passagers debout de transports en commun

La perte d'équilibre chez l'humain est un phénomène courant de la vie quotidienne. Plusieurs causes peuvent être identifiées, dont notamment des perturbations extérieures. On peut citer par exemple les glissements ou des déplacements de la base de support (un freinage d'urgence dans un tramway par exemple). Ces incidents engendrent des blessures qui coûtent très cher au niveau du budget de la santé.

Le scénario qui nous intéresse particulièrement est celui des passagers debout dans les transports en commun. La combinaison de plusieurs études accidentologiques fait ressortir un risque de blessure important pour ce type de situations. En effet, il apparaît qu'une part importante des lésions recensées dans les transports en commun intervient dans des incidents sans collision. Le chiffre varie de 54% pour Bjornstig et al. (2005) à 63% pour Kirk et al. (2003). Une des raisons majeures est l'accélération ou décélération du véhicule provoquant au moins 50% des blessures (Bjornstig et al., 2005; Halpern et al., 2005). De plus, sans grande surprise, les passagers debout et les personnes âgées sont les plus exposés dans ces scénarios.

D'autres éléments indiquent que ce problème risque de devenir plus en plus préoccupant. Par exemple, les nouveaux designs de véhicule intègrent de plus en plus de

passagers debout. De plus, la population âgée, et donc à risque, est en forte augmentation en France et ailleurs (cf. Figure 6.3). Par conséquent, il y a un fort besoin d'aborder la question de la sécurité des passagers debout des transports en commun pour qu'ils restent accessibles à toutes les populations de la société.

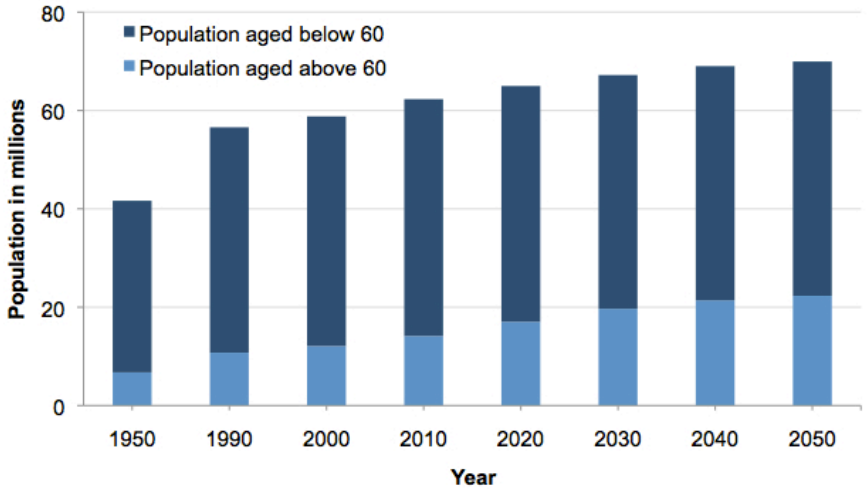

Figure 6.3: La proportion des personnes âgées dans la population française depuis 1950 et projeté jusqu'à 2050 par l'Institut National de la Statistique et des Etudes Economiques (Insee, 2006).

Comment traiter ce problème ?

Pour traiter ce problème, il faut comprendre les principaux phénomènes de la chute ou du rattrapage d'équilibre. Plus précisément, il est nécessaire d'évaluer la cinématique d'une personne suite à une perturbation de son équilibre afin d'estimer les risques de chute ou d'impact secondaire avec l'environnement. Or, dans les situations étudiées, la réaction des personnes suite à la perturbation a une influence prépondérante sur la cinématique du rattrapage ou de la chute. Il est donc nécessaire de prendre cette réaction en compte. De plus cette réaction est fortement dépendante des capacités physiques et cognitives des personnes, capacités typiquement dégradées lors du vieillissement.

Les questions qu'on se pose sont donc : (i) comment cette réaction évolue en fonction des paramètres de la perturbation (tel que son intensité mais aussi sa durée) ? (ii) Quel est l'effet de l'âge sur cette réaction ?

Il existe 2 approches distinctes pour étudier ces questions : expérimentale ou numérique

Les études expérimentales : utiles mais pas prédictives

On trouve dans le domaine de la biomécanique une littérature relativement abondante sur les problèmes de chute et de maintien de l'équilibre. La procédure généralement utilisée est classique : l'équilibre de sujets volontaires est perturbé par différents moyens, tels qu'une modification de la friction du sol ou des accélérations de la base de support, et leur réaction est enregistrée et analysée.

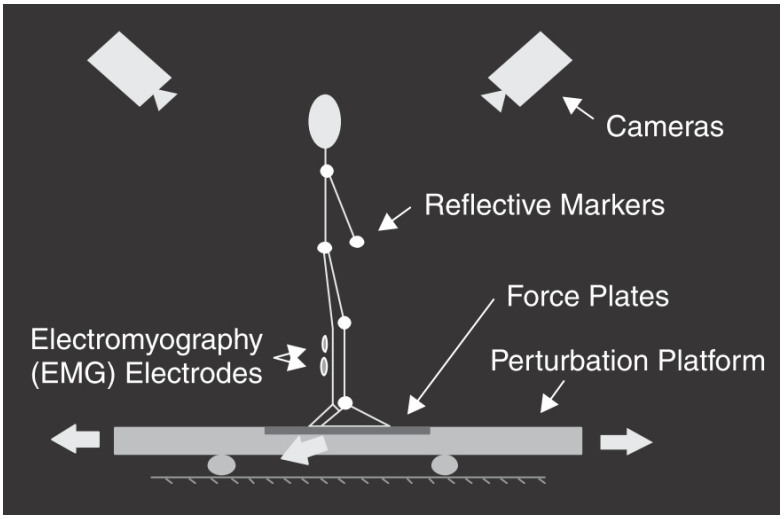

Figure 6.4: Le moyen d'essai couramment utilisé pour générer des perturbations de type transport en commun (Maki et al., 2003)

Ces études expérimentales font ressortir des caractéristiques importantes du rattrapage d'équilibre. Par exemple, on observe que les sujets utilisent souvent 3 stratégies de rattrapage - ou actions de contrôle - qui sont souvent caractérisées en termes cinématique (Horak and Nashner, 1986) : la stratégie dite "de cheville" qui représente la rotation du corps entier autours des chevilles; la stratégie de hanche qui représente la rotation en antiphase du haut et du bas du corps; et enfin le fait de faire un ou plusieurs pas de rattrapage. Ces stratégies sont souvent exploitées en parallèle et leur utilisation dépend du niveau de perturbation, des contraintes environnementales etc.

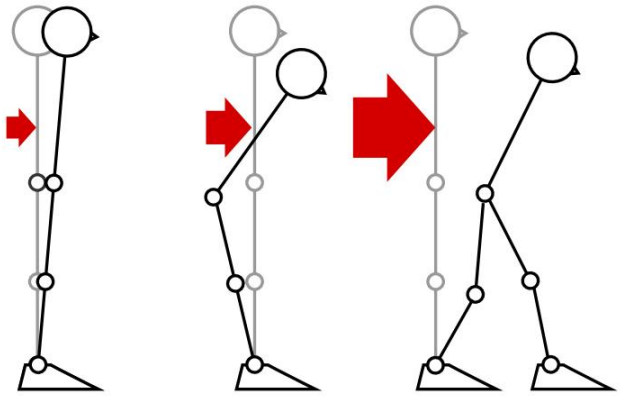

Figure 6.5: Les stratégies fondamentales utilisées par les humains pour rattraper leur équilibre: La stratégie dite de cheville (gauche), de hanche (centre) et de pas de rattrapage (droite) (Kanamiya et al., 2010)

(Maki et al., 1994). Il apparaît aussi que la stratégie de pas de rattrapage est très fréquemment utilisée, en particulier chez les personnes âgées.

Ces études expérimentales nous apportent donc une connaissance assez précise des actions de rattrapage employées par des sujets suite à une perturbation de leur équilibre. En revanche, elles ne répondent pas complètement à nos questions de bases. Une des raisons majeure est que les résultats des différentes études sont difficilement comparables, notamment du fait de l'absence de protocole de test standard. De plus, dans le cas d'un mouvement de la surface d'appui, les perturbations appliquées sont souvent mal définies, et correspondent rarement à ce que l'on observe réellement dans les transports en commun. Une autre limitation vient du fait qu'il est très délicat, voire impossible, d'effectuer des essais sur des personnes fragiles (typiquement des personnes âgées) qui sont pourtant les personnes à risque. Il est donc quasiment impossible de prédire les conséquences d'une perturbation de l'équilibre à partir de ces données expérimentales. Il apparaît alors nécessaire de mettre en place un modèle pour répondre à nos questions.

Modéliser l'équilibre dynamique

Il existe plusieurs approches de modélisation de l'équilibre dans la littérature en biomécanique et en neurosciences. Les plupart de ces modèles ne considèrent que l'équilibre

postural, c'est-à-dire statique ou faiblement perturbé. Dans ce cas, les aspects dynamiques du mouvement ne sont pas pris en compte. De plus, aucun de ces modèles ne considère le fait de faire un pas de rattrapage.
En revanche, notre cas d'étude est bien différent. Nous sommes intéressés par modéliser la conséquence de perturbations relativement importantes, où des pas de rattrapage sont couramment mis en oeuvre. On parle alors d'équilibre dynamique, par opposition à l'équilibre postural.

La modélisation de l'équilibre dynamique est abordée de manière plus formelle dans le domaine de la robotique bipède. Etant donné que ces machines ressemblent à des humain et sont soumises à des contraintes similaires (l'unilatéralité des contacts pied/sol par exemple), on constate que les avancés dans ce domaine pourrait donner des pistes pour développer notre modèle de rattrapage d'équilibre.

On peut considérer le bipède comme un système de corps rigides qui doit respecter les lois de la mécanique lors de la réalisation d'un mouvement : les efforts extérieures (en l'occurrence, la pesanteur et les forces de contacts avec le sol) doivent équilibrer les efforts inertiels liés au mouvement (Barthelemy and Bidaud, 2007). Cette condition peut être représentée comme:

$$W^i = W^g + W^c \tag{6.1}$$

où W^i , W^g , W^c sont respectivement les torseurs des efforts d'inertie, de la gravité et des contacts.
Pour que les mouvements soient théoriquement réalisables, le système doit respecter la condition 6.1. Il faut de plus respecter un certain nombre de contraintes sur les efforts de contact (unilatéralité et non glissement par exemple) et le système (limitation des forces motrices par exemple). Pour des robots bipèdes, cette faisabilité des mouvements est souvent évaluée à l'aide d'un critère basé sur un point de référence, appelé le ZMP ou Zero Moment Point, en stipulant que celui-ci doit se trouver à l'intérieur de la Base de Support. Mais la difficulté majeure dans la modélisation de l'équilibre dynamique est de représenter le risque de chute. En effet, la condition 6.1, qui reflète la conformité du mouvement avec les lois de la mécanique, n'implique pas que le sys-

tème ne va pas chuter.
Dans ce travail, nous avons défini la stabilité d'un système comme la possibilité de générer un mouvement qui ne donne pas lieu à une chute étant donné les actions de contrôle et les contraintes du système. Cette notion se base sur le concept de noyau de viabilité, proposé par Wieber. Ce noyau regroupe l'ensemble des états du système à partir desquels il est possible d'éviter la chute (c.f. Figure 6.6 Wieber, 2008, 2002).

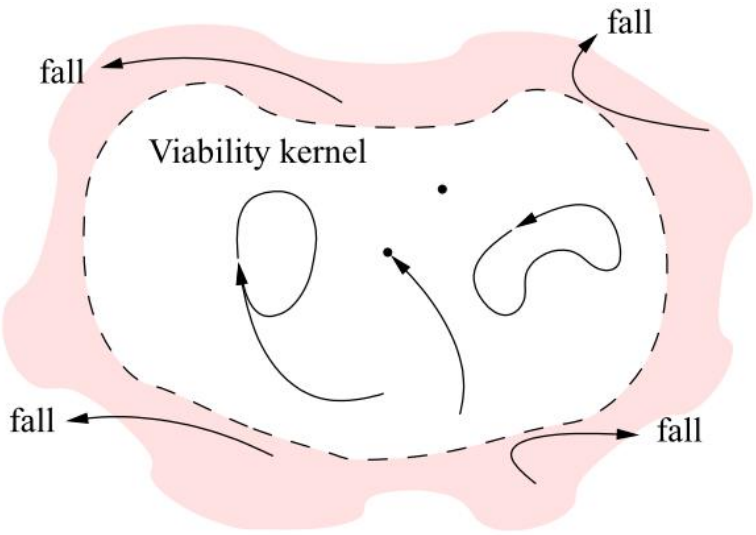

Figure 6.6: Le noyau de viabilité rassemble tous les états à partir desquels il est possible d'éviter une chute (Wieber, 2002)

Cette représentation définit parfaitement la stabilité en théorie, mais en pratique il est quasiment impossible de calculer précisément ce noyau du point de vue numérique Wieber (2008). Cependant, nous avons pu identifier deux approches qui permettent de contourner cette difficulté.

La première repose surle concept de *capturabilité*, proposé récemment par Pratt et collègues (Koolen et al., 2012; Pratt et al., 2012). Cela revient à estimer les états pour lesquels l'équilibre pourra être rétabli en utilisant toutes les actions de contrôles (notamment les pas) au maximum. Cela revient à approximer le noyau de viabilité de Wieber (2002). Cette approche, très intéressante, est cependant assez limitée dans le contexte de ce travail. En effet nous ne cherchons pas à savoir uniquement si un état

est "rattrapable" ou non (bien que ce soit une information utile) mais plutôt à savoir comment l'équilibre va être rattrapé.

Une deuxième approche consiste trouver un critère qui garantisse de rester à l'intérieur du noyau de viabilité, sans pour autant avoir à estimer ce noyau avec précision. Une solution a été proposée également par Wieber (2008). Elle repose sur le fait que la chute d'un bipède est équivalente à la divergence de son CdM et tous ses dérivés à l'infini. Ainsi, l'intégrale de la norme de n'importe quelle dérivée du CdM aura une valeur finie pour les mouvements stables. Par conséquent, il est possible de générer des mouvements stables en minimisant une dérivée du centre de masse. Cette idée a ensuite été formalisée sous la forme d'une commande prédictive par Herdt et al. (2010a), sur lequel notre premier modèle de rattrapage d'équilibre est basé.

Un premier modèle de rattrapage

Le principe de la commande prédictive (aussi appelé MPC) consiste à résoudre une série des problèmes d'optimisation sur un horizon du temps. Le contrôleur consiste en une fonction coût et en un modèle interne du système, plus simple par rapport au système réel. La fonction coût formalise l'objectif à atteindre dans le temps, tel que l'état désiré du système, et le modèle interne permet d'estimer la conséquence de la commande calculé sur un horizon du temps. Une fois cette commande déterminée, elle est appliquée au système complet et le résultat est réintégré en entrée de la commande prédictive. Une nouvelle solution est alors déterminée sur un horizon de temps légèrement décalé par rapport au précédent, et ainsi de suite.
Parmi plusieurs contrôleurs de marche de robot bipède basés sur la commande prédictive, celui de Herdt et al. (2010a) est unique en ce qui concerne le placement des pas. Le contrôleur se base sur la régulation de vitesse de CdM par rapport à une référence, en utilisant la stratégie de cheville (déplacer son Centre de Pression dans le polygone de support) et de pas de rattrapage.
Ce contrôleur a été adapté pour représenter des situations de rattrapage d'équilibre.

Implémentation

On fait l'hypothèse que pour le rattrapage d'équilibre, l'objectif principal est de ramener au plus vite la vitesse du système à zéro. Cela est accompli par une minimisation de la vitesse de CoM tout au long de l'horizon du temps. La fonction de coût prend aussi en compte l'impulsion (jerk) du CoM, pour générer un mouvement plus lisse, et l'écart entre le CoP et la cheville, pour obtenir une posture finale plus confortable. Ces deux termes sont faiblement pondérés pour ne pas trop affecter l'objectif principal. La dynamique du système est représentée par un modèle de pendule inversé linéaire couramment utilisé en robotique.
La fonction coût est donc :

$$\min \quad \frac{1}{c_1^2}\|\dot{C}_{k+1} - \dot{C}_{k+1}^{ref}\|^2 + \frac{1}{c_2^2}\|\dddot{C}_k\|^2 + \frac{1}{c_3^2}\|Z_{k+1} - F_{k+1}\|^2, \quad (6.2)$$

où c_1 , c_2 et c_3 sont les coefficients de pondération, $u = \begin{bmatrix} \dddot{C}_k \\ \bar{F}_{k+1} \end{bmatrix}$ sont les variables de contrôle, ici le jerk du CdM $\dddot{C}_k$ et les positions de pas de rattrapage $\bar{F}_{k+1}$. A ce niveau, les durées de pas sont fixées à l'avance.
Le mouvement du système est soumis à des contraintes linéaires d'inégalité qui consiste à (i) contraindre le ZMP à rester dans le polygone de sustentation défini par les pieds au sol et (ii) contraindre la vitesse maximum des pieds.

Comparaison avec les résultats expérimentaux

Pour comparer les prédictions de ce modèle par rapport aux données expérimentales, on choisit un paradigme expérimental simple de la littérature où les sujets sont lâchés dans une posture statique instable (le fameux tether-release). Deux études, dont les paramètres et résultats sont bien décrits, sont utilisées pour la comparaison. L'étude de Hsiao-Wecksler and Robinovitch (2007) qui impose un pas de rattrapage et l'étude de Cyr and Smeesters (2009b) sans aucune contrainte sur le nombre de pas. L'angle d'inclinaison initial est l'entrée principale du modèle, avec la géométrie moyenne des sujets et les instants des pas de rattrapage. La variable de comparaison est la position

des pas de rattrapage.
Les résultats sont tracés dans les Figure 6.7 et 6.8.

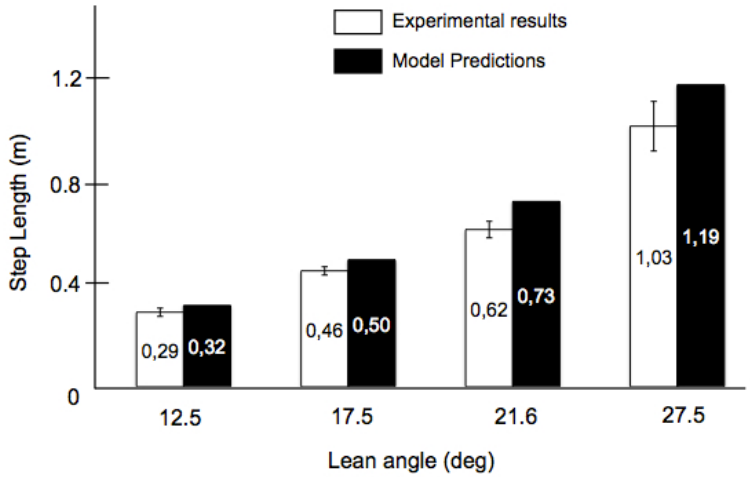

Figure 6.7: Longueurs des pas de rattrapage pour le scénarios de Hsiao-Wecksler and Robinovitch (2007): expérimentales (en blanc, moyenne et écart-type) vs simulées par la première version du modèle(noir)

Dans les deux cas, les prédictions du modèle sont du même ordre que les résultats expérimentaux, ce qui confirme nos hypothèses de travail. Cependant, on observe que les prédictions de notre modèle sont toujours plus grandes que les résultats expérimentaux et que cette différence est bien corrélée avec le niveau de l'inclinaison (Figure 6.7). Cela peut être dû à la non-considération de l'inertie du haut du corps, qui est une limitation du modèle pendule inversé. Les tendances sont identiques pour le cas de plusieurs pas où les prédictions du modèle sont globalement correctes, sauf une sur-estimation de la longueur par notre modèle.
Malgré ces résultats encourageant, nous estimons que la non-considération de l'inertie du haut du corps et le fait de fixer les durées de pas sont des limitations importantes de ce modèle. Ces limitations sont donc abordées dans la suite de ce travail.

Développement

Pour prendre en compte les effets inertiels du haut du corps, nous choisissons un modèle simple qui consiste en un volant d'inertie centré au CdM (c.f. Figure 6.9).

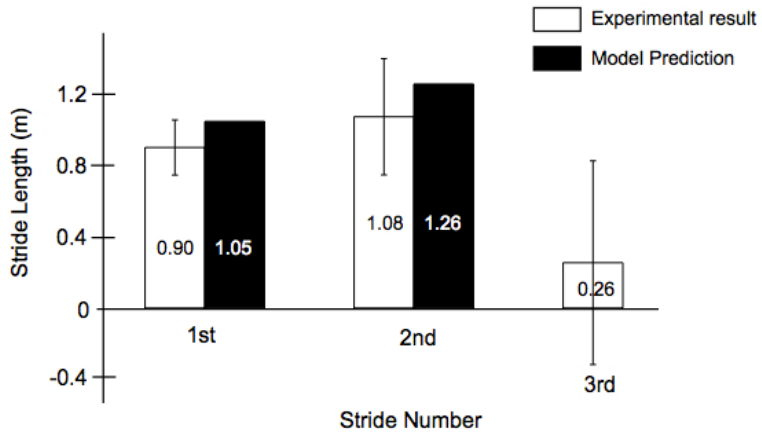

Figure 6.8: Les positions des trois pas de rattrapage pour le scénario de Cyr and Smeesters (2009a): Expérimentales (en blanc, moyenne et écart-type) vs simulées par la première version du modèle(noir)

La dynamique de ce nouveau système est représentée par l'équation suivante :

$$mh\,\ddot{c}_x + j\,\ddot{\theta} = mg(c_x - z_x) \tag{6.3}$$

dont on peut calculer le ZMP:

$$z = c_x - \frac{h}{g}\,\ddot{c}_x - \frac{j}{mg}\,\ddot{\theta}. \tag{6.4}$$

où j représente l'inertie de ce segment et θ son orientation.
Comme l'objectif principale du contrôleur est de revenir au plus vite à une posture statique, la fonction coût consiste notamment à minimiser la vitesse du CdM $\dot{C}_{k+1}$ et du volant d'inertie $\dot{\Theta}_{k+1}$ tout au long de l'horizon. De plus, pour **obtenir une véritable optimisation de la durée de pas** dans notre contrôleur, l'accélération de la jambe $\ddot{F}'_{k+1}$ est aussi pénalisée. Ce paramètre peut être rapproché du couple à fournir pour accélérer le pied en vol vers l'avant. Cela donne la fonction coût suivante:

$$\min\ \frac{1}{c_1^2}\|\dot{C}_{k+1}\|^2 + \frac{1}{c_2^2}\|\dot{\Theta}_{k+1}\|^2 + \frac{1}{c_3^2}\|\ddot{F}'_{k+1}\|^2. \tag{6.5}$$

Cependant, les mouvement générés sont considérablement améliorés si on minimise les

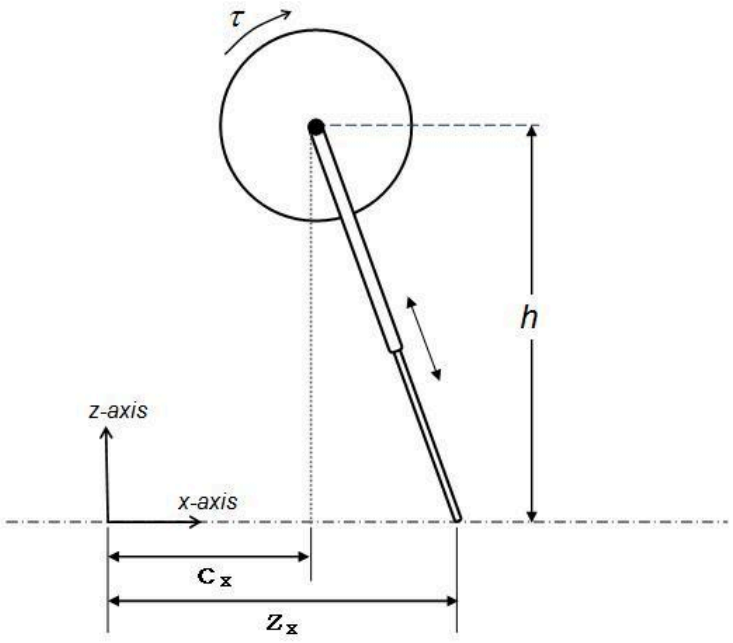

Figure 6.9: Le modèle de pendule inversé linéaire avec un volant d'inertie pour prendre en compte les effets inertiels du haut du corps

dérivées troisièmes du mouvements $\dddot{C}_k$ et $\dddot{\Theta}_k$ ainsi que la distance entre la position Z_{k+1} du CoP and le centre du pied d'appuis. Par conséquent, on minimise :

$$\min \ \frac{1}{c_1^2}\|\dot{C}_{k+1}\|^2 + \frac{1}{c_2^2}\|\dot{\Theta}_{k+1}\|^2 + \frac{1}{c_3^2}\|\ddot{F}'_{k+1}\|^2 + \frac{1}{c_4^2}\|\dddot{C}_k\|^2 + \frac{1}{c_5^2}\|\dddot{\Theta}_k\|^2 + \frac{1}{c_6^2}\|Z_{k+1} - F_{k+1}\|^2, \quad (6.6)$$

avec comme variable de contrôle $u = \begin{bmatrix}\dddot{C}_k & \dddot{\Theta}_k & \bar{F}_{k+1}\end{bmatrix}^T$. Le choix des pondérations c_1 à c_6 permet de réguler différentes stratégies pendant le rattrapage d'équilibre.
Le système est soumis à des contraintes d'inégalités linéaires, notamment sur le CoP, l'accélération de la jambe ainsi que sur le couple et l'angle de rotation de volant d'inertie.

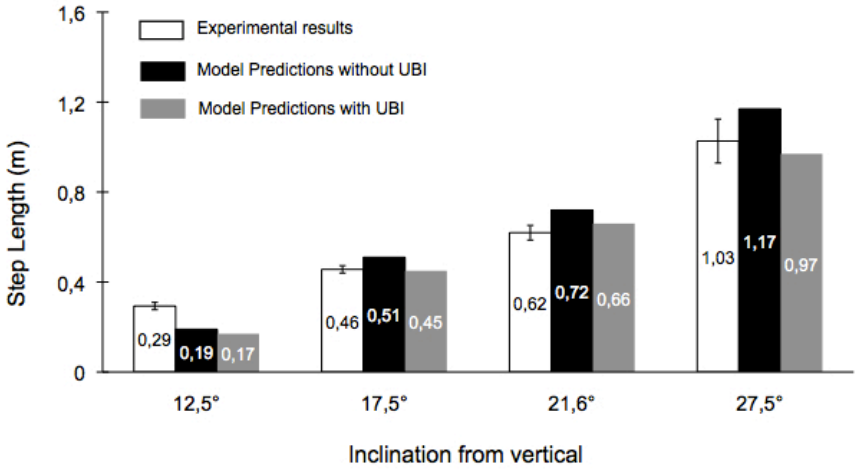

Figure 6.10: Les longueurs de pas de rattrapage pour le scénario de Hsiao-Wecksler and Robinovitch (2007) avec l'optimisation de la durée de pas: Expérimentale (en blanc, moyenne et écart-type) contre simulée avec (noir) et sans (gris) considération de l'inertie du haut du corps.

Comparaison avec les résultats expérimentaux

Pour comparer les prédictions de notre modèle, prenons les mêmes scénarios de rattrapage que nous avons considéré dans la précédente section. Les résultats sont montrés dans les Figures 6.10 à 6.14.

Les figures 6.10 et 6.11 comparent les longueurs et les durées de pas observées dans les essais (en blanc, moyenne et écart-type) et les prédictions du modèle sans (noir) et avec (gris) l'inertie du haut du corps. On peut constater que l'utilisation de l'inertie du haut du corps réduit la distance de rattrapage. Cette réduction est bien corrélée avec le niveau d'inclinaison initial, c'est-à-dire avec la perturbation. De plus, dans la plupart des cas, les prédictions incluant l'inertie sont plus proches des résultats expérimentaux, ce qui confirme notre hypothèse que cette inertie joue un rôle important dans ces scénarios de rattrapage.

La Figure 6.12 montre le pic d'accélération du volant d'inertie pour différents niveaux d'inclinaison. On peut remarquer la corrélation entre ce pic et le niveau d'inclinaison, une tendance cohérente avec la littérature sur le rattrapage d'équilibre (e.g. Park et al., 2004).

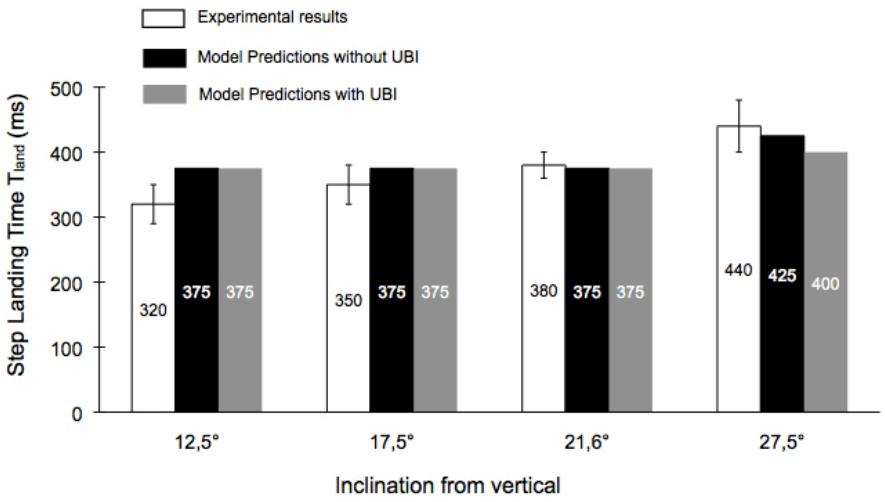

Figure 6.11: Les durée de pas optimisées par le contrôleur pour les différentes scénarios de citetHsiao-Wecksler2007.

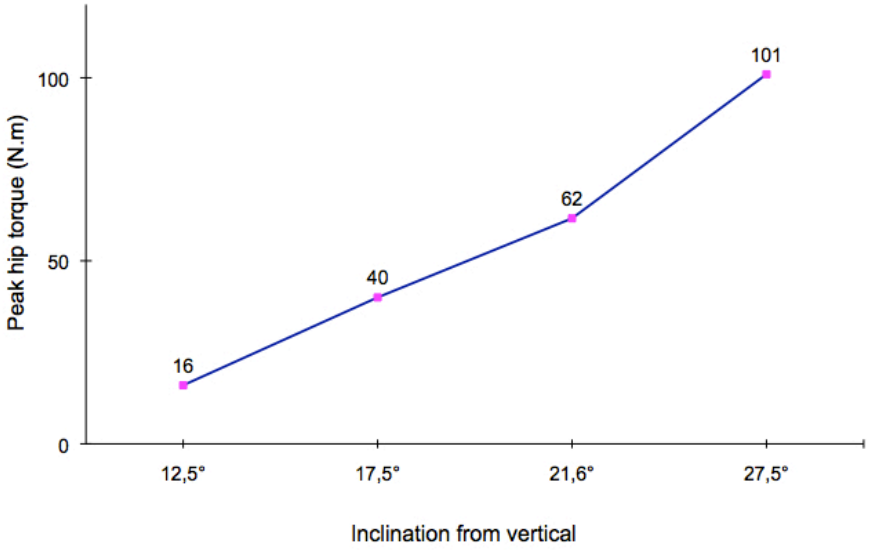

Figure 6.12: Le pic de couple du volant d'inertie prédit par le modèle pour 4 scénario par Hsiao-Wecksler and Robinovitch (2007).

Les Figures 6.13 et 6.14 montrent les résultats pour le scénario à plusieurs pas de rattrapage de Cyr and Smeesters (2009a). On peut voir une bonne cohérence entre les expériences et les simulations en termes de position et de durée de pas. Il faut notez que le troisième pas, non prédit par notre modèle, a été observé pour seulement

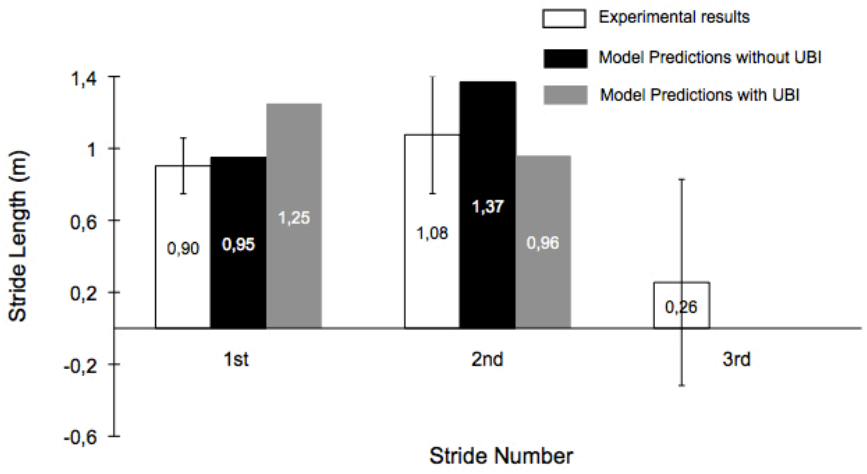

Figure 6.13: Les positions des pas pour le scénario de Cyr and Smeesters (2009a) avec optimisation de la durée de pas: Résultats expérimentaux (en blanc, moyenne et écart-type) contre résultats de simulation (avec et sans l'inertie du haut du corps).

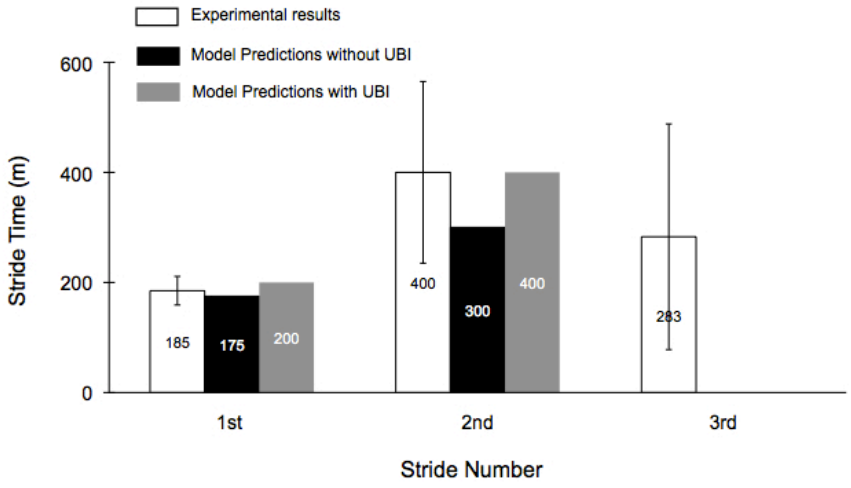

Figure 6.14: Les durées de pas optimisées, avec et sans inertie du haut du corps, comparé avec les résultats expérimentaux pour le scénario de Cyr and Smeesters (2009a).

2 sujets sur 28.

Pour conclure, les comparaisons présentées dans cette partie démontrent la capacité de notre modèle à prédire des comportements de rattrapage d'équilibre réalistes

pour des perturbations simple et une performance de rattrapage maximale. On peut aussi noter que notre modèle reproduit des caractéristiques du rattrapage humain observées dans les études expérimentales, comme l'utilisation des stratégies en parallèle, l'utilisation de l'inertie du haut du corps corrélée avec la perturbation, ou l'optimisation de la durée de pas.

Des scénarios applicatifs

Considérons maintenant des cas plus applicatifs. Trois cas de figure ont été testés: 1) un scénario de perturbation courte, mais pour laquelle les sujets pouvaient adopter des stratégies sous optimales; 2) un scénario de perturbation relativement longue, posant le problème de l'estimation de la perturbation à venir et de sa prise en compte dans le rattrapage; 3) une étude prospective sur les effets de l'âge sur le rattrapage d'équilibre.

Rattrapage sous optimal

Dans cette partie nous nous sommes intéressés à simuler des situations testées expérimentalement lors d'une étude précédente (Robert, 2006). Dix sujets volontaires ont été perturbés par une translation soudaine de leur base de support vers l'arrière. Le profil d'accélération était une demi-sinusoïde d'amplitude 1G d'une durée de 400 ms. La distance du rattrapage n'était pas contrainte expérimentalement et aucune instruction particulière à ce sujet n'était donnée aux volontaires. Dans un deuxième temps, quatre de ces dix sujets ont été soumis à la même perturbation, mais la distance de rattrapage était contrainte par un obstacle, forçant les sujets à se rattraper avec un niveau de performance proche de leur maximum. Sans surprise les caractéristiques du rattrapage entre les deux séries sont très différentes. On peut en déduire que, sans contrainte particulière, la réaction des sujets est relativement éloignée de la performance maximale (distance de rattrapage minimum). De fait, la réaction simulée en utilisant le modèle et les paramètres de la section* précédente est assez éloignée du résultat de la première série d'essais, mais beaucoup plus proche de la deuxième.

Nous avons donc choisi de modifier l'importance relative des paramètres de notre

fonction de coût. Nous nous sommes notamment intéressés à deux paramètres : le coût associé à l'accélération maximal du pied en vol ($\|\ddot{F}'_{k+1}\|^2$), que l'on peut relier à l'effort nécessaire pour faire ce pas, et le coût associé au Jerk du CdM ($\|\dddot{C}_k\|^2$), qui correspond à la continuité des mouvements. En faisant varier les pondérations associées à ces deux coûts nous pouvons alors représenter les deux types de réactions observées expérimentalement.

Anticipation de la perturbation

Dans cette section nous nous sommes intéressés à simuler des perturbations relativement longues, typiquement un profil de freinage d'urgence d'une durée de deux secondes (une seconde de montée en accélération et une seconde de plateau à 4 m.s-2). En particulier se pose la question : $1/$ de l'estimation, et la prise en compte dans la réaction, de ce que sera la perturbation au court de l'horizon de temps à venir; $2/$ de la fréquence à laquelle la réaction est mise à jour (la fréquence à laquelle est appelé le contrôleur prédictif).

Le modèle interne du contrôleur a été légèrement modifié afin de prendre en compte les mouvements estimés de la base de support dans la dynamique du système. Différentes estimations ont été testées (de la perturbation exacte à aucune anticipation). De même, différentes fréquences d'appel du contrôleur ont été testées. Les Figures 6.15 illustrent les résultats obtenus et notamment (i) l'énorme influence de la qualité de l'estimation de la perturbation à venir sur l'efficacité du rattrapage, (ii) la nécessité d'une replanification de la réaction fréquente lorsque la perturbation à venir est mal estimée.

Effet de l'âge

Nous avons ensuite interrogé la capacité de notre modèle à représenter le rattrapage de différents types de population, en particulier les personnes âgées. Dans cette section nous avons souhaité voir si nous pouvions "faire vieillir" notre modèle. Cela consiste à (i) identifier des paramètres du modèle qui sont représentatifs de caractéristiques physiques ou cognitives normalement dégradées avec l'âge; (ii) modifier les valeurs de ces paramètres, initialement ajustés pour une population jeune (section 4); (iii)

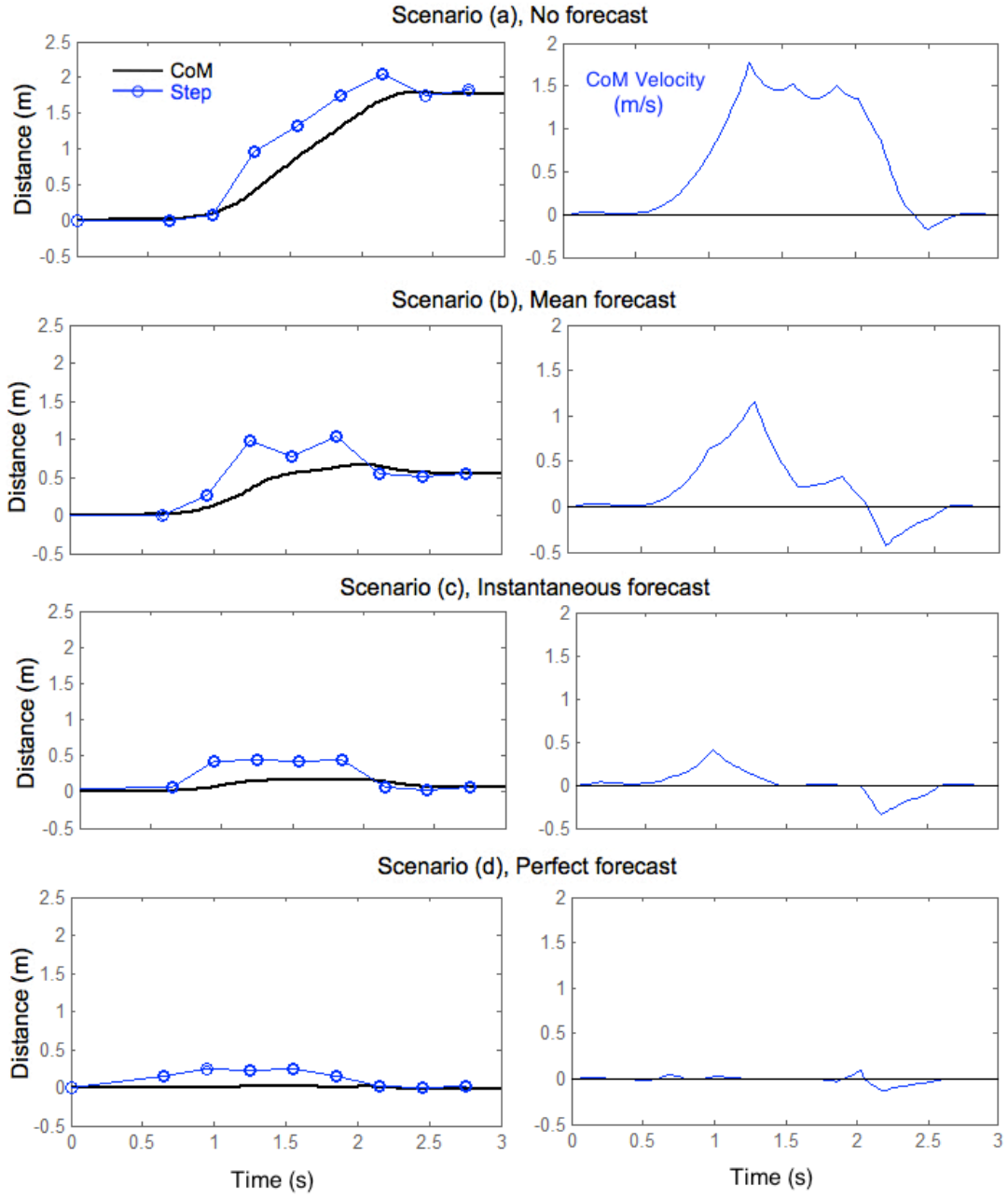

Figure 6.15: Rattrapage d'équilibre pour une perturbation longue selon 4 modalités d'anticipation de la perturbation de qualité croissante : évolution temporelle de la position (gauche - noir) et de la vitesse (droite - bleu) du CdM, ainsi que position des pas (gauche, point bleus).

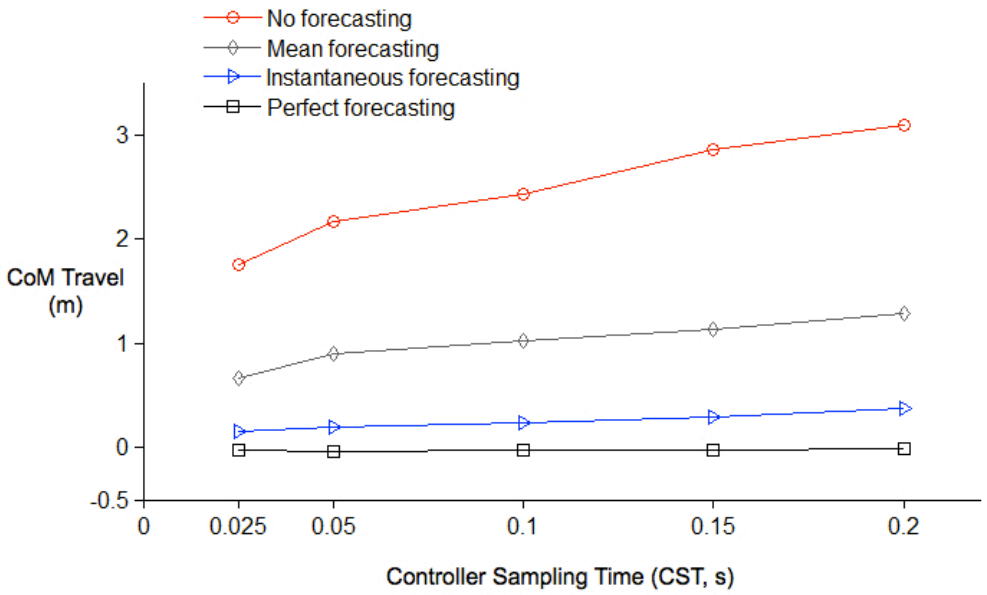

Figure 6.16: Distance totale parcourue par le CdM avant le rattrapage en fonction de la fréquence de replanification de la réaction, pour plusieurs modalités d'estimation de la perturbation.

observer l'influence de ces modification sur la réponse du modèle (distance de rattrapage, nombre et longueur des pas, ...) et (iv) vérifier si cette influence correspond aux différences de rattrapage entre sujets âgés et sujets jeunes rapportées dans la littérature.

Nous nous sommes penchés sur trois paramètres : la dégradation des capacités physiques a été représentée en réduisant l'accélération maximale du pied en vol et la base de support fonctionnelle, et la dégradation des capacités attentionnelles et sensorimotrices a été représentée en augmentant le temps de réaction. Les résultats (cf. Figures 6.17) indiquent que le modèle dégradé à tendance à faire, pour une même perturbation, des pas plus grands et plus longs. De même, la perturbation maximale admissible est drastiquement réduite. Ces résultats vont dans le sens des observations reportées dans la littérature. Bien que des travaux supplémentaires soient nécessaires afin d'identifier les valeurs réalistes de ces paramètres, ces résultats montrent le potentiel du modèle.

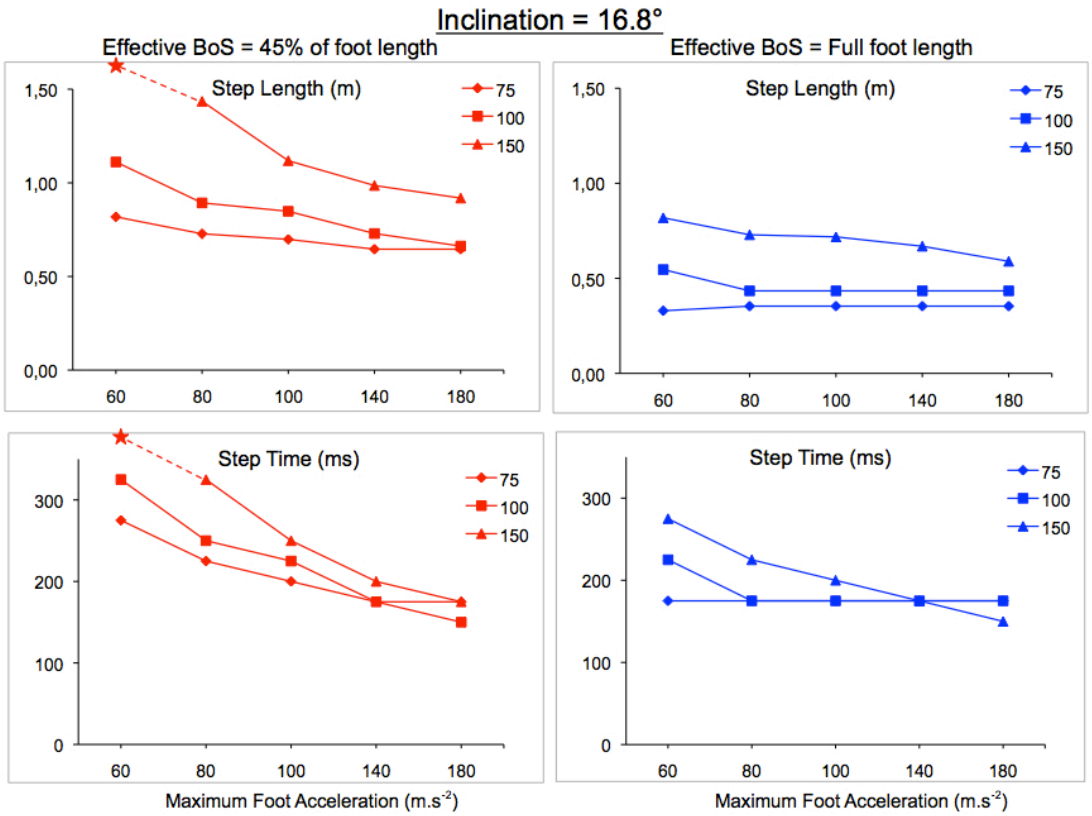

Figure 6.17: Longueur et durée des pas de rattrapage simulées pour des perturbations de type tether-release (cf. Chapitre 4), pour 3 différentes valeurs de temps de réaction (75 ms - losanges, 100 ms – carrés et 150 ms – triangles), deux valeurs de longueur effective de la base de support (100% à droite, 45% à gauche) et différents niveaux d'accélération maximale du pied en vol.

Conclusion et perspective

L'objectif de cette thèse était de proposer un modèle capable de prédire le rattrapage d'équilibre de sujets humains suite à des perturbations relativement importantes.

Nous avons tout d'abord adapté un contrôleur initialement développé pour la marche des robots bipèdes. Ce contrôleur a ensuite été modifié afin d'intégrer notamment l'inertie du haut du corps et de moduler la durée des pas. Le modèle a ensuite été validé pour des cas de perturbation simple et de performance de rattrapage maximale à l'aide de données expérimentales issues de la littérature. Nous avons ensuite cherché à évaluer les performances du modèle dans des situations plus complexes, afin d'aborder les questions (i) du rattrapage à performance sous optimale, (ii) de l'estimation de la perturbation à venir (iii) du rattrapage pour les sujets âgés. Les résultats qualitatifs obtenus sont encourageants sur les capacités du modèle. Par la suite il sera intéressant de continuer à développer certains aspects de ce modèle, notamment en modifiant le modèle mécanique contrôlé ou en intégrant les aspects d'intégration sensoriel. Enfin il faudrait finaliser les travaux entrepris dans le dernier chapitre du manuscrit, et tester le modèle dans d'autre cas applicatifs (lors de la marche par exemple).

Bibliography

Adkin, A. L., Frank, J. S., Carpenter, M. G., and Peysar, G. W. (2000). Postural control is scaled to level of postural threat. *Gait & Posture*, 12(2):87 -- 93.

Afnor (2003). Applications ferroviaires - freinage - syst mes de freinage des transports publics urbains et suburbains - partie 1 : Exigences de performances. nf en 13452-1. Technical report, Association Fran aise de Normalisation (AFNOR).

Aftab, Z., Wieber, P.-B., and Robert, T. (2010). Comparison of capture point estimation with human foot placement: Applicability and limitations. In *Actes des 5i mes Journ es Nationales de la Robotique Humano de, June 3-4 2010, Futuroscope Poitiers (France)*.

Alexandrov, A., Frolov, A., and Massion, J. (2001). Biomechanical analysis of movement strategies in human forward trunk bending. i. modeling. *Biological Cybernetics*, 84(6):425--434.

Alexandrov, A. V. and AA, F. (2005). Feedback equilibrium control during human standing. *Biological Cybernetics*, 93(5):309--322.

Anderson, F. C. and Pandy, M. G. (2001). Dynamic optimization of human walking. *Journal of Biomechanical Engineering*, 123(5):381--390.

Arampatzis, A., Karamanidis, K., and Mademli, L. (2008). Deficits in the way to achieve balance related to mechanisms of dynamic stability control in the elderly. *Journal of Biomechanics*, 41(8):1754 -- 1761.

Atkeson, C. and Stephens, B. (2007). Multiple balance strategies from one optimization criterion. In *Humanoid Robots, 2007 7th IEEE-RAS International Conference on*, pages 57--64.

Aubin, J. (1991). *Viability theory*. Birkhauser.

Azevedo, C., Amblard, B., Espiau, B., and Assaiante, C. (2004). A synthesis of bipedal locomotion in human and robots. research repport, INRIA.

Azevedo, C., Poignet, P., and Espiau, B. (2002). Moving horizon control for biped robots without reference trajectory. In *Proceedings- IEEE International Conference on Robotics and Automation*, volume 3, pages 2762--2767.

Bardy, B. G. (2002). *Coordination dynamics: Issues and trends*, chapter Postural Coordination Dynamics in Standing Humans, pages 103--121. Springer.

Barrett, R. S. and Lichtwark, G. A. (2008). Effect of altering neural, muscular and tendinous factors associated with aging on balance recovery using the ankle strategy: a simulation study. *Journal of Theoretical Biology*, 254(3):546--554.

Barthelemy, S. and Bidaud, P. (2007). tat de l art sur le contr le de l quilibre. Technical report, ISIR (LRP).

Bende, J. (2000). City bus safety - a casualty study from the view of the accidents research (cited by Kirk et al. 2003). Technical report, Institute for Vehicle Safety Munich.

Bhatt, T., Wening, J. D., and Pai, Y.-C. (2005). Influence of gait speed on stability: recovery from anterior slips and compensatory stepping. *Gait & Posture*, 21(2):146--156.

Bjornstig, U., Albertsson, P., Bjornstig, J., Bylund, P., Falkmer, T., and Petzall, J. (2005). Injury events among bus and coach occupants- non-crash injuries as important as crash injuries. *IATSS Research*, 29(1):79.

Bonnet, V., Fraisse, P., Ramdani, N., Lagarde, J., Ramdani, S., and Bardy, B. (2009). A robotic closed-loop scheme to model human postural coordination. In *IEEE/RSJ International Conference on Intelligent Robots and Systems*.

Bonnet, V., Lagarde, J., Fraisse, P., Ramdani, N., Ramdani, S., Poignet, P., and Bardy, B. (2007). Modeling human postural coordination to improve the control of balance in humanoids. In *IEEE-RAS International Conference on Humanoid Robots*, pages 324--329. IEEE.

Bonnet, V., Ramdani, S., Fraisse, P., Ramdani, N., Lagarde, J., and Bardy, B. G. (2011). A structurally optimal control model for predicting and analyzing human postural coordination. *Journal of Biomechanics*, 44(11):2123 -- 2128.

Borah, J., Young, L., and Curry, R. (1988). Optimal estimator model for human spatial orientation. *Annals of the New York Academy of Sciences*, 545(1):51--73.

Bortolami, S. B., DiZio, P., Rabin, E., and Lackner, J. R. (2003). Analysis of human postural responses to recoverable falls. *Exp Brain Res*, 151(3):387--404.

Bothner, K. E. and Jensen, J. L. (2001). How do non-muscular torques contribute to the kinetics of postural recovery following a support surface translation. *Journal of Biomechanics*, 34(2):245--250.

Bottaro, A., Casadio, M., Morasso, P. G., and Sanguineti, V. (2005). Body sway during quiet standing: is it the residual chattering of an intermittent stabilization processfi. *Human Movement Science*, 24(4):588--615.

Bottaro, A., Yasutake, Y., Nomura, T., Casadio, M., and Morasso, P. (2008). Bounded stability of the quiet standing posture: an intermittent control model. *Human Movement Science*, 27(3):473--495.

Brown, L. A., Shumway-Cook, A., and Woollacott, M. H. (1999). Attentional demands and postural recovery: The effects of aging. *The Journals of Gerontology Series A: Biological Sciences and Medical Sciences*, 54(4):M165--M171.

Carty, C. P., Barrett, R. S., Cronin, N. J., Lichtwark, G. A., and Mills, P. M. (2012). Lower limb muscle weakness predicts use of a multiple- versus single-step strategy to recover from forward loss of balance in older adults. *The Journals of Gerontology Series A: Biological Sciences and Medical Sciences*.

Chaffin, D. and Andersson, G. (1984). *Occupational Biomechanics*. J. Wiley & Sons, New York, NY, 4th edition.

Corso, P., Finkelstein, E., Miller, T., Fiebelkorn, I., and Zaloshnja, E. (2006). Incidence and lifetime costs of injuries in the united states. *Injury Prevention*, 12(4):212--218.

Creath, R., Kiemel, T., Horak, F., Peterka, R., and Jeka, J. (2005). A unified view of quiet and perturbed stance: simultaneous co-existing excitable modes. *Neuroscience Letters*, 377(2):75 -- 80.

Cyr, M.-A. and Smeesters, C. (2009a). Kinematics of the threshold of balance recovery are not affected by instructions limiting the number of steps in younger adults. *Gait & Posture*, 29(4):628--633.

Cyr, M.-A. and Smeesters, C. (2009b). Maximum allowable force on a safety harness cable to discriminate a successful from a failed balance recovery. *Journal of Biomechanics*, 42(10):1566--1569.

de Graaf, B. and van Weperen, W. (1997). The retention of balance: an exploratory study into the limits of acceleration the human body can withstand without losing equilibrium. *Human Factors*, 39(1):111--118.

Desmurget, M. and Grafton, S. (2000). Forward modeling allows feedback control for fast reaching movements. *Trends Cogn Sci*, 4(11):423--431.

Diedam, H. (2009). Fast nmpc algorithms for humanoid robot walking. Master's thesis, University of Heidelberg.

Diedam, H., Dimitrov, D., Wieber, P., Mombaur, K., and Diehl, M. (2008). Online walking gait generation with adaptive foot positioning through linear model predic-

tive control. In *Proceedings of the IEEE/RSJ International Conference on Intelligent Robots and Systems*.

Diener, H., Horak, F., and Nashner, L. (1988). Influence of stimulus parameters on human postural responses. *Journal of neurophysiology*, 59(6):1888--1905.

Do, M., Breniere, Y., and Brenguier, P. (1982). A biomechanical study of balance recovery during the fall forward. *Journal of Biomechanics*, 15(12):933--939.

Do, M. C., Schneider, C., and Chong, R. K. (1999). Factors influencing the quick onset of stepping following postural perturbation. *Journal of Biomechanics*, 32(8):795--802.

Doke, J. and Kuo, A. (2007). Energetic cost of producing cyclic muscle force, rather than work, to swing the human leg. *Journal of Experimental Biology*, 210(13):2390--2398.

Dumas, R., Cheze, L., and Verriest, J.-P. (2007). Adjustments to mcconville et al. and young et al. body segment inertial parameters. *Journal of Biomechanics*, 40:543--553.

Englsberger, J., Ott, C., Roa, M. A., Albu-Schaffer, A., and Hirzinger, G. (2011). Bipedal walking control based on capture point dynamics. In *IEEE/RSJ International Conference on Intelligent Robots and Systems (IROS)*, pages 4420 --4427.

Flash, T. and Hogan, N. (1985). The coordination of arm movements: an experimentally confirmed mathematical model. *The Journal of Neuroscience*, 5:1688--1703.

Geyer, H., Seyfarth, A., and Blickhan, R. (2006). Compliant leg behaviour explains basic dynamics of walking and running. *Proceedings of the Royal Society B*, 273(1603):2861.

Goswami, A. (1999). Postural stability of biped robots and the foot-rotation indicator (fri) point. *The International Journal of Robotics Research*, 18(6):523.

Halpern, P., Siebzehner, M. I., Aladgem, D., Sorkine, P., and Bechar, R. (2005). Non-collision injuries in public buses: a national survey of a neglected problem. *Emergency Medicine Journal*, 22(2):108--110.

Heinrich, S., Rapp, K., Rissmann, U., Becker, C., and Konig, H. (2010). Cost of falls in old age: a systematic review. *Osteoporosis International*, 21(6):891--902.

Herdt, A., Diedam, H., Wieber, P., Dimitrov, D., Mombaur, K., and Diehl, M. (2010a). Online walking motion generation with automatic foot step placement. *Advanced Robotics*, 24:719--737.

Herdt, A., Perrin, N., and Wieber, P. (2010b). Walking without thinking about it. In *IEEE/RSJ International Conference on Intelligent Robots and Systems (IROS) 2010*, pages 190--195. IEEE.

Hirai, K., Hirose, M., Haikawa, Y., and Takenaka, T. (1998). The development of honda humanoid robot. In *Proc. IEEE International Conference on Robotics and Automation*, volume 2, pages 1321--1326 vol.2.

Hof, A., Gazendam, M., and Sinke, W. (2005). The condition for dynamic stability. *Journal of Biomechanics*, 38(1):1--8.

Hofmann, A. (2006). *Robust Execution of Bipedal Walking Tasks From Biomechanical Principles*. PhD thesis, Computer Science and Artificial Intelligence Laboratory, Massachusetts Institute of Technology.

Hogan, N. (1984). An organizing principle for a class of voluntary movements. *The Journal of Neuroscience*, 4:2745--2754.

Horak, F. B. and Nashner, L. M. (1986). Central programming of postural movements: adaptation to altered support-surface configurations. *Journal of Neurophysiology*, 55(6):1369--1381.

Hsiao, E. T. and Robinovitch, S. N. (1999). Biomechanical influences on balance recovery by stepping. *Journal of Biomechanics*, 32(10):1099--1106.

Hsiao-Wecksler, E. T. and Robinovitch, S. N. (2007). The effect of step length on young and elderly women's ability to recover balance. *Clinical Biomechanics (Bristol, Avon)*, 22(5):574--580.

Insee (2006). Projections de population pour la france m tropolitaine l horizon 2050 (population trends in france - looking ahead to 2050 - an increasing and ageing population). Online.

Kagami, S., Kitagawa, T., Nishiwaki, K., Sugihara, T., Inaba, M., and Inoue, H. (2002). A fast dynamically equilibrated walking trajectory generation method of humanoid robot. *Autonomous Robots*, 12:71--82. 10.1023/A:1013210909840.

Kajita, S., Kanehiro, F., Kaneko, K., Fujiwara, K., Harada, K., Yokoi, K., and Hirukawa, H. (2003). Biped walking pattern generation by using preview control of zero-moment point. In *IEEE International Conference on Robotics and Automation*, volume 2, pages 1620--1626. Citeseer.

Kajita, S. and Tani, K. (1991). Study of dynamic biped locomotion on rugged terrain-derivation and application of the linear inverted pendulum mode. *IEEE International Conference on Robotics and Automation*, 2:1405 --1411 vol.2.

Kajita, S., Yamaura, T., and Kobayashi, A. (1992). Dynamic walking control of a biped robot along a potential energy conserving orbit. *IEEE Transactions on Robotics & Automation*, 8:431--438.

Kanamiya, Y., Ota, S., and Sato, D. (2010). Ankle and hip balance control strategies with transitions. In *Robotics and Automation (ICRA), 2010 IEEE International Conference on*, pages 3446 --3451.

Karamanidis, K. (2006). *Motor behaviour during sudden perturbation and repetitive non-strategic tasks in consideration of muscle-tendon unit capacities: effects of aging and running*. PhD thesis, Institute of Biomechanics and Orthopaedics German Sport University, Cologne.

Kawato, M. (1999). Internal models for motor control and trajectory planning. *Current Opinion in Neurobiology*, 9(6):718--727.

King, G., Luchies, C., Stylianou, A., Schiffman, J., and Thelen, D. (2005). Effects of step length on stepping responses used to arrest a forward fall. *Gait & Posture*, 22(3):219--224.

Kirk, A., Grant, R., and Bird, R. (2003). Passenger casualties in non-collision incidents on buses and coaches in great britain. In *Proceedings of the 18th International Technical Conference on the Enhanced Safety of Vehicles*. © US Department of Transportation.

Komura, T., Leung, H., Kudoh, S., and Kuffner, J. (2005). A feedback controller for biped humanoids that can counteract large perturbations during gait. In *Proceedings of the 2005 IEEE International Conference on Robotics and Automation (ICRA)*, pages 1989--1995. IEEE.

Koolen, T., Boer, T. D., Rebula, J., Goswami, A., and Pratt, J. (2012). Capturability-based analysis and control of legged locomotion, part 1: Theory and application to three simple gait models. *International Journal of Robotics Research*, submitted.

Kuzelicki, J., Zefran, M., Burger, H., and Bajd, T. (2005). Synthesis of standing-up trajectories using dynamic optimization. *Gait & Posture*, 21(1):1 -- 11.

Leboeuf, F., Bessonnet, G., Seguin, P., and Lacouture, P. (2006). Energetic versus sthenic optimality criteria for gymnastic movement synthesis. *Multibody System Dynamics*, 16(3):213--236.

Lee, W. A. and Deming, L. R. (1988). Age-related changes in the size of the effective support base during standing. *Physical Therapy*, 68:859.

Lim, H.-O. and Takanishi, A. (2000). Waseda biped humanoid robots realizing human-like motion. In *Proceedings of 6th International Workshop on Advanced Motion Control*.

Loram, I. D. and Lakie, M. (2002). Human balancing of an inverted pendulum: position control by small, ballistic-like, throw and catch movements. *The Journal of physiology*, 540(Pt 3):1111--1124.

Lord, S., Clark, R., and Webster, I. (1991a). Physiological factors associated with falls in an elderly population. *Journal of the American Geriatrics Society*, 39(12):1194--200.

Lord, S. R., Clark, R. D., and Webster, I. W. (1991b). Postural stability and associated physiological factors in a population of aged persons. *Journal of Gerontology*, 46(3):M69--M76.

Lord, S. R., Sherrington, C., and Menz, H. B. (2001). *Falls in Older People: Risk Factors and Strategies for Prevention*. Cambridge University Press.

Madigan, M. and Lloyd, E. (2005). Age and stepping limb performance differences during a single-step recovery from a forward fall. *The Journals of Gerontology Series A: Biological Sciences and Medical Sciences*, 60(4):481--485.

Maki, B. and McIlroy, W. (1997). The role of limb movements in maintaining upright stance: the" change-in-support" strategy. *Physical Therapy*, 77(5):488.

Maki, B. and McIlroy, W. (2007). Cognitive demands and cortical control of human balance-recovery reactions. *Journal of Neural Transmission*, 114:1279--1296.

Maki, B., McIlroy, W., and Fernie, G. (2003). Change-in-support reactions for balance recovery. *IEEE Engineering in Medicine and Biology Magazine*, 22(2):20 -- 26.

Maki, B., McIlroy, W., and Perry, S. (1994). Compensatory responses to multidirectional perturbations. In Taguchi, K., Igarashi, M., and Mori, S., editors, *Vestibular and Neural Front.*, pages 437--440, Amsterdam, the Netherlands. Elsevier Science Publishers BV.

Martin, L., Cahouët, V., Ferry, M., and Fouque, F. (2006). Optimization model predictions for postural coordination modes. *Journal of Biomechanics*, 39(1):170 -- 176.

Maurer, C., Mergner, T., and Peterka, R. (2006). Multisensory control of human upright stance. *Experimental Brain Research*, 171:231--250. 10.1007/s00221-005-0256-y.

McIlroy, W. and Maki, B. (1993). Task constraints on foot movement and the incidence of compensatory stepping following perturbation of upright stance. *Brain Research*, 616(1-2):30--38.

McIlroy, W. and Maki, B. (1996). Age-related changes in compensatory stepping in response to unpredictable perturbations. *Journals of Gerontology Series A: Biological Sciences & Medical Sciences*, 51A:M289--M296.

McIlroy, W. E. and Maki, B. E. (1994). The deceleration response to transient perturbation of upright stance. *Neuroscience Letters*, 175:13 -- 16.

McIlroy, W. and Maki, B. (1994). Compensatoy arm movements evoked by transient perturbations of upright stance. In Taguchi, K., Igarashi, M., and Mori, S., editors, *Vestibular and Neural Front.*, pages 489--492, Amsterdam, the Netherlands. Elsevier Science Publishers BV.

Mergner, T., Maurer, C., and Peterka, R. (2003). *Progress in Brain Research*, volume 142, chapter A multisensory posture control model of human upright stance. Elsevier Science B.V.

Mille, M.-L., Rogers, M. W., Martinez, K., Hedman, L. D., Johnson, M. E., Lord, S. R., and Fitzpatrick, R. C. (2003). Thresholds for inducing protective stepping responses to external perturbations of human standing. *J Neurophysiol*, 90(2):666--674.

Moglo, K. and Smeesters, C. (2005). The threshold of balance recovery is not affected by the type of postural perturbation. In *ISB XXth Congress - ASB 29th Annual Meeting*.

Morasso, P. and Schieppati, M. (1999). Can muscle stiffness alone stabilize upright standing? *Journal of Neurophysiology*, 82(3):1622--1626.

Nashner, L. M. and McCollum, G. (1985). The organization of human postural movements: A formal basis and experimental synthesis. *Behavioral and Brain Sciences*, 8:135--150.

Nenchev, D. and Nishio, A. (2007). Experimental validation of ankle and hip strategies for balance recovery with a biped subjected to an impact. In *IEEE/RSJ International Conference on Intelligent Robots and Systems (IROS)*, pages 4035 --4040.

Nishiwaki, K., Kagami, S., Kuniyoshi, Y., Inaba, M., and Inoue, H. (2002). Online generation of humanoid walking motion based on a fast generation method of motion pattern that follows desired zmp. In *IEEE/RSJ International Conference on Intelligent Robots and Systems*, volume 3, pages 2684--2689. IEEE.

Nishtwaki, K., Nagasaka, K., Inaba, M., and Inoue, H. (1999). Generation of reactive stepping motion for a humanoid by dynamically stable mixture of pre-designed motions. In *Proceedings of IEEE International Conference on Systems, Man, and Cybernetics (IEEE SMC'99)*, volume 6, pages 902--907. IEEE.

Owings, T. M., Pavol, M. J., and Grabiner, M. D. (2001). Mechanisms of failed recovery following postural perturbations on a motorized treadmill mimic those associated with an actual forward trip. *Clinical Biomechanics (Bristol, Avon)*, 16(9):813--819.

Pai, Y., Maki, B., Iqbal, K., McIlroy, W., and Perry, S. (2000). Thresholds for step initiation induced by support-surface translation: a dynamic center-of-mass model provides much better prediction than a static model. *Journal of Biomechanics*, 33(3):387--392.

Pai, Y. C. and Patton, J. (1997). Center of mass velocity-position predictions for balance control. *Journal of Biomechanics*, 30(4):347--354.

Pai, Y. C., Rogers, M. W., Patton, J., Cain, T. D., and Hanke, T. A. (1998). Static versus dynamic predictions of protective stepping following waist-pull perturbations in young and older adults. *Journal of Biomechanics*, 31(12):1111--1118.

Pai, Y.-C., Wening, J. D., Runtz, E. F., Iqbal, K., and Pavol, M. J. (2003). Role of feedforward control of movement stability in reducing slip-related balance loss and falls among older adults. *Journal of Neurophysiology*, 90(2):755--762.

Pandy, M. G., Garner, B. A., and Anderson, F. C. (1995). Optimal control of non-ballistic muscular movements: a constraint-based performance criterion for rising from a chair. *Journal of Biomechanical Engineering*, 117(1):15--26.

Park, J. H. and Cho, H. C. (2000). An online trajectory modifier for the base link of biped robots to enhance locomotion stability. In *Robotics and Automation, 2000. Proceedings. ICRA '00. IEEE International Conference on*, volume 4, pages 3353 --3358 vol.4.

Park, S., Horak, F., and Kuo, A. (2004). Postural feedback responses scale with biomechanical constraints in human standing. *Experimental Brain Research*, 154(4):417--427.

Pavol, M. J., Owings, T. M., Foley, K. T., and Grabiner, M. D. (2001). Mechanisms leading to a fall from an induced trip in healthy older adults. *The Journals of Gerontology Series A: Biological Sciences and Medical Sciences*, 56(7):M428--M437.

Peterka, R. (2002). Sensorimotor integration in human postural control. *Journal of Neurophysiology*, 88(3):1097--1118.

Pijnappels, M., Bobbert, M. F., and van Die n, J. H. (2005). How early reactions in the support limb contribute to balance recovery after tripping. *Journal of Biomechanics*, 38(3):627--634.

Popovic, M. B., Goswami, A., and Herr, H. (2005). Ground reference points in legged locomotion: Definitions, biological trajectories and control implications. *The International Journal of Robotics Research*, 24(12):1013--1032.

Pratt, J., Carff, J., Drakunov, S., and Goswami, A. (2006). Capture point: A step toward humanoid push recovery. In *Proceedings of the 2006 6th IEEE-RAS International Conference on Humanoid Robots*, pages 200--207.

Pratt, J., Koolen, T., Boer, T. D., Rebula, J., Cotton, S., Carff, J., Johnson, M., and Neuhaus, P. (2012). Capturability-based analysis and control of legged locomotion , part 2: Application to m2v2 , a lower body humanoid. *International Journal of Robotics Research*, submitted.

Robert, T. (2006). *Analyse biomécanique du maintien de l'équilibre debout suite à une accélération transitoire de la surface d'appui - Application à l'amélioration de la protection des passagers de transports en commun*. PhD thesis, Institut National des Sciences Appliquées de Lyon.

Robert, T. and Verriest, J. (2007). Latency of the active mechanical response following a translation of the support surface. *Computer Methods in Biomechanics and Biomedical Engineering*, 10:141--142.

Runge, C. F., Shupert, C. L., Horak, F. B., and Zajac, F. E. (1999). Ankle and hip postural strategies defined by joint torques. *Gait & Posture*, 10(2):161--170.

Schillings, A., Wezel, B. V., and Duysens, J. (1996). Mechanically induced stumbling during human treadmill walking. *Journal of Neuroscience Methods*, 67(1):11 -- 17.

Schulz, B., Ashton-Miller, J., and Alexander, N. (2005). Compensatory stepping in response to waist pulls in balance-impaired and unimpaired women. *Gait & posture*, 22(3):198--209.

Sociale, S. (2001). Les clés du bien vieillir: Prévention des chutes chez les seniors. Technical report, Comité Français d'Education pour la Santé (CFES).

Stephens, B. (2007). Humanoid push recovery. In *IEEE-RAS International Conference on Humanoid Robots*. Citeseer.

Stephens, B. and Atkeson, C. (2010). Push recovery by stepping for humanoid robots with force controlled joints. In *International Conference on Humanoid Robots 2010*.

Szturm, T. and Fallang, B. (1998). Effects of varying acceleration of platform translation and toes-up rotations on the pattern and magnitude of balance reactions in humans. *Journal of vestibular research: equilibrium & orientation*, 8(5):381--397.

Takenaka, T., Matsumoto, T., Yoshiike, T., Hasegawa, T., Shirokura, S., Kaneko, H., and Orita, A. (2009). Real time motion generation and control for biped robot -4th report: Integrated balance control. In *IEEE/RSJ International Conference on Intelligent Robots and Systems*.

Thelen, D., Schultz, A., Alexander, N., and Ashton-Miller, J. (1996). Effects of age on rapid ankle torque development. *The Journals of Gerontology Series A: Biological Sciences and Medical Sciences*, 51(5):M226--32.

Thelen, D., Wojcik, L., Schultz, A., Ashton-Miller, J., and Alexander, N. (1997). Age differences in using a rapid step to regain balance during a forward fall. *The Journals of Gerontology: Series A*, 52(1):M8.

Uno, Y., Kawato, M., and Suzuki, R. (1989). Formation and control of optimal trajectory in human multijoint arm movement. *Biological Cybernetics*, 61:89--101.

Van den Bogert, A., Pavol, M., and Grabiner, M. (2002). Response time is more important than walking speed for the ability of older adults to avoid a fall after a trip. *Journal of biomechanics*, 35(2):199--205.

van der Burg, J. C. E., Pijnappels, M., and van Die n, J. H. (2007). The influence of artificially increased trunk stiffness on the balance recovery after a trip. *Gait Posture*, 26(2):272--278.

van der Kooij, H., Jacobs, R., Koopman, B., and Grootenboer, H. (1999). A multisensory integration model of human stance control. *Biological Cybernetics*, 80:299--308.

van der Kooij, H., Jacobs, R., Koopman, B., and van der Helm, F. (2001). An adaptive model of sensory integration in a dynamic environment applied to human stance control. *Biological cybernetics*, 84(2):103--115.

Verriest, J.-P., Hetier, M., Chevalier, M.-C., Robert, T., and Beillas, P. (2010). Kinematics of a standing passenger subjected to an emergency braking deceleration pulse. In *Proceedings of the 6th World Congress of Biomechanics, 1 - 6 August 2010, Singapore (Singapore).*

Wieber, P. (2005). Some comments on the structure of the dynamics of articulated motion. In *Fast Motions in Biomechanics and Robotics*.

Wieber, P. (2008). Viability and predictive control for safe locomotion. In *IEEE-RSJ International Conference on Intelligent Robots & Systems*.

Wieber, P. and Chevallereau, C. (2006). Online adaptation of reference trajectories for the control of walking systems. *Robotics and Autonomous Systems*, 54(7):559--566.

Wieber, P. B. (2002). On the stability of walking systems. In *Proceedings of the International Workshop on Humanoid and Human Friendly Robotics*.

Wieber, P.-B. (2006). Trajectory free linear model predictive control for stable walking in the presence of strong perturbations. In *IEEE-RAS International Conference on Humanoid Robots*.

Wight, D. L., Kubica, E. G., and Wang, D. W. L. (2008). Introduction of the foot placement estimator: A dynamic measure of balance for bipedal robotics. *Journal of Computational and Nonlinear Dynamics*, 3:11009.

Winter, D. (1990). *Biomechanics and Motor Control of Human Movement*. Wiley, New York.

Winter, D. A. (1992). Foot trajectory in human gait: a precise and multifactorial motor control task. *Physical Therapy*, 72(1):45--53.

Winter, D. A., Patla, A. E., Prince, F., Ishac, M., and Gielo-Perczak, K. (1998). Stiffness control of balance in quiet standing. *Journal of Neurophysiology*, 80(3):1211--1221.

Winter, D. A., Patla, A. E., Rietdyk, S., and Ishac, M. G. (2001). Ankle muscle stiffness in the control of balance during quiet standing. *Journal of Neurophysiology*, 85(6):2630--2633.

Wojcik, L., Thelen, D., Schultz, A., Ashton-Miller, J., and Alexander, N. (1999). Age and gender differences in single-step recovery from a forward fall. *The Journals of Gerontology Series A: Biological Sciences and Medical Sciences*, 54(1):M44--M50.

Wu, M., Ji, L., Jin, D., and chung Pai, Y. (2007). Minimal step length necessary for recovery of forward balance loss with a single step. *J Biomech*, 40(7):1559--1566.

Yin, K. and van de Panne, M. (2006). Omnidirectional humanoid balance control: Multiple strategies for reacting to a push. Technical report, University of British Columbia, Computer Science Department.

Yun, S.-K. and Goswami, A. (2011). Momentum-based reactive stepping controller on level and non-level ground for humanoid robot push recovery. In *Proceedings of IEEE/RSJ International Conference on Intelligent Robots and Systems*.

Zarrugh, M., Todd, F., and Ralston, H. (1974). Optimization of energy expenditure during level walking. *European Journal of Applied Physiology and Occupational Physiology*, 33(4):293--306.